2010

Characterization of the Functional Role of the Intracellular Cholesterol Transporter StARD4 in Knockout Mice, and Investigation of Epigenetic Modulation of ApoA-I Transcription

Joshua Riegelhaupt

Characterization of the Functional Role of the Intracellular Cholesterol Transporter StARD4 in Knockout Mice, and Investigation of Epigenetic Modulation of ApoA-I Transcription

A Thesis presented to the Faculty of

The Rockefeller University

in Partial Fulfillment of the Requirements for

the degree of Doctor of Philosophy

by

Joshua Riegelhaupt

June 2010

CHARACTERIZATION OF THE FUNCTIONAL ROLE OF THE INTRACELLULAR CHOLESTEROL TRANSPORTER StARD4 IN KNOCKOUT MICE AND INVESTIGATION OF THE EPIGENTIC MODULATION OF APOA-I TRANSCRIPTION

Joshua Riegelhaupt, Ph.D.
The Rockefeller University 2010

Cholesterol is crucial for mammalian survival by playing important roles, such as regulating membrane fluidity and as a precursor for the synthesis of steroid and sex hormones, bile acids, and Vitamin D. In addition, cellular and organismal regulation of cholesterol is important for health. For example, increased levels of plasma LDL cholesterol are a risk factor for coronary heart disease and stroke. Intracellular cholesterol levels are regulated by a variety of mechanisms, but numerous studies indicate a very important role for transcriptional regulation by Sterol Regulatory Binding Proteins (SREBPs), Liver X Receptors (LXRs) and Unfolded Protein Response (UPR) or ER stress families of transcription factors. StARD4 is regulated by SREBPs and we have chosen to make a mouse knockout model to characterize its role *in-vivo*.

StARD4, expressed primarily in liver and macrophages, is a known intracellular cholesterol transporter previously shown to be down-regulated ~2 fold in liver, by high cholesterol feeding. It is thought to be involved in the dynamics of cholesterol movement between ER, plasma membrane, endosomes and lipid droplets. Based on these observations, I hypothesized

that a knockout of StARD4 in a mouse model would show altered intracellular cholesterol sorting, and figuring out the basis of such a defect would provide insight into the general mechanisms of intracellular sterol transport. To my surprise, StARD4 knockouts were viable and for the most part phenotypically normal. They showed no alteration in plasma or liver cholesterol or triglycerides. In addition, no abnormalities were found in glucose metabolism, macrophage cholesterol efflux, or atherosclerosis susceptibility. Based on these observations, I hypothesize that *in-vivo,* the absence of StARD4 is compensated for by other genes and/or pathways. In the future, it will be necessary to identify these compensatory mechanism(s) to truly understand the physiological role of StARD4.

I also studied another aspect of cholesterol metabolism related to its transport in plasma in high density lipoproteins (HDLs). HDL is involved in the reverse cholesterol transport mechanism, whereby excess cholesterol is removed from peripheral tissues and transported to the liver for excretion. The major protein of HDL is apoA-I and in mouse models it has been shown that animals transgenic for apoA-I have increased HDL levels. This suggests increased apoA-I transcription as a mechanism for increasing HDL, which might be preventive or therapeutic for coronary heart disease. With this as a goal, as part of my thesis I studied the epigenetic regulation of apoA-I transcription. I found that increased apoA-I transcription in liver cell culture cell lines was associated with highly unmethylated CpGs in the

apoA-I promoter, and the reverse, in cultures with poor apoA-I expression. I also found histone marks associated with apoA-I expression. This project was discontinued in favor of the StARD4 knockout mouse project. However, it might be continued in the future to reveal drug targets that alter epigenetic regulation of apoA-I in a manner that raises HDL levels.

Acknowledgments

I would like to take a moment to thank the many people who have helped me along my path before and during my PhD experience. First and foremost, I would like to extend my deepest gratitude to my PhD mentor, **Jan Breslow**. Above all else, Jan taught me the virtue of patience and humbleness. I can not think of a kinder or more encouraging person to have been my guide through the ups and downs of the PhD experience. At no point, did Jan lose faith in my ability or intelligence and for this I am greatly appreciative.

I am also thankful to the members of team Breslow of which there have been many. It began with my relationship with **Marc Waase**, who happened to work on similar projects to my own. This was quickly expanded to include my post doc mentors, **Ralph Burkhardt**, **Changcheng Zhou**, El Doctor **Jose Manuel Rodriquez** and **Jeanne Garbarino**. I also enjoyed the time spent with all other members of the Breslow lab, which included, **Brian Pridgen**, **Megan Roblee**, **Eimear Kenny** and **KY Chen**. I had the pleasure of working with a Cornell medical student, **Daniel Cruz**, whose company I greatly enjoyed over the summer we were together. I wanted to thank **Helen Yu** for all her work sectioning my mouse aortas and **Katie Tsang** for making the lab run so smoothly. I would also like to thank the two clinical scholars **Manish Ponda** and **Swaroop Pendyala** who taught me a lot of things about medical biology that I would not have learned otherwise. I am also grateful to **Lauren Glenz** who helped run the day to day administrative functions of the laboratory. The Tri-institutions have many useful resources that I was able to use during my time here and I would like to thank the people who I worked with; **Suzanna Couto** (MSKCC Pathology), **Chingewen Yang** (RU Gene Targeting), **Rada Norinsky** (RU Transgenics), **Connie Zhao** (RU Genomics) and all their staffs. I am also grateful to my classmates, the PhD entering class of 2005, whom I have been able to share the joys and stresses of our time at Rockefeller together. Specifically, I would like to thank my roommate **Florian Gehre**, for the great times we spent together.

My graduate career would not have run as smoothly without the help of everyone behind the scenes in the Deans office at the Rockefeller University. **Sid Strickland**, **Emily Harms**, **Marta Delgado**, **Kristen Cullen**, **Cristian Rosario** and **Michelle Sherman**.

I thank my committee members: **Sid Strickland** and **David Allis**, for their advice and assistance over the past years. I would also like to thank my external member, **David Cohen** (Harvard) for his comments and help.

Finally, I would like to thank my family. My parents, **Elliot Riegelhaupt** and **Susan Steinberg** are much of the influence that has

gotten me here today and without their constant love and support, I would not be who I am. Their hardwork and concomitant family devotion is a wonderful reminder of what it takes to be successful in this world. My brothers **Paul** and **Mike** and sister **Rachel** always provide a great friendship which I can rely on no matter where I am in life. My grandparents, **Lillian** and **Milton** are people who I look up to in admiration for the struggles they have endured in life and for the successes they have achieved. My aunt and uncle, **Lu** and **Michael** and my cousins, **Ilana** and **Talia**, are wonderful support networks for me. Finally, my girlfriend **Sasha Growick**, who had the pleasure of being with me for almost all of my time at Rockefeller. Thanks for all your love and support. I could not have done it without you.

Table of Contents

Chapter 2: Generation and Characterization of the StARD4 K.O.

Chapter 3: Epigenetic Regulation of ApoA-I

Chapter 4: Materials and Methods

Chapter 5: Discussion and Future Direction

List of Figures

List of Tables

List of Abbreviations

25OH	25-hydroxycholesterol
ABC	ATP-binding cassette
ACAT	acyl-coenzyme A: cholesterol acyl transferase
ACOT	acyl-CoA thioester hydrolase
Apo	apolipoprotein
ATF	activating transcription factor
BFIT	brown fat inducible thioesterase
bHLH-Zip	basic helix-loop-helix-leucine zipper
CACH	cytolosolic acetyl-CoA hydrolase
CERT	ceramide transfer protein
CETP	cholesterol ester transfer protein
ChIP	chromatin immuno-precipitation
CpG	cytosine guanine
Cyp	cytochrome P450
DGA	diacylglycerol acyltransferase
DLC	deleted in liver cancer
ER	endoplasmic reticulum or estrogen receptor
ERSE	ER stress response element
GPBP	Goodpasture antigen-binding protein
GTT1	gestation trophoblastic tumor 1
HAT	histone acetyltransferase
HDAC	histone deacetylase
HDL	high density lipoprotein
HEK	Human Embryonic Kidney Cells
HepG2	human liver carcinoma cell line
HMG CoA	hydroxymethylglutaryl coenzyme A
HMGR	HMG CoA reductase
HMGS	HMG CoA synthase
HPL	hepatic lipase
HuH7	human hepato cellular carcinoma cell line
IL	interleukin
IP	immuno-precipitation
IRE	inositol requiring enzyme
IMM	inner mitochondrial membrane
Insig	insulin-induced-gene
IVC	inferior vena cava
Lcat	lecithin:cholesterol acyltransferase
LDL	low density lipoprotein
LDL-C	low density lipoprotein cholesterol
LDLR	LDL receptor
LPL	lipoprotein lipase
LPS	lipopolysacharride
LXR	liver X receptor
LXRE	LXR response element

MBD	Methyl Binding Domain
MENTAL	MLN64 N-terminal domain
MENTHO	MLN64 N-terminal domain homologue
MLN64	metastatic lymph node 64
MMP	matrix metalloprotease
NaCL	sodium chloride
NOS	nitric oxide synthase
NPC	Niemann pick type c
OMM	outer mitochondrial membrane
ORF	open reading frame
ORP	OSBP related protein
OSBP	oxysterol binding protein
Osh	OSBP-homologous
PC	phosphatidylcholine
PCR	polymerase chain reaction
PCTP	phosphatidylcholine transfer protein
PE	phosphatidylethanolamine
PERK	PKR-like ER protein kinase
PH	pleckstrin homology domain
PLTP	phospolipid transfer protein
PM	plasma membrane
RCT	reverse cholesterol transport
RhoGAP	rho GTPase activating protein
RNAi	RNA interference
RPM	rotations per minute
RT	reverse transcriptase
S1P	site 1 protease
S2P	site 2 protease
SAM	Sterol alpha motif
SCAP	SREBP cleavage activating protein
SCP-2	sterol carrier protein
SNP	single nucleotide polymorphism
SR-B1	scavenger receptor class B1
SRE	sterol regulatory element
SREBP	sterol regulatory element binding protein
SSD	sterol sensing domain
StAR	steroidogenic acute regulatory protein
StARD	START domain containing
START	StAR-related lipid transfer
THEA	thioesterase adipose associated
TSA	trichostatin A
TNF	tumor necrosis factor
UPR	unfolded protein response
Utr	untranslated region
VLDL	very low density lipoprotein

Chapter 1: Introduction

Cholesterol's Physiological Importance

Cholesterol, the most abundant sterol in the human body, is essential for life, as its precursors and metabolites are involved in various cellular signaling events and cell functions (Soccio and Breslow 2004). Systemically, cholesterol is made available to mammals from dietary sources and eventual uptake from plasma lipoproteins (Goldstein and Brown 2009) and from *de novo* synthesis from acetyl-CoA using 20-30 enzymes and cofactors (Bloch 1975). However, its excess, especially high plasma levels of LDL-C (or commonely referred to as, "bad cholesterol"), is toxic and contributes to several diseases (Soccio and Breslow 2004). Most notably are atherosclerosis and stroke, accounting for nearly a million American deaths each year (Tabas 2002). Therefore, it is critical that the body maintain appropriate cholesterol homeostasis, and understanding the mechanisms involved is important for developing new remedies for disorders of cholesterol metabolism.

Cholesterol is a 27-carbon molecule that is rigid, planar, amphipathic, composed of a four ring steroid nucleus, a polar hydroxyl group and an alkyl side chain. Cholesterol provides rigidity and structure to the plasma membrane, retaining membrane permeability and playing an important role in lipid rafts composition; structures that serve as scaffolds for various cell signaling pathways (van Meer, Voelker et al. 2008).

Cholesterol covalently interacts with and modifies other proteins, perhaps best exemplified by its role in regulation of sonic hedgehog, a major player in normal human development (Tabas 2002). As a precursor of the steroid and stress hormones, notably the adrenal hormones, corticosterone, cortisol and aldosterone and the gonadal hormones progesterone, estradiol and testosterone, cholesterol plays a vital role in developmental/reproductive biology, as well as in stress response (Payne and Hales 2004). Additionally, cholesterol is a precursor for bile acids, which play varied and important physiological roles. First, they are essential for absorption of lipids and all other fat soluble nutrients in the gut. Second, they are responsible for activation of signaling pathways, like the FXR nuclear hormone pathway, that regulates triglyceride, cholesterol, energy and glucose homeostasis (Thomas, Pellicciari et al. 2008). Finally, cholesterol is the building block for vitamin D3 (or cholecalciferol), which is essential in calcium homeostasis. (Tabas 2002).

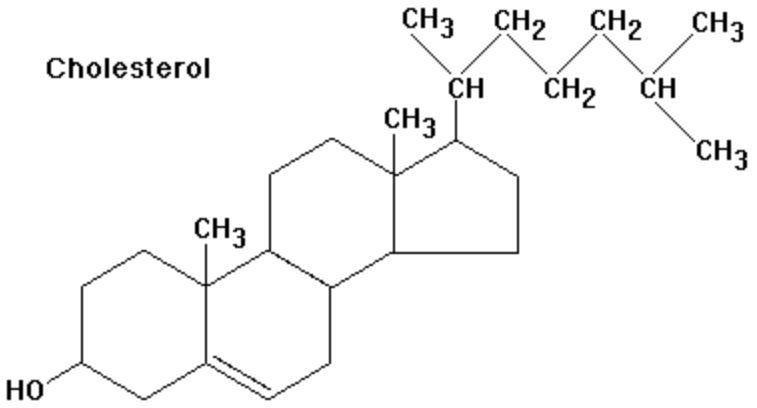

Figure 1.1 - Structural Composition of a Cholesterol Molecule

Cholesterol plays an extremely important role in the body and its level must be carefully regulated. This includes tight regulation of the pathways for synthesis, as well as cellular influx and efflux. Pathways exist to deal with excess cellular cholesterol, for example the repression of endogenous synthesis, esterification of cholesterol by the enzyme acyl-coenzyme A:cholesterol acyltransferase (ACAT) and the ultimate efflux out of the cell as part of the reverse cholesterol transport (RCT) pathway (Tabas 2002). However, upon failure, this excess can lead to the development of atherosclerotic plaques, which occur when excess cholesterol, carried in lipoproteins, settles in the subendothelial space of the vasculature. The excess cholesterol in turn signals for the infiltration of monocytes which transform into foam cells that eventually undergo necrosis. When foam cells necrose, vascular smooth muscle cells migrate into the space and form a cap. Eventually, the build up of the plaque

induces inflammatory and apoptotic pathways that lead to plaque rupture. Rupture then leads to an acute thrombotic vascular infarction of that tissue which is the pathogenic cause of myocardial infarctions and thrombotic stroke (Hansson 2005). Finally, due to its important role in bile synthesis, excess cholesterol can lead to the development of gallstones, which force over half a million Americans per year to undergo cholecystectomy (removal of the gallbladder) (Portincasa, Moschetta et al. 2006).

Cholesterol *de novo* Synthesis and Dietary Uptake

There are two mechanisms by which the body acquires cholesterol; *de novo* synthesis and dietary intake. About 1 gram of cholesterol is synthesized per day versus 300-500mg absorbed from the diet (Ikonen 2006). Cholesterol in ingested food is emulsified by bile acids, absorbed into intestinal epithelial cells and packaged into chylomicrons. The latter enter the lymphatics from which they drain into the venous system and become plasma lipoproteins.

Cholesterol synthesis occurs in all organs. The cellular signaling pathway controlling cholesterol synthesis, commonly referred to as the HMG-CoA Reductase pathway, has been extensively researched for over 20 years as it is the target of a blockbuster pharmaceutical therapy (Tobert 2003). Briefly, Acetyl-CoA, the metabolic product of glycolysis and fatty acid oxidation, is converted by 20-30 enzymes to four key intermediates, mevalonate, farnesyl pyrophosphate, squalene and lanosterol and then

ultimately to cholesterol. (Goldstein, DeBose-Boyd et al. 2006). The pharmaceutical drug class of statins inhibit one of these enzymes called HMG-CoA Reductase, the rate limiting step in the production of mevalonate and ultimately cholesterol (Tobert 2003).

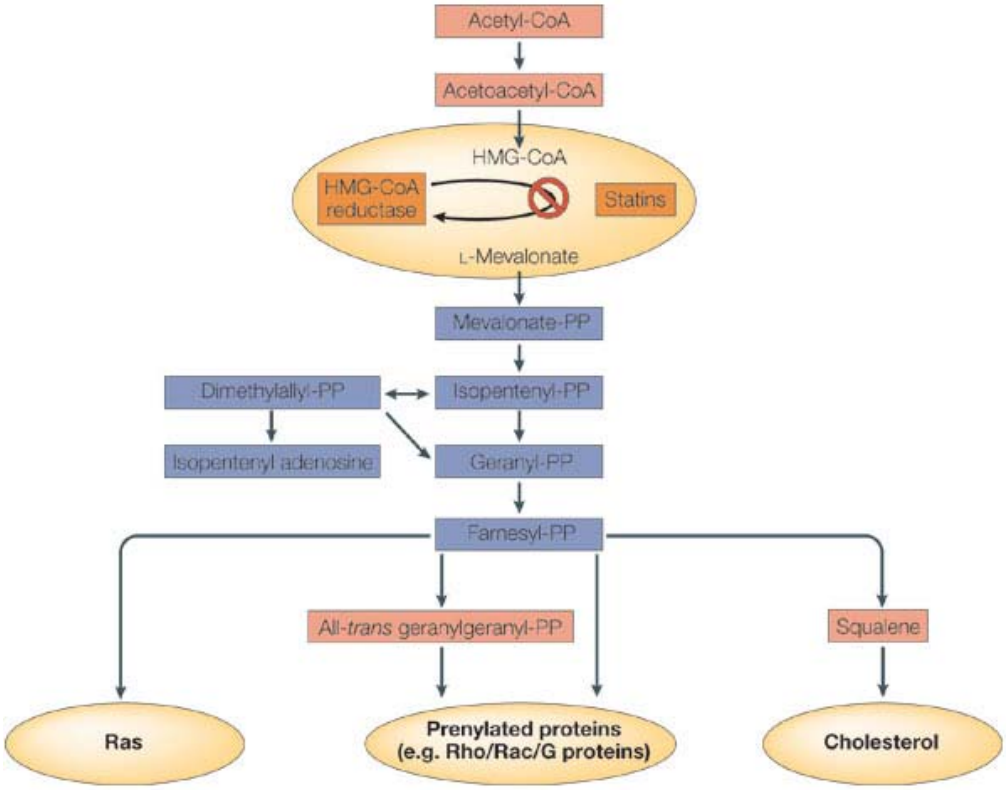

Figure 1.2 - Brief Overview of the HMG-CoA Reductase pathway
The diagram represents the HMG-CoA Reductase pathway for cholesterol synthesis and some of the other effected products, like Ras and Rho, by pathway intermediates which play important roles in cell proliferation, differentiation and migration. Some of the anti-inflammatory responses of statins have been attributed to off-target effects on these proteins (Menge, Hartung et al. 2005).

The complexity of cholesterol metabolism requires a controlling entity to balance overall cholesterol homeostasis and this burden falls primarily on the liver. To this end, the liver balances the rate of synthesis and storage (in the form of cholesterol esters in lipid droplets or free

cholesterol in the plasma membrane), with the rate of efflux (both into the blood stream in lipoproteins and out of the body through the bile excretion pathways) and rate of influx (from the bloodstream) (Ikonen 2006).

Lipoprotein Transport of Cholesterol in the Blood

Cholesterol and cholesterol esters are shuttled throughout the plasma in particles called lipoproteins. The non-polar cholesterol esters and triglycerides in the core of the lipoprotein are solublized by apolipoproteins, while phospholipids and free cholesterol remain on the surface (Gotto, Pownall et al. 1986). The transport of these lipoproteins resembles a circular pathway. From the intestine, chylomicrons, triglyceride rich and containing apolipoprotein B-48 (ApoB48), are secreted. Within the plasma, chylomicrons are metabolized into chylomicron remnants and undergo receptor mediated endocytosis by the liver (Redgrave 2004). The liver secretes another triglyceride rich particle called very low density lipoprotein (VLDL), that contains additional apolipoproteins, ApoE and varied ApoC particles as well as ApoB100 (Chang, Chang et al. 2006). As VLDL makes it way through the vasculature, it is converted to IDL (intermediate density lipoprotein) via the action of a lipoprotein lipase (LPL) and then to LDL (low density lipoprotein). At this stage, LDL has also lost ApoE and the ApoCs lipoproteins (Chang, Chang et al. 2006). The last major lipoprotein, HDL (high density lipoprotein), or commenly referred to as, “good cholesterol,”

is produced as an ApoA-I containing discoidal particle in the liver and intestine. Upon secretion into plasma, HDL begins its journey to maturity, evolving as it acquires free cholesterol from peripheral cells (Krieger 1999). Free cholesterol in discoidal HDL is esterified by LCAT in plasma, changing the shape of the particle to spherical with cholesterol ester in the center. Both LDL and HDL are ultimately taken up in the liver by the LDL receptor (LDLR) and by scavenger receptor B1 (SRBI), respectively (Krieger 1999). A more comprehensive coverage of the HDL particle and ApoA-I will be discussed in subsequent sections.

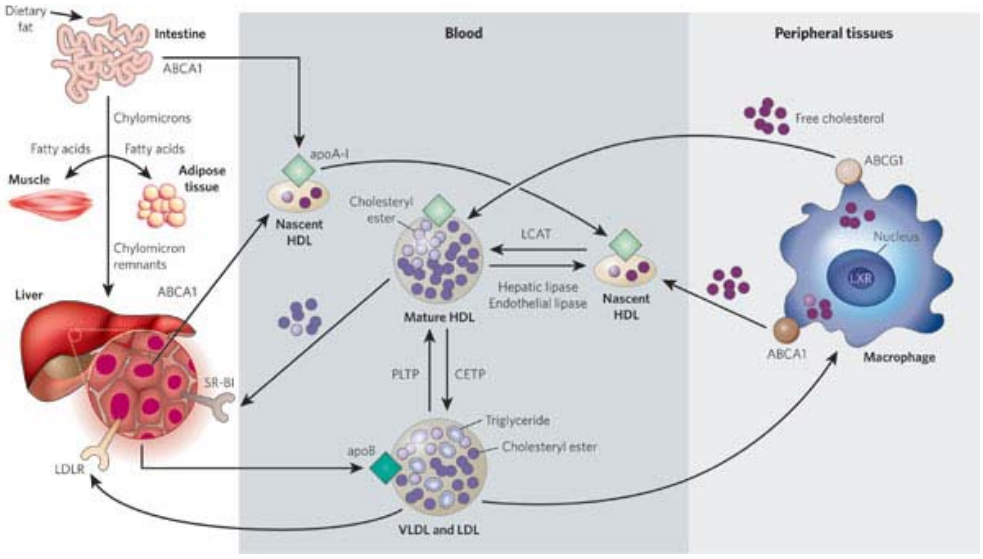

Figure 1.3 - Lipoprotein Metabolism
The intestine absorbs dietary fat and packages it into chylomicrons, which are transported to peripheral tissues through the blood. In muscle and adipose tissue, lipoprotein lipase breaks down the particles and the fatty acid component enters these tissues. The subsequent remnant is taken up by the liver. The liver then creates ApoB particles and enriches them with lipid particles to create VLDL, which is subsequently excreted into the plasma. Lipolysis of this particle by lipoprotein lipase ultimately creates LDL which can be recycled to the liver by the LDL receptor. The other component of this pathway is HDL. Produced by both the intestine and liver as a lipid free ApoA-I particle, HDL is formed in a multi-step process. Starting when ApoA-I recruits cholesterol from peripheral tissues via the ABCA1 transporter, the particle matures, collects more cholesterol from peripheral tissues via the ABCG1 transporter and then ultimately converts to a mature HDL particle as its free cholesterol is esterified to cholesterol ester by lecithin cholesterol acyltransferase (LCAT). Finally, HDL's cholesterol is taken up by the liver by way of the SR-BI receptor or by transfer to LDL and VLDL by the cholesterol ester transfer protein (CETP) (Rader and Daugherty 2008).

Studying Cholesterol Metabolism and Atherosclerosis in a Mouse Model

Mus musculus, commonly known as the laboratory mouse, is currently the most used animal model for studying atherosclerosis and its underlying pathways. This was not always the case, as there are major phenotypic differences between humans and mice that make studying

atherosclerosis in mice challenging. Notably, there are significant differences, both quantitatively and qualitatively, in cholesterol turnover between mice and humans (Dietschy and Turley 2002). First, LDL tends to be cleared at a much higher rate in mice versus humans and thus mice tend to have higher HDL versus LDL and VLDL, when compared to humans. This is considered to be anti-atherogenic as VLDL and LDL are considered to be the problematic apolipoproteins in regard to development of atherosclerosis and as such makes mice a more difficult model for studying the progression of cardiovascular disease (Ikonen 2006). Second, differences in lipoprotein composition and size in species of humans and mice has also been shown to effect the rate of atherosclerotic development (Veniant, Withycombe et al. 2001). Third, mouse livers can edit ApoB100 mRNA to produce and secrete ApoB48 labelled particles, a process only done in intestines in humans. Fourth, mice can degrade dietary cholesterol via LXR (discussed in subsequent chapters), a process humans cannot do due to promoter differences in the downstream LXR gene, Cyp7A1. Finally, mice do not express CETP (discussed in subsequent chapters). Therefore, researchers, through dietary or genetic manipulation, have realized ways to manipulate mouse baseline lipid levels to push the system to be pro-atherogenic.

The most common way to do this, is by knockout of the LDLR or ApoE genes (Ikonen 2006). Both genes are involved in lipoprotein

clearance as $LDLR^{-/-}$ affects LDL clearance and $ApoE^{-/-}$ affects remnant clearance. LDLR, expressed throughout the body, is the receptor for LDL. ApoE is a ligand found on both chylomicrons and VLDL and is involved in each particle's clearance from plasma. A study by Dansky *et al* further delineated that the C57Bl6 mouse strain is a more sensitive strain to the progression of atherosclerosis, then the FVB mouse line (Dansky, Charlton et al. 1999; Teupser, Tan et al. 2006). With this background in mind, one of the major aims of this thesis was the development of a C57Bl6 mouse knockout model of a gene called StARD4. StARD4 is an intracellular cholesterol transporter whose knockout, will hopefully shed insight on pathways and mechanisms that control cholesterol's fate intracellularly. The details behind the discovery and background for the StARD4 gene will be covered extensively in following sections.

The HDL Lipoprotein

Cholesterol is the main component of an HDL particle and there is an inverse correlation between atherosclerosis and plasma HDL levels cholesterol (Rader and Daugherty 2008). First identified in studies using ultracentrifugation to separate lipoproteins by density, HDL has evolved into one of the risk factors analyzed to assess overall cardiovascular risk by clinicians (Rader 2006). The most popular mechanistic explanation for HDL's anti-atherogenic role is its involvement in what has been termed reverse cholesterol transport (RCT). First proposed by Glomset *et al* in

1968, RCT encompasses a mechanism by which HDL facilitates the uptake of peripheral cholesterol and then carries this cholesterol to the liver for excretion into the bile (Glomset 1968). Furthermore, HDL's function has been expanded by *in-vitro* work to include anti-inflammatory, antioxidant, anti-thrombotic (Barter, Nicholls et al. 2004) and nitric oxide-inducing mechanisms (Mineo, Deguchi et al. 2006). For these reasons, HDL remains an attractive and highly researched lipoprotein for the development of novel therapeutics against atherosclerosis.

HDL Components: ApoA-I & ApoA-II

The biosynthesis of an HDL particle is complex. In plasma, nascent HDL consisting of ApoA-I phospholipid discs, attracts excess free cholesterol from membranes and HDL free cholesterol is esterified by the plasma enzyme LCAT. This changes the shape of the HDL particle to spherical with a core of cholesterol ester and a surface of ApoA-I (some particles also have ApoA-II) and phospholipids (Rader 2006). ApoA-I comprises the majority of the protein in a HDL particle, approximately 70% (Lewis and Rader 2005). It was shown in the Breslow laboratory by Andy Plump, that ApoA-I knockout mice have low levels of HDL (Plump, Azrolan et al. 1997). Furthermore, on a pro-atherogenic, ApoE $^{-/-}$ background, a human ApoA-I transgene was able to increase HDL and suppress atherosclerosis (Plump, Scott et al. 1994). Therefore, upregulation of endogenous ApoA-I has remained an attractive target for

the development of therapeutics to raise HDL. Only recently, has a small molecules advanced up unto phase II clinical trials to raise HDL levels via ApoA-I alterations (Resverlogix – RVX-208) and scientific research into the transcriptional regulation of ApoA-I remains an active area of research for the development of therapeutics against atherosclerosis. The other major component of HDL, ApoA-II, plays a bit more confounding role in HDL metabolism. Although only constituting about 20% of the HDL protein, its deletion in mice still leads to markedly decreased HDL levels; on the order of 60% lower (Weng and Breslow 1996). However, oddly enough, over-expression of ApoA-II raises HDL, but also increases atherosclerosis (Warden, Hedrick et al. 1993). This makes ApoA-II a more confusing target for study.

Lipid Acquisition and Particle Maturation

Newly secreted HDL must acquire phospholipids and cholesterol in order to mature. The first step in this process is lipidation of ApoA-I through the ABCA1 cholesterol pump found in peripheral tissues (Rader 2006). Genetic precedent for the importance of ABCA1 comes from Tangiers disease, whose genetic basis is a lack of ABCA1 and whose physiological phenotype includes low levels of HDL and ApoA-I as well as yellowed tonsils hepto-splenomegally due to cholesterol laden macrophages (Bodzioch, Orso et al. 1999). ABCAI knockout mice have phenotypes similar to patients with Tangier disease (McNeish, Aiello et al.

2000). Although ABCA1 is ubiquitously expressed, it seems that the majority of the lipidation of the nascent ApoA-I particle by ABCA1 takes place in the liver and intestines. While nascent particles acquire free cholesterol via ABCA1, more mature HDL particles use a different cholesterol pump, ABCG1 and there is evidence that other uncharacterized pathways, such as the role of SR-B1in reorganizing plasma membrane cholesterol, direct contact or limited diffusion might play a role in HDL particle maturation (Yancey, de la Llera-Moya et al. 2000; Rader 2006).

It is estimated that in mice, over 90 mg of cholesterol per kilogram of body weight is effluxed daily from extrahepatic tissues to the HDL particle (Dietschy and Turley 2002). However, the exact mechanism behind the lipidation of HDL particles remains a highly researched area. What is evident is that all extrahepatic cells require cholesterol, some of which can't be metabolized and thus the tissues require a mechanism for the efflux of cholesterol to occur. Thus from this basic understanding, it seems that large tissues such as skeletal muscle, adipose tissue and the skin would play large roles in contributing to the HDL particle (Rader 2006). This has been shown *in vitro,* as all of these cells lines have been shown to efflux cholesterol to ApoA-I and HDL particles.

Two other proteins that play a large role in the development of the HDL particle are phospolipid transfer protein (PLTP) and lecithin:cholesterol acyltransferase (LCAT). PLTP helps the HDL particle

acquire phospholipids from triglyceride rich particles; VLDL & LDL (Huuskonen, Olkkonen et al. 2001). LCAT, is responsible for esterification of cholesterol to cholesterol ester in the hydrophobic lipid core of the HDL particle. LCAT probably acts on surface cholesterol which upon esterification becomes the much more hydrophobic cholesterol ester. This changes the shape of the particle with the cholesterol ester migrating spontaneously into the core of a spherical particle. Mouse models that knockout either gene, result in reductions in plasma HDL levels. Thus enhanced expression of these 2 genes are legitimate targets for novel HDL raising therapies (Rietra, Slaterus et al. 1978) (Kuivenhoven, Pritchard et al. 1997).

HDL Catabolism: SR-BI & CETP

The major site for uptake of the HDL particle is the liver. The best described mechanism for this process is mediated by the scavenger receptor class BI (SR-BI). SR-BI is responsible for what has been termed selective uptake; the uptake of HDL esterified cholesterol, without subsequent degradation of the HDL particle itself (Trigatti, Rigotti et al. 2000; Rader 2006). Interestingly and in accordance with SR-BI's hypothesized role as an overall regulator of RCT, mouse knockouts of SR-BI show increased HDL levels and over-expression mouse models show a reduction in HDL levels (Zhang, Da Silva et al. 2005). Furthermore, mouse studies of hepatic over-expression of SR –BI on atherosclerotic backgrounds show a

reduction in HDL levels with a concomitant reduction in atherosclerosis (Ueda, Gong et al. 2000). However, to date there is very little direct evidence in humans for the role of SR-BI and HDL in atherosclerosis. No SR-BI deficient patients have so far been reported and there are but a few genetic polymorphisms of the SR-BI gene (*SCARBI*) which in general have not been shown to be associated with HDL levels (Osgood, Corella et al. 2003).

An alterative pathway for HDL catabolism is mediated by the cholesterol ester transfer protein (CETP). CETP's role is to transfer triglycerides from apoB-containing lipoproteins and exchange them with cholesterol esters from the HDL particle (Rader 2006; Tall 2007). Humans genetically deficient in CETP, were discovered in Japan and have extremely high levels of HDL cholesterol and reduced ApoA-I catabolism (Brown, Inazu et al. 1989). In cholesterol ester turnover studies in humans, the majority of the excreted biliary cholesterol was first found to be transferred to apoB-containing lipoproteins, presumably by CETP (Schwartz, VandenBroek et al. 2004). For these reasons, inhibiting CETP in humans became an attractive target for drug development, and one such inhibitor, Torcetripib, has been tested in clinical trials. As hypothesized, Torcetripib increased HDL cholesterol levels by 50%, but unfortunately also increased the incidence of myocardial infarctions comparable to placebo (Clark, Sutfin et al. 2004). These results may have been

confounded by off-target effects of the drug, such as raising blood pressure, but also raise the possibility that inhibition of CETP may have impeded reverse cholesterol transport and this mechanism might have been detrimental.

A better mechanism for raising HDL cholesterol levels would be to increase the synthesis of its principal apolipoprotein ApoA-I. This would both increase the favorable effects of HDL on the vasculature and increase reverse cholesterol transport. A worthy goal would be to mimic the increase of ApoA-I production in transgenics due to copy number, by developing a method to increase ApoA-I production pharmacologically.

Transcriptional Control of ApoA-I

One method of increasing plasma ApoA-I and HDL cholesterol levels would be to increase ApoA-I synthesis in liver and/or intestine. This could be done via increased ApoA-I gene transcription and many studies have appeared in the last ~20 years on the cis- and trans- elements that regulate ApoA-I transcription. The human ApoA-I gene is located at chromosome 11q23 at 116 MB. It is in a complex with three other apolipoprotein genes from proximal to distal; ApoA-I, ApoC-III, ApoA-IV and ApoA-V (Malik 2003). The ApoC-III gene is in the opposite orientation of the ApoA-I and ApoA-IV genes (Malik 2003). Each of these genes has its own liver regulatory element in the proximal promoter, but there appears to be a single intestinal enhancer for all three genes at ~

550bp up-stream of the ApoC-III start site. For the ApoA-I gene many studies have shown the proximal promoter liver regulatory element to be between 220-110bps from the start of transcription (Ginsburg, Ozer et al. 1995). Multiple transcription factors have been shown to bind to different regions within this cis-element. Mutational analysis has revealed that maximal ApoA-I liver expression depends on the integrity of the whole region, suggesting a level of interaction between transcription factors. Examples of transcription factors that play some role in regulation of ApoA-I are shown in figure 1.4. Of these, HNF-4α appears to be the most important in maintaining hepatocyte expression (HNF-4 is also enriched in intestine) (Malik 2003). In mice with *hnf4*$^{-/-}$, developed using tetraploid embryo complementation (*hnf4*$^{-/-}$ are embryonic lethal) to allow for normal fetal liver development, the *hnf4*$^{-/-}$ livers have abolished ApoA-I expression (Li, Ning et al. 2000). Additionally, expression of ApoA-I in hepatic and intestinal cell cultures was greatly diminished when the cells were transfected with an expression vector encoding a dominant-negative HNF-4 (Fraser, Keller et al. 1997). Although not with the consistency of HNF-4, some data suggest the proximal promoter region -220 to -110 also binds FoxA/HNF-3 (see diagram of the -220 to -110 region in figure 1.4). How FoxA/HNF-3 and HNF-4 might interact is not clear. Interestingly, the three dimensional structure of FoxA/HNF-3 resembles a globular domain of the linker histone H5. This suggests that FoxA/HNF3 might affect ApoA-I

transcription by interacting with a nucleasome binding domain, thereby mediating epigenetic modulation of ApoA-I gene expression (Malik 2003).

A)

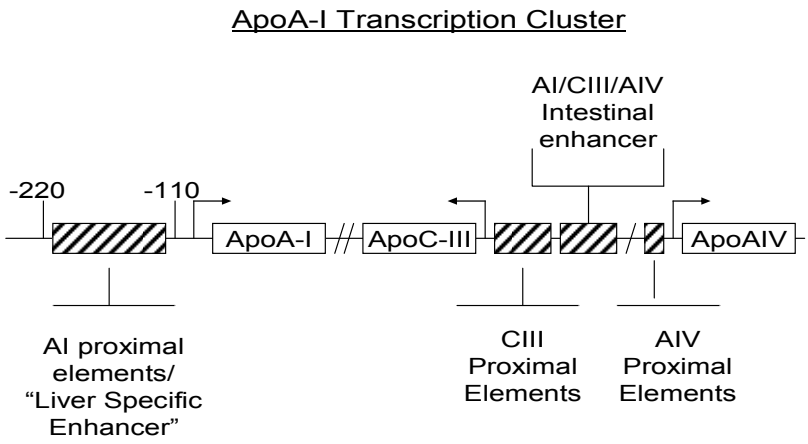

B)

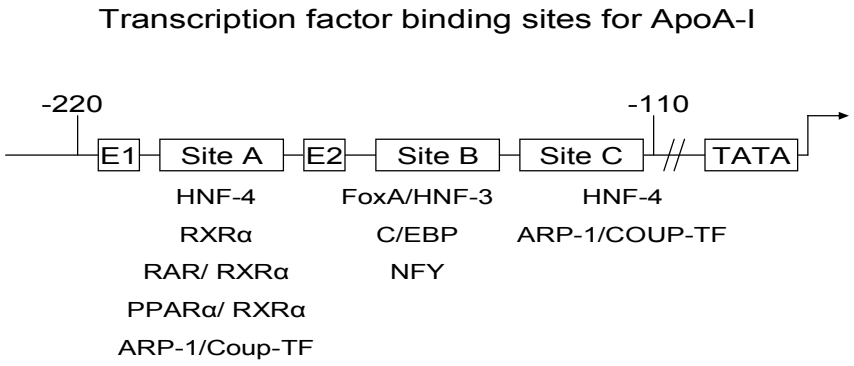

Figure 1.4 - ApoA-I Transcription Cluster & Associated Transcription Factors
A pictorial representation of the ApoA-I/ApoC-III/ApoAIV gene cluster and their associated promoter/enhancer elements. All three genes share an intestinal element, while each has a unique liver promoter region. B) An enlarged image of region -220 to -110 with all reported associated transcription factor binding sites. The most influential of these factors appears to be HNF-4, which binds both Site A and Site C (Malik 2003).

Epigenetics

Epigenetics is a term that defines all meiotically and mitotically heritable changes in gene expression that are not coded in the DNA sequence itself (Egger, Liang et al. 2004). These modifications can take place on the DNA sequenece itself or on the protein elements that package DNA into chromasomes. These proteins are called histones and they package and wind the DNA such that the DNA forms a spool around the histone proteins to compact the DNA sequence into chromatin and eventually chromosomes. Three systems, DNA methylation, histone modification and RNA silencing are the most common forms of epigenetic regulation. A perturbation in any one of these systems can lead to inappropriate or novel expression/silencing of genes and produce distinct phenotypes. The possible implications of this are broad for the development of treatments involving activation of beneficial genes or silencing of harmful ones. This is currently receiving great attention in the cancer field, notably in attempts to activate or reactivate tumor suppressor genes (Hong, Moorefield et al. 2007). Epigenetics is a relatively nascent field and it has yet to be comprehensively applied to other diseases, including atherosclerosis. In this regard, I thought an interesting potential thesis project would be to examine the epigenetic regulation of ApoA-I.

The only literature on the epigenetic regulation of ApoA-I is a series of papers published between 1989 and 1991 performed by the Razin group

in Israel in collaboration with the Breslow laboratory at Rockefeller University (Shemer, Eisenberg et al. 1991) (Shemer, Kafri et al. 1991) (Shemer, Walsh et al. 1990). These papers used methylation-specific restriction enzymes, the only technique available at the time, to study DNA methylation of the ApoA-I gene in various tissues of C57BL/6J mice and relate the patterns observed to whether or not the gene was actually expressed. They showed that in expressing tissues, like liver and intestine, the ApoA-I proximal promoter region was unmethylated, whereas in non-expressing tissues like kidney, sperm and leukocytes this region was methylated (Shemer, Walsh et al. 1990). In contrast, in all tissues the 3'-end of the ApoA-I gene was hypomethylated, except for intestine where it was partially methylated (Shemer, Eisenberg et al. 1991). Furthermore, in a mouse model expressing the human ApoA-I transgene only in the liver, but not any other tissue, hypomethylation of the human ApoA-I proximal promoter region was limited to liver with full methylation in other tissues including the intestine. Interestingly, the neighboring genes CIII and A-IV also show DNA-methylation patterns that correspond with expression (Shemer, Eisenberg et al. 1991). ApoC-III is expressed primarily in the liver and ApoA-IV in the intestine. Accordingly, the 5' promoter region of ApoC-III is demethylated in the liver, whereas, the 5' promoter region of ApoA-IV is demethylated in the intestine. In summary, for the adjacent ApoA-I, C-III, A-IV genes, promoter DNA demethylation corresponded to

high expression and partial or full methylation to low or background expression (Shemer, Eisenberg et al. 1991).

In the approximately 20 years since the Razin/Breslow papers were published there have been major improvements in epigenetic technology and understanding of molecular mechanisms and key players involved in histone modifications and epigenetic regulation (Jenuwein and Allis 2001). For this reason, as part of my thesis work, I revisited the original DNA methylation experiments with greatly improved modern technology. I also examined the role of histone methylation and the histone code (not known at the time of the original experiments) in regulating ApoA-I gene transcription. Especially with regard to the latter, I hoped to discover new aspects of the regulation of ApoA-I transcription that could be exploited to develop therapies to raise HDL levels.

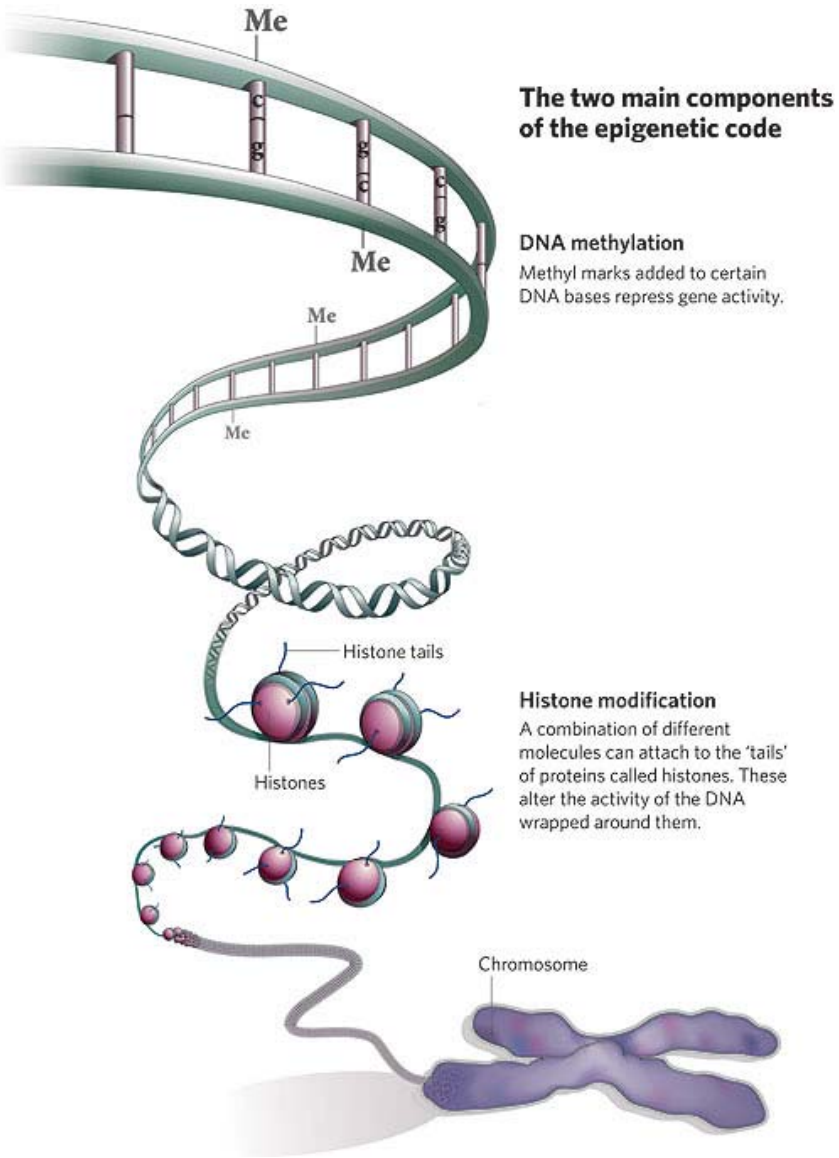

Figure 1.5 - Representation of the Two Major Epigenetics Modifications
Epigenetics represents of the modifications of DNA not coded by the genetic code. The two major examples shown above are DNA methylation and histone modification. Both exert their influence at differing times. Methylation occurs on the actual DNA strand, while the histone modifications occur after DNA has wrapped itself into the nucleosome structure and then has its associated protruding histone tails. All these histones, eventually wrap into more complex 3-dimensional structures to become chromosomes (Qiu 2006).

Histone Code Determination

The histones that make up a nucleosome are subject to many forms of modification including, methylation, acetylation, phosphorylation,

ubiquitination and sumoylation (Bernstein, Meissner et al. 2007). However, these modifications appear to have a level of order to them; occurring at specific sites that make up what has become known as the histone code (Tomasetto, Regnier et al. 1995; Jenuwein and Allis 2001). Although the roles of many of these modifications are not fully understood, there is some insight into how histone N-terminal tail lysine acetylation and methylation regulate gene expression. In general, histone N-terminal tail lysine acetylation appears to be associated with transcriptional activation. This may be due to neutralization of the positively charged histone lysines causing loosening of their attachment to the negatively charged DNA, thereby allowing for transcription factor insertion and gene activation (Bernstein, Meissner et al. 2007). It appears that histone lysine methylation is more complicated as its effects on transcription appear to be residue and modification dependent. In model organisms, it was shown for several genes, that tri-methylation of histone H3 lysine 4 (H3K4) activates, whereas tri-methylation of histone H3 lysine 27 (H3K27) represses transcription (Hake and Allis 2006). These modifications and control mechanisms have never been described for the ApoA-I gene and therefore as part of my thesis, I attempted to map the, "epigenetic framework" of the ApoA-I gene.

Histone Code Modification

The acetylation and deacetylation of the histone tails is catalyzed by histone acetyltransferases (HAT) and histone deacetylases (HDACs), respectively. Over time, it was revealed that many of the histone acetyltransferases were previously identified as transcriptional co-activators that are recruited to genes by sequence specific transcriptional activators (Moggs and Orphanides 2004). This suggested a novel role for transcriptional activators; namely the recruitment of factors to alter chromatin structure. The key role of these chromatin alterations is illustrated in the way that xenobiotics target nuclear receptors and alter gene expression. For example, peroxisome proliferators, dioxins and estrogenic chemicals act via the peroxisome proliferator-activated receptor-α, aryl hydrocarbon receptor and estrogen receptor, respectively (Moggs and Orphanides 2004). These factors seem to induce alterations in chromatin structure that allow RNA polymerase II and its associated helpers to access the gene that needs to be transcribed. The molecular mechanism for this process has been well studied for the estrogen receptor-α (ERα) (Moggs and Orphanides 2001). Ligand binding to ERα induces conformational changes that allow for 40-50 co-regulatory proteins to bind specific estrogen response element sequences near or within the ERα target genes.

Some of the co-regulators include nucleosome remodeling enzymes like BRG1 and BRM1 and histone-modifying enzymes like HAT, HDAC1 and HDAC7 that ultimately allow de-compaction of local chromatin structure. HDAC inhibitors such as Trichostatin A (TSA) or SiRNAs targeted to some of these HATs or HDACs could be used to perturb the histone code. More specifically, this might help us understand that key switches that regulate the on versus off activity of the ApoA-I promoter. These specific histone markers might then be pharmacologically targeted to increase apoA-I expression and raise HDL cholesterol levels.

Cholesterol's Role in Regulation of Gene Expression

Cholesterol has the ability to regulate its own homeostatic balance at the transcriptional level by effect one of three pathways: the sterol regulatory element binding protein (SREBP) pathway, the liver X receptor pathway (LXR) or the unfolded protein response (UPR)/ endoplasmic reticulum (ER) stress pathway. Each pathway will be discussed thoroughly in the next sections.

The SREBP Pathway

The mechanisms that regulate the *de novo* synthesis, uptake and oxidative catabolism of lipids, involves a family of ER membrane associated transcription factors termed sterol regulatory element binding proteins or SREBPs (Raghow, Yellaturu et al. 2008). As the regulation itself is intrinsically complicated, these transcription factors are subject to

various levels of feedback/feed-forward regulation at the transcriptional, translational and post-translational level.

The SREBP family of basic helix-loop-helix-leucine zipper (bHLH-LZ) transcription factors is comprised of SREBP-1a, SREBP-1c and SREBP-2 encoded by two genes *SREBP-1* and *SREBP-2* (Raghow, Yellaturu et al. 2008). SREBP-1a and SREBP-1c differ only in the length of their N-terminal binding domain, which occurs due to the use of alternate promoters for the transcription of each (Eberle, Hegarty et al. 2004). More importantly, the genes, SREBP-1a, SREBP-1c and SREBP-2 differ in their tissue specificity and target gene selectivity, which conveys each protein with a unique role (Espenshade 2006). SREBP-1a and SREBP-1c regulate genes involved in the synthesis of monounsaturated and polyunsaturated fatty acids and their ultimate incorporation into triglycerides and phospholipids. In contrast, SREBP-2's role is primarily focused on activating genes involved in the uptake and biosynthesis of cholesterol (Espenshade 2006). SREBP-1c is predominantly localized to the liver, while the other two are expressed fairly ubiquitously. SREBP's are known to regulate over 30 genes involved in various aspects of uptake and synthesis of cholesterol, fatty acids, triglycerides and phospholipids (Horton, Goldstein et al. 2002).

The SREBP family members are localized to the ER as inert membrane proteins after synthesis (Goldstein, DeBose-Boyd et al. 2006).

In this state, they are an approximate 1150 amino acid precursor protein, depending on which SREBP, containing two hydrophobic membrane spanning regions separated by a short hydrophilic loop that projects into the lumen of the ER. The N-terminal binding domain and the C-terminal regulatory domain both project into the cytoplasm (figure 1.6). When sterols are replete, a protein called SREBP cleavage-activating protein (Kanno, Wu et al.) binds cholesterol and assumes a conformation that allows SREBP to bind the ER protein insulin induced gene (Insig) (Peng, Schwarz et al. 1997). This binding, prevents SREBP-SCAP interaction with Coat protein complex-II (COPII) membrane vesicle formation and ultimately stops the translocation of this transcription factor to the Golgi (Raghow, Yellaturu et al. 2008). In this sense, SCAP, which contains a sterol sensing domain similar to HMGCR, acts as a sensor for membrane cholesterol levels (Goldstein, DeBose-Boyd et al. 2006). In the opposite situation, when the cell is in a cholesterol depleted state, SCAP dissociates from Insig, allowing for the translocation of the SCAP-SREBP complex from the ER to the Golgi (Raghow, Yellaturu et al. 2008). As a built in feedback loop, oxysterols, cholesterol derivatives, interact with Insig in such a way that it will bind SCAP and prevent the translocation of the SCAP-SREBP proteins (Raghow, Yellaturu et al. 2008).

Upon arrival to the Golgi, SREBPs undergoes two sequential proteolytic events, one mediated by the site 1 protease (S1P) extracellularly

and the other within the transmembrane domain by site 2 protease (S2P) (Espenshade 2006). This releases the N-terminal transcription factor domain from the membrane allowing for translocation of SREBPs, as a dimer, to the nucleus by importin β (Rawson 2003). Upon arrival to the nucleus, SREBPs binds to the sterol regulatory elements (SRE's) in the promoter of target genes and activates transcription. As a result, both cholesterol synthetic and cholesterol uptake genes are transcribed and the cell then replenishes its cholesterol stores and this then feeds back and inactivates SREBPs (Espenshade 2006). Further regulating this well balanced homeostatic cycle, is the half life of nuclear SREBP, as it is rapidly targeted for degradation in the nucleus.

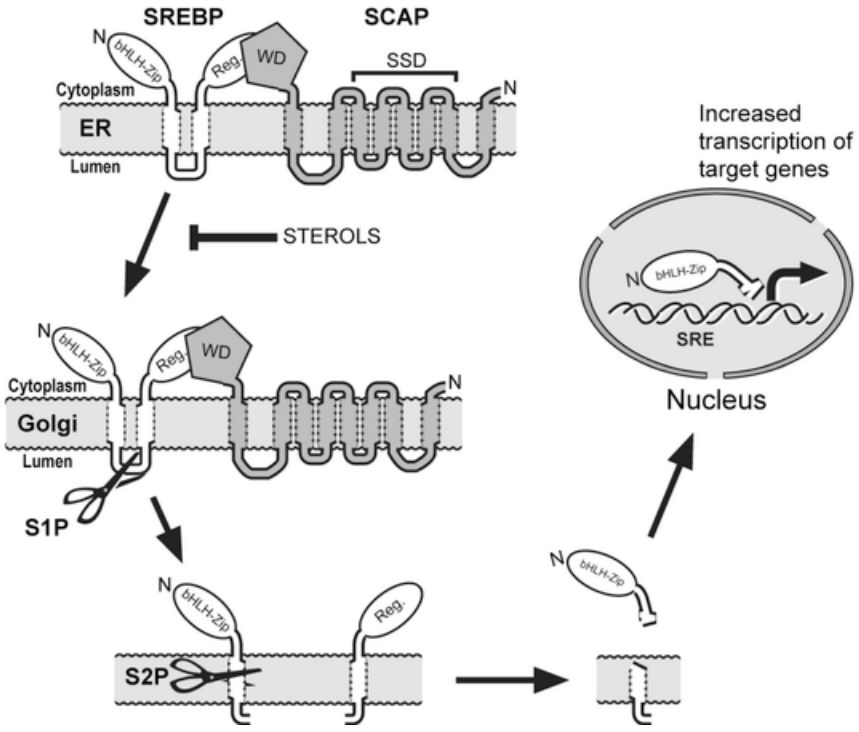

Figure 1.6 - SREBP Role in Cholesterol Regulation
Above is representation of the fate of the SREBP pathway. When sterols are high, SCAP through its SSD domain binds Insig (not pictured) and sequesters SREBP in the membrane of the ER. Upon sterol depletion, the SCAP-SREBP complex is allowed to move to the Golgi, where it is cut into its active precursor by two proteases, S1P and S2P. The shortened active form of SREBP is then moved to the nucleus where it activates transcription of genes involved in cholesterol synthesis and uptake.

The LXR Pathway

The second important family of transcription factors involved in cholesterol regulation of gene expression is liver X receptor or LXR. LXRs regulate genes involved in reverse cholesterol transport, dietary cholesterol absorption, bile acid metabolism, glucose metabolism and fatty acid biosynthesis (Repa and Mangelsdorf 2002).

The LXR receptor genes, LXR-α and LXR-β, are members of the nuclear hormone receptor superfamily of ligand-activated transcription

factors (Repa and Mangelsdorf 2002). Also known as NR1H3 and NR1H2 respectively, the proteins are composed of a central DNA-binding domain, consisting of a zinc-finger and a large lipophilic ligand binding core that binds its endogenous ligands, oxysterols and other intermediates of the cholesterol biosynthesis pathway (Tontonoz and Mangelsdorf 2003). As is alluded to in its name, LXR-α and LXR-β are most highly expressed in liver. However, while LXR-β is ubiquitously expressed, LXR-α's expression beyond the liver is restricted to the spleen, adipose tissue, lung and pituitary glands.

Interestingly, and one of the major reasons LXR's have become studied in the atherosclerotic research community, is LXR's role in inhibiting atherosclerosis. As stated before, mice are particularly resistant to forming atherosclerotic lesions. This is due to multiple variables, but one of them is the mouse specific up-regulation of a gene called cholesterol 7α hydroxylase (CYP7A1), the rate limiting enzyme in bile acid synthesis and a key component of RCT (Repa and Mangelsdorf 2002). CYP7A1, also happens to be the first gene described as an LXR target gene (Peet, Turley et al. 1998). Consistent with this anti-atherosclerotic role, $LDLR^{-/-}$ or $ApoE^{-/-}$ mice fed agonists for LXR show significant reduction in the size of their atherosclerotic lesions (Claudel, Leibowitz et al. 2001; Joseph, McKilligin et al. 2002). Further investigation into the effect of LXR on atherosclerotic development led researchers to discover LXR's role is most

widely exerted in macrophages. This was well exemplified when researchers conducted a bone marrow transplant experiment. First endogenous monocytes and macrophages from LDLR$^{-/-}$ and ApoE$^{-/-}$ mice were irradiated and destroyed (Tangirala, Bischoff et al. 2002). Subsequently, the mice received bone marrow transplants from either WT, LXR-$\alpha^{-/-}$ or LXR-$\beta^{-/-}$ mice to replace the lost macrophages and monocytes. The bone marrow and thus the macrophages from LXR-$\alpha^{-/-}$ or LXR-$\beta^{-/-}$ transplants were less functional compared to wild-type, amassing larger plaque lipid droplets. Furthermore the mice who received their bone marrow from LXR-$\alpha^{-/-}$ or LXR-$\beta^{-/-}$ mice had significantly greater atherosclerotic lesions when compared to the mice transplanted with WT bone marrow (Tangirala, Bischoff et al. 2002).

On a molecular level, upon ligand binding, LXRs undergo a conformational change that allows it to bind retinoid X receptor (RXR) which acts as a heterodimer to activate transcription of selected genes (Repa and Mangelsdorf 2002). In contrast to SREBP, LXR is expressed when endogenous cholesterol levels are high. Ligands for LXR have been identified as oxysterols, as well as glucose and D-glucose-6-phosphate (Repa and Mangelsdorf 2002; Mitro, Mak et al. 2007). Among oxysterols, 22(R)-hydroxycholesterol, 24(S)-hydroxycholesterol and 24(S), 25 epoxycholesterol have been identified as high affinity ligands for LXR (Lala, Syka et al. 1997; Schoonjans, Brendel et al. 2000; Fu, Menke et al.

2001). Interestingly, 27-hydroxycholesterol, the most abundant oxysterol in plasma is only a weak activator of LXR. Additionally, synthetic, non-steroidal LXR-selective agonists exist like T0314407, T0901317, GW3965 (Collins, Fivush et al. 2002).

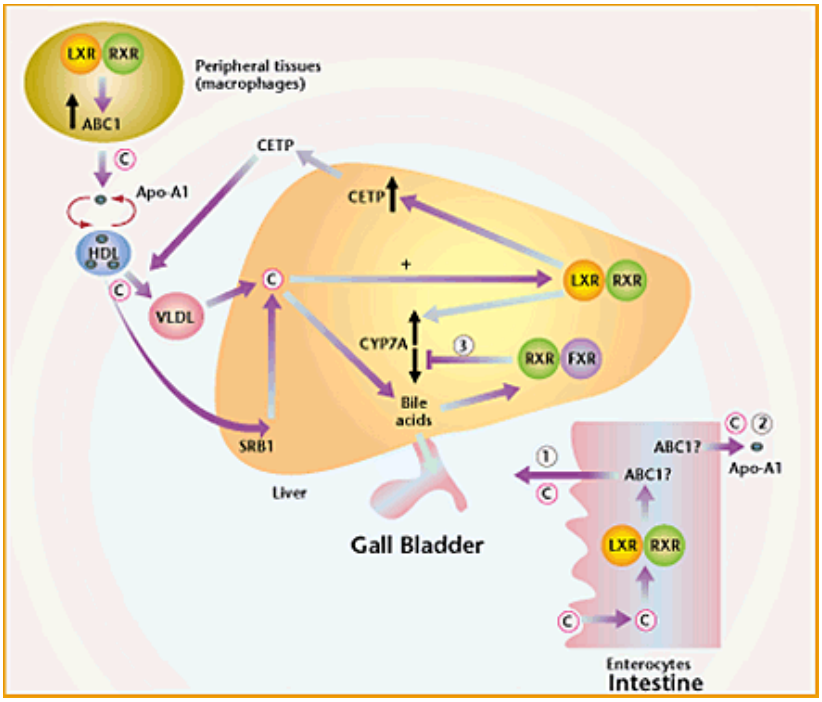

Figure 1.7 - Roles of LXR in the Liver, Peripheral Tissue and Intestine. Nuclear hormone receptors (LXR and RXR) coordinate reverse cholesterol transport from peripheral tissues to the liver allowing for cholesterol conversion into bile acids and cholesterol excretion in the intestine. As described, they help by activating expression of the cholesterol transporter ABC1 in cholesterol loaded peripheral cells, notably macrophage foam cells, leading to enhanced efflux of free cholesterol and the eventual formation of mature HDL. Additionally, LXR's up-regulate CETP, CYP7A1, LPL, PLTP SR-B1 and other genes involved in RCT and eventual excretion of cholesterol through the intestine and out of the body (Tall, Costet et al. 2000).

LXRs also act as regulators of hepatic lipogenesis and glucose metabolism. LXRs enhance SREBP-1c expression which can lead to hypertriglyceridemia (Schultz, Tu et al. 2000). Additionally, treatment of mice with synthetic LXR ligands can cause hepatic steatosis (Schultz, Tu et al. 2000). LXR's can activate glucokinase, phosphoenolpyruvate carboxykinase and glucose-6-phosphatase, thus decreasing hepatic glucose output and increasing hepatic glucose utilization (Jamroz-Wisniewska, Wojcicka et al. 2007). It has even been shown that LXRs have anti-inflammatory activity, repressing genes like iNOS, Cox2, IL-6, IL-1, βMCP-1, MCP-3 and MMP9 after LPS, TNF-α or IL-1-β stimulation (Yan and Olkkonen 2008).

Unfolded Protein Response / Endoplasmic Reticulum Stress Response

The ER is the repository of nearly 50% of cellular membranes, a major site of calcium storage, the major location of sterol and lipid synthesis and the site of protein synthesis. The ER plays a critical role in sensing cellular homeostasis (Schroder 2008). Crucial to the cell, is that only properly folded and modified proteins are exported from the ER to the Golgi, while all other mishaps in protein production are degraded. Three major pathways have been elucidated that can disrupt this process and induce the unfolded protein response (UPR) or ER stress response. They are the generation of reactive oxygen species (Gross, Wan et al.), excessive secretory protein synthesis and cholesterol overloading of the ER (Shen,

Zhang et al. 2004). The UPR is characterized by the activation of three transmembrane proteins, PKR-like ER protein kinase (Bartz, Kern et al.), inositol requiring enzyme 1 (IRE-1) and activating transcription factor 6 (ATF6) (Foufelle and Ferre 2007).

Mechanistically, these factors are regulated in a similar manner to the SREBP proteins. Normally bound to Bip/GRP78, an ER chaperone protein, the three proteins are sequestered to the ER membrane (Kaufman, Scheuner et al. 2002). However, BiP binds to misfolded proteins, which then allows for the release of PERK, IRE-1 and ATF6. Perk, phosphorylates elf2α, attenuating translation of most mRNAs (Fels and Koumenis 2006). IRE-1 homodimerizes and undergoes autophosphorylation which eventually leads to splicing of XBP1 (Foufelle and Ferre 2007). ATF6 translocates to the Golgi and eventually shuttles to the nucleus to activate expression of genes involved in the UPR response (Haze, Yoshida et al. 1999).

The initial phase of the UPR focuses on recovery. The three proteins orchestrate a symphony of changes that include, increasing the ER folding capacity by increasing the ER synthesis of phospholipids and re-esterifying sterols. Additionally, they down-regulate the overall load on the ER, by decreasing overall transcription and translation (Foufelle and Ferre 2007). However, if all the countermeasures fail, apoptotic pathways are eventually activated to eliminate the perceived unhealthy cell. It is this eventual fate

that has implicated UPR in disease such as atherosclerosis, diabetes and neurodegenerative diseases (Marciniak and Ron 2006; Scheper and Hoozemans 2009).

Accumulation of free cholesterol in the ER is a known activator of the UPR (Tabas 2002). Normally the cell does not experience this difficulty, due to the activity of ACAT, but in atherosclerosis these mechanisms are overwhelmed and the UPR is activated. Specifically, macrophages in plaques start accumulating excess free cholesterol via scavenger receptors whose expression is independent of cellular cholesterol status (Zhou, Lhotak et al. 2005). Initially, the UPR enhances cell survival, but eventually the intracellular free cholesterol is too great and the cell undergoes apoptosis exacerbating the progression of atherosclerosis (Zhou, Lhotak et al. 2005).

Intracellular Cholesterol Transport

Cholesterol is essential for mammalian cell membranes, but the cholesterol:protein ratio varies considerably between membranes (Ikonen 2008). Cholesterol is enriched in the plasma membrane (PM), where it constitutes 20% to 45% of lipid molecules (Maxfield and Wustner 2002). It is also abundant in the endocytic recycling compartment and in the Golgi, especially the *trans*-Golgi compartments (Mukherjee, Zha et al. 1998). In contrast, the other major membrane constituent of the cell, the ER, which has already been described as a major player in cholesterol regulation, has a

low cholesterol content, estimated at approximately 1% of total cellular cholesterol (Lange 1991). Interestingly, the membranes of the ER and PM are close to equal in area, but yet still have striking differences in cholesterol concentration (Liscum and Munn 1999). It is these contrasting characteristics of the ER, be its involvement in sterol homeostasis, ranging from controlling signaling pathways such as SREBP and the UPR discussed previously to regulating its own surprisingly low cholesterol levels, that spur the interest of the researcher community in intracellular cholesterol sorting.

The exact mechanisms responsible for creating and maintaining this drastic difference in membrane cholesterol levels has not been determined. However, transport and sorting mechanism must exist to include or exclude cholesterol from organelles. Understanding this is crucial to understanding overall sterol homeostasis and ultimately relates back to questions concerning the development of atherosclerosis (Soccio and Breslow 2004).

It has been known for some time that cholesterol is transferred between intracellular compartments by both vesicular and non-vesicular mechanisms (Soccio and Breslow 2004). Vesicular trafficking, is a mechanism for moving membrane components and luminal cargo between subcellular organelles along cytoskeletal tracks in an ATP dependent manner (Mobius, van Donselaar et al. 2003; Ikonen 2008). Disruption of the cytoskeleton with Brefeldin A or depleting ATP with metabolic poisons

have both been shown to disrupt intracellular sterol transport by vesicular mechanisms (Prinz 2007).

In contrast, there is also evidence that cholesterol is transported by non-vesicular mechanisms. This includes transportation of cholesterol by cytosolic lipid transfer proteins or directly, by membrane contact. Blocking vesicular pathways up to as high as 90%, does not significantly alter the cholesterol gradient across the organelles, suggesting that a non-vesicular mechanism may play an important role in compensating the cellular cholesterol trafficking (Prinz 2007). Further highlighting the proposed role for non-vesicular cholesterol trafficking, there are no known vesicular methods for transferring cholesterol between various cellular compartments and the mitochondria; the location of steroid synthesis. This also holds true for movement of sterols between intracellular organelles and lipid droplets, lipid storage depots consisting of a core of sterol esters and triglycerides (Prinz 2007). Therefore, it seems that there is much to be learned about the non-vesicular pathways of transport and its role in cholesterol movement intracellularly.

Non-vesicular transporters or cytosolic lipid transfer proteins are proteins that contain a hydrophobic pocket, providing shelter for a hydrophobic cholesterol molecule as it travels through the hydrophilic cytosol. These proteins fall into five families. The following sections will cover these families in depth, starting with the niemann pick C proteins and

then proceeding to the caveolins, the oxysterol binding protein-related proteins, the sterol carrier protein 2 and ending with an extra emphasis given to the steroidogenic acute regulatory-related lipid transfer domain proteins, of which one member, StARD4, is the basis of much of the work done in this thesis.

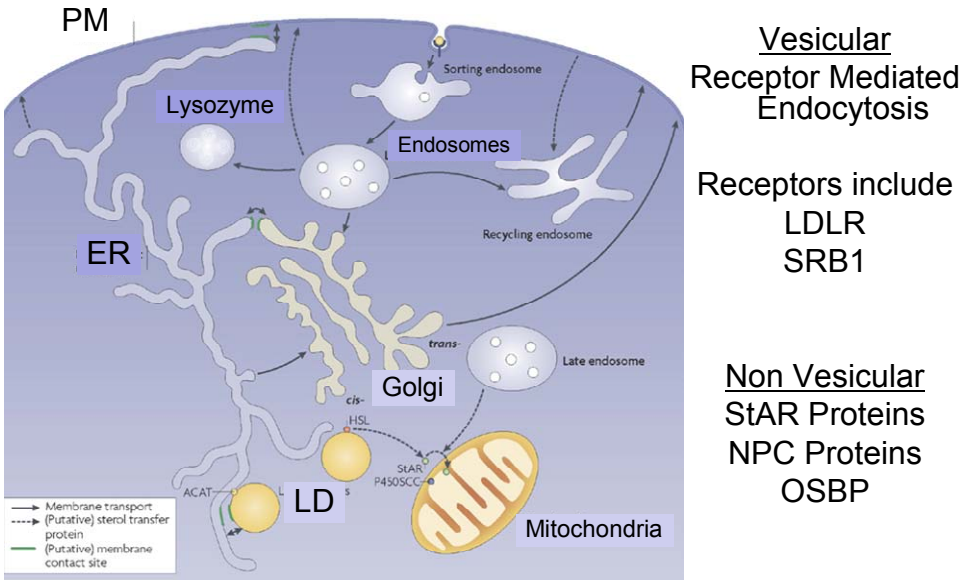

Figure 1.8 – Vesicular and Non-Vesicular Intracellular Cholesterol Transport. Cholesterol has two mechanisms by which it can travel through the hydrophilic cytosol, vesicular and non vesicular. Vesicular encompasses the classical pathways involved in receptor mediated endocytosis exemplified by the absorption of an LDL particle. Non vesicular is protein mediated by families of proteins such as the StAR proteins.

Niemann Pick C Proteins

Niemann Pick Type C (NPC) is a fatal neurodegenerative disease, that is an autosomal recessive lipid storage disorder characterized by

intracellular free cholesterol accumulation in late endosomal/lysosomal cellular compartments (Soccio and Breslow 2004). Mutations in either of the genes, NPC1 or NPC2 is the genetic cause for the disease (Sturley, Patterson et al. 2004). NPC1 is a late endosomal membrane protein with 13 predicted transmembrane segments, including a sterol sensing domain (Prinz 2002). NPC2 is a soluble cholesterol-binding protein in the lumen of late endosomes and lysosomes (Naureckiene, Sleat et al. 2000). Evidence points to a role for the two proteins in the pathway necessary for trafficking LDL derived cholesterol out of lysosomes (Sleat, Wiseman et al. 2004). Strangely, although NPC2 has been shown to bind cholesterol with a stoichiometery of 1:1, the structure of NPC2 has been solved and appears to be too small to accommodate a cholesterol molecule(Friedland, Liou et al. 2003; Ko, Binkley et al. 2003). A recent paper by Brown and Goldstein, reveals, by elucidation of the structure NPC, the process by which the NPC1 and NPC2 transfer cholsterol. The working model is that after lysosomal hydrolysis of LDL cholesterol esters, cholesterol binds NPC2, which transfers it to NPC1 N-Terminal domain, reversing its orientation and allowing insertion of its isooctyl side chain into the outer lysosomal membrane (Kwon, Abi-Mosleh et al. 2009).

Although most models of NPC involve defective or slowed transport of cholesterol away from late endosomes, the precise mechanisms controlling the process are unknown. The two main components of lipid

rafts, cholesterol and sphingomyelin, have high affinity for one another and accumulation of one can cause accumulation of the other (Simons and Gruenberg 2000). In concordance, NPC1 deficient neurons store a greater amount of sphingomyelin than cholesterol (Gondre-Lewis, McGlynn et al. 2003). However, work in NPC1 deficient mice show neuronal accumulation of cholesterol (Reid, Sakashita et al. 2004). Alternatively, it is possible that NPC1/2's protein mutations cause general late endosome problems. This is supported by over-expression studies done with Rab7 and Rab9, two GTPases involved in late endosomal function, that can correct the cholesterol and sphingomyelin accumulation associated with NPC cells (Choudhury, Dominguez et al. 2002). On an atherosclerotic background, $ApoE^{-/-}$ mice whose macrophages are homozygous for NPC1 deficiency have larger lesions with evidence of arterial medial degradation and atherothrombosis (Welch, Sun et al. 2007).

The Caveolins

Caveolins are abundant membrane proteins associated with cholesterol and sphingomyelin (Prinz 2007). When caveolins oligomerize, they form caveolae; cholesterol and sphingomyelin rich flask shaped membrane invaginations found in some cells. Caveolins are likely to play important roles in cholesterol homeostasis and distribution (Parton and Simons 2007). It has been suggested that caveolins transport cholesterol from the ER to the PM as a part of complex, much like a plasma

lipoprotein, with heat shock protein 56, cyclophilin A and cyclophilin 40 (Prinz 2007). However, the exact role of caveolins in cholesterol transport remains debated.

There are three caveolins; 1, 2 and 3. Caveolins are located on the cytoplasmic side of caveolae and serve as structural components of caveolae and as scaffolding proteins for various signaling molecules (Cohen, Hnasko et al. 2004). Surprisingly, given caveolin-1's role in caveolae formation, caveolin-1 mouse knockouts are viable with normal lipid profiles (Drab, Verkade et al. 2001). Bred onto the atherosclerotic background, caveolin-$1^{-/-}$ $ApoE^{-/-}$ double knockout mice have reduced atherosclerosis despite higher levels of plasma non-HDL cholesterol and triglycerides (Frank, Lee et al. 2004). It might be that caveolins play a role in uptake of cholesterol in macrophages, explaining the reduction found in the atherosclerosis mouse model, however much more is needed to be done to elucidate the role of the caveolins in the intracellular non vesicular pathways.

Oxysterol Binding Protein (OSBP) – Related Proteins (ORPs)

OSBP was initially identified because it binds oxysterols, oxygenated cholesterol derivatives and regulators of cholesterol metabolism (Kandutsch and Shown 1981). ORP's are part of a large family of lipid binding proteins related to OSBP, of which there at least 12 members, that play numerous roles including lipid distribution and

metabolism, cell signaling and vesicular transport (Prinz 2007). Structurally, ORP's contain the C-terminus lipid binding domain with the signature OSBP motif, EQVSHHPP. The N-terminus is variable and contains a range of motifs like FFAT, pleckstrin homology or an anykrin repeats. Alternative splicing of the ORPs is common and results in long and short forms of the proteins with different subcellular localizations and binding specificities. A large amount of the work on ORPs has been done in yeast *S. cerevisiae*, which has seven OSH (OSBP homolog) proteins (Prinz 2007). Yeast mutants for any one of the seven OSH genes have little to no defect in PM to ER sterol transfer suggesting a level of redundancy (Raychaudhuri, Im et al. 2006). However, conditional deletion of all seven genes slows exogenous sterol transport, causes vacuolar fragmentation and accumulation of lipid droplets ultimately ending in cell death (Beh, Cool et al. 2001; Beh and Rine 2004)

Unfortunately, little is known about the mammalian ORPs and whether they work as sterol transfer proteins is yet to be elucidated. ORPS are made up of six subfamilies based on sequence homology. They are OSBP and ORP4, ORP1/2, ORP/8, ORP3/6/7 and ORP 9/10/11. OSBPs localize to the cytoplasm, but relocate to the Golgi upon treatment with 25-hydroxycholesterol (Fairn and McMaster 2008). Over-expression of OSBP increases cholesterol and sphingomyelin synthesis, while RNAi knockdown shows no change in cholesterol or fatty acid synthesis (Fairn

and McMaster 2008). In mice, adenoviral over-expression of OSBP in liver leads to an increase in plasma VLDL and TG concentrations, due to an up-regulation of SREBP-1c (Yan and Olkkonen 2008). Other ORP's like Orp-1 have been shown to increase atherosclerotic lesions in an $LDLR^{-/-}$ mice when over-expressed in macrophages, suggesting a role in macrophage sterol metabolism (Yan and Olkkonen 2008). ORP2 over-expression in CHO or Hela cells causes up-regulation of cellular cholesterol efflux , decreased cholesterol esterification and reduced triglycerides (Laitinen, Lehto et al. 2002). Although the roles and characteristics of some of the other ORP's has been described, little is known about the role of these proteins *in-vivo* and there is much room for researchers to discover novel aspects of OSBP behavior and ultimately intracellular cholesterol transport.

Sterol Carrier Protein 2 (SCP-2)

SCP-2 is a small 13.3 kDA protein that is also called non-specific lipid transfer protein (nsLTP). The protein is formed by the cleavage of two other larger proteins, SCP-x and pro-SCP-2, both of which are encoded by the same gene with distinct promoters (Prinz 2007). Both proteins are made with a c-terminal peroxisomal targeting signal and are therefore likely involved in β-oxidation of fatty acids. As further evidence of this, mice lacking the gene for SCP-2 have defects in fatty acid oxidation (Seedorf, Raabe et al. 1998).

Additional implicated roles for SCP-2 include transport of sterols and other lipids between sub-cellular compartments. A fraction of SCP-2 is found in the cytoplasm and numerous studies have demonstrated that SCP-2 can transfer cholesterol between liposomes and/or membranes (Gallegos, Atshaves et al. 2001). Much additional work is needed in order to further elucidate the role of SCP-2 to elucidate its role in intracellular transport.

Steroidogenic Acute Regulatory-Related Lipid Transfer Domain Protein Family (StAR Protein Family)

StAR-related lipid transfer (START) domains are ~210 amino acid lipid binding domains implicated in intracellular transport, cell signaling and lipid metabolism. The first described member of the family was steroidogenic acute regulatory protein (StAR), which is responsible for transfer of cholesterol to the mitochondria in steroid producing cells (Stocco 2001). The human and mouse genomes each have 15 genes encoding start domains and further phylogenetic analysis divides the families into six subfamilies (Soccio, Adams et al. 2002). The X-ray crystal structures of MLN64, StARD4 and phosphatidylcholine transfer protein (PCTP) have all been solved. All three share a helix-grip fold with α-helices at the N and C terminus separated by nine β-sheets and two α-helices (Soccio, Adams et al. 2002). The following sections of the background will cover the START subfamilies in depth.

StARD name	Other names	Mouse	Human
StARD1	***StAR***	8, 24.5 Mb	8, 37.4 Mb
StARD2	***PCTP***	11, 90.7 Mb	17, 53.6 Mb
StARD3	***MLN64***, *es64, CAB1*	11, 99.1 Mb	17, 37.3 Mb
StARD4	*CRSP*	18, 33.4 Mb	5,110.5 Mb
StARD5	None	7, 73.3 Mb	15, 77.6 Mb
StaRD6	None	18, 70.8 Mb	18, 52.0 Mb
StARD7	*GTT1*	2, 128.3 Mb	2, 94.7 Mb
StARD8	*KIAA0189-RhoGAP*	X, 81.9 Mb	X, 64.1 Mb
StARD9	*KIAA1300*	2, 121.1 Mb	15, 38.4 Mb
StARD10	*PCTP*-like, *SDCCAG28, CGI-5*	7, 91.1 Mb	11, 74.8 Mb
StARD11	***GPBP***, *COL4A3BP*	13, 93.9 Mb	5, 73.5 Mb
StARD12	***DLC-1***, *Arhgap7, p122-RhoGAP*	8, 35.5 Mb	8, 12.7 Mb
StARD13	*GT650, 4902678-RhoGAP*	5, 150.3 Mb	13, 31.7 Mb
(*StARD14*)	***CACH***	13, 88.9 Mb	5, 80.8 Mb
(*StARD15*)	***THEA***, *BFIT, KIAA0707*	4, 104.5 Mb	1, 54.8 Mb

Table 1.1 - Nomenclature and Chromosomal Locations of the START Genes
All human START genes except *CACH* and *THEA* have been assigned formal names of *StARD1—StARD13*, but some common names are widely used. Physical map positions (chromosome, position in megabases) in the mouse and human genomes are based on the Ensembl data base (www.ensembl.org)

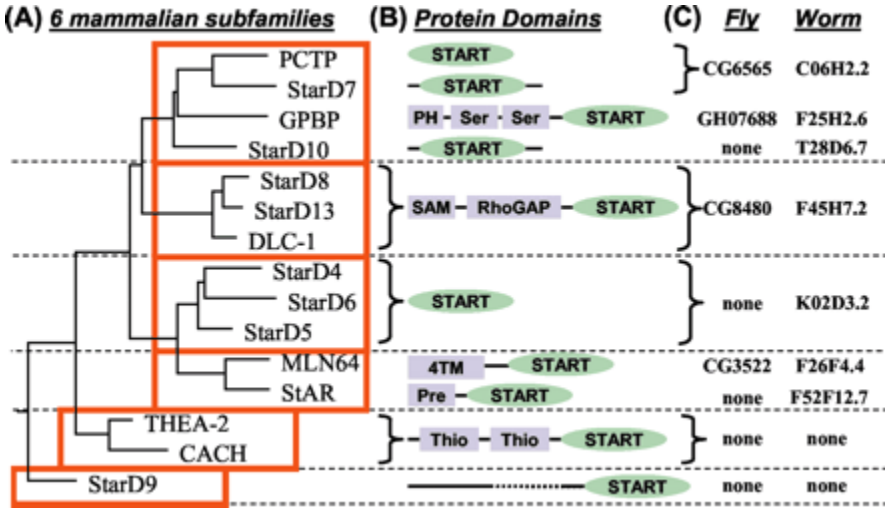

Figure 1.9 - Phylogenetic Structure of the START Family.
The 15 human START domain proteins were aligned using ClustalW and the resulting phylogenetic tree with 6 subfamilies was created. Start domains are represented in green and other common regions in grey. (4tm - four transmembranes, Pre - mitochondrial precursor, Thio – acyl-CoA thioesterase).

The StAR Subfamily (StAR & MLN64)

StAR

The rate limiting step in steroidogenesis is controlled by StAR's delivery of cholesterol to the P450 side chain cleavage enzyme residing on the inner mitochondrial membrane (IMM), which converts cholesterol to pregnenolone (Miller and Strauss 1999). Phosphorylation of pre-existing StAR and synthesis of new StAR is the result of pituitary hormone signaling (Miller and Strauss 1999). Mouse knockouts of StAR have a phenotype mimicking congenital lipoid adrenal hyperplasia, which have marked defects in steroidogenesis in the adrenal glands and gonads (Caron, Soo et al. 1998). However, there is some evidence to point to an alternative mechanisms of steroidogenesis, as StAR null fetuses produce normal amounts of placental progesterone (Bose, Sugawara et al. 1996).

The importance of StAR is due to its role in transporting cholesterol to the IMM, a destination that proves difficult to reach as cholesterol must first arrive at the outer mitochondrial membrane (OMM) and then transfer through the inter-membranous space to get to the IMM. Originally synthesized as a 37 kDa precursor, StAR is cleaved at its N-terminus to is active 30kDa form upon arrival in the mitochondria (Bose, Baldwin et al. 2000; Soccio and Breslow 2003). It is likely, that StAR's activity occurs in the OMM as studies where StAR is fused to mitochondrial proteins in the OMM, IMM and inter-membranous space only have activity at the OMM

(Bose, Lingappa et al. 2002). Unclear is how StAR performs other functions. It has been proposed that perhaps StAR simply drops off cholesterol. Or perhaps, StAR in its molten globule state alters the OMM to facilitate cholesterol desorption to the IMM (Bose, Baldwin et al. 2000). Whatever the role might be, it is clear that StAR plays a vital role in steroidogenosis in the mitochondria.

MLN64 (StARD3)

First discovered as a gene amplified in breast, gastric and esophageal cancer, MLN64 localizes to late endosomes (Akiyama, Sasaki et al. 1997). Its association with cancers is probably due to its close genetic proximity to the oncogene c-*erb*-B2 with which it coamplifies (Tomasetto, Regnier et al. 1995). Structurally, MLN64's N-terminus includes four transmembrane helices and the C-terminus shares 37% homology with StAR (Moog-Lutz, Tomasetto et al. 1997). Its X-ray crystal structure is consistent with a molecule capable of binding cholesterol in a 1:1 manner (Tsujishita 2003). Much like StAR, MLN64 transfers cholesterol *in-vitro* and stimulates steroidogenosis (Watari, Arakane et al. 1997). MLN64 is detectable in all tissues and could be responsible for the placental steroidogenesis mentioned earlier.

MLN64 has an additional role as a participant in the NPC pathway. It is thought, that after LDL deposits cholesterol into the endosome, NPC2, NPC1 and then MLN64 might act sequentially to move cholesterol to its

eventual cytosolic acceptor (Strauss, Liu et al. 2002). Unfortunately, MLN64 has not been reported in NPC disease and mouse knockouts of MLN64 were overall phenotypically normal (Kishida, Kostetskii et al. 2004).

StARD4 Subfamily: StARD4, StARD5 & StARD6

StARD4, StARD5 and StARD6 form a family of START domain proteins based on phylogenetic analysis and are closely related to StAR and MLN64. StARD4 was identified first as a gene down-regulated 2-fold by dietary cholesterol in a microarray study (Soccio, Adams et al. 2002). Based on this proximity to other START domain proteins and the microarray data, it is likely that the StARD4 subfamily members participate in cholesterol metabolism (Soccio, Adams et al. 2005).

StARD4 and StARD5 are both widely expressed with their highest levels reached in the liver, whereas StARD6's expression is isolated to the testis and neurons (Soccio, Adams et al. 2005). StARD4 and StARD5 share 30% amino acid homology (Soccio and Breslow 2003). Both proteins bind cholesterol as a ligand, but StARD5 additionally binds 25-hydroxycholesterol (Rodriguez-Agudo, Ren et al. 2006). StARD4 and StARD5 were both shown to be able to activate steroidogenosis by the mitochondrial p450scc when analyzed by co-transfection assays for StAR-like activity (Ponting and Aravind 1999; Soccio, Adams et al. 2005). It has also been postulated that StARD4 and StARD5 might deliver cholesterol in

rate limiting manner to mitochondrial cyp27, which generates 27-hydroxycholesterol, the initial step in what is known as the alternative bile acid synthesis pathway (Pandak, Ren et al. 2002). Additionally, 27-hydroxycholesterol is an activator of LXR and RCT, implicating a role for StARD4 in cholesterol removal from the body. The bile acid theory has been supported by data showing that transfection of an overexpressing StARD4 plasmid in primary hepatocytes is capable of increasing the rate of bile acid production (Rodriguez-Agudo, Ren et al. 2008). This same study also showed an increase in neutral lipid droplets, identified by oil red o staining.

Interestingly, in both mouse liver and cultured cells, StARD4, unlike StARD5, shows the characteristics of a gene regulated by the SREBP pathway. In concordance, the StARD4 promoter has a functional SRE element (Ponting and Aravind 1999). In contrast, StARD5 is not regulated by sterols, but rather ER stress. The ER in general is a cholesterol poor organelle, despite its role in cholesterol synthesis and therefore, StARD5 might play a role in helping to reduce ER stress (Soccio and Breslow 2003). However, as an added wrinkle, StARD4 has an ERSE like element in its promoter and can be up-regulated by ER stress through the ATF6 transcription factor (Yamada, Yamaguchi et al. 2006). StARD6 on the other hand, expressed exclusively in the testis might be important for male

fertility as sterols play key roles from meiosis to capacitation (Byskov, Baltsen et al. 1998; Travis and Kopf 2002).

To better understand the role of StARD4 physiologically, a major part of the work done in this thesis is focused on characterizing and understanding the phenotype of the StARD4 mouse knockout.

PCTP Subfamily: PCTP (StARD2), StARD7 (GTT1), StARD10 & StARD11 (GPBP/CERT)

A little more distantly related then some of the other START domain proteins, the PCTP subfamily's only common homology to StAR proteins is its START domain. Its exonic organization differs and PCTP proteins also bind a variety of different lipids (Soccio and Breslow 2003).

PCTP (StARD2)

PCTP or phosphatidylcholine transfer protein is an extremely specific lipid transporter binding to PC in a 1:1 stochiometric manner. It is responsible for intermembrane transport of PC and no other lipids or phospholipids (Wirtz 1991; Kanno, Wu et al. 2007). It is thought that PCTP transfers PC from its site of synthesis at the ER to the plasma membrane and mitochondria. In support of this, upon treatment of cells with clofibrate, PCTP transfers to the mitochondria; a movement induced by a phosphorylation at serine 110 (de Brouwer, Westerman et al. 2002).

Widely expressed, PCTP's highest levels are found in liver. PCTP knockout mice exist and have been reported to have normal bile excretion

levels, normal production of lung surfactant, composed primarily of PC and normal leukotriene biosynthesis, but the study was confounded by low bile excretion levels in wild type mice that might have masked the results in the knockouts (van Helvoort, de Brouwer et al. 1999). When the mouse knockout is challenged by a lithogenic diet, known to promote cholesterol gallstone formation, biliary secretion rates of bile acids, cholesterol and phospholipids are increased, yet the mice maintain normal hepatocellular secretion of PC (Wu, Hyogo et al. 2005). Over-expression of PCTP in chinese hamster ovary cells (CHO) results in a dose dependent increase in the efflux of lipids through the ABCA1 transporter suggesting that PCTP might play a role in replenishing the plasma membrane with PC after it gets utilized by ABCA1 (Baez, Barbour et al. 2002).

Finally, at 6 months of age, PCTP and ApoE double knockouts had a slight reduction in atherosclerosis, which in males was accompanied by a decrease in plasma cholesterol (Wang, Baez et al. 2006).

StARD7 (GTT1)

Few functional studies of StARD7 or GTT1 (gestation trophoblastic tumor 1) have appeared in the literature. StARD7 was first identified by its over-expression in choriocarcinoma cell lines compared to cells lines derived from normal trophblastic tissue and nonmalignant hydatidiform moles (Durand, Angeletti et al. 2004). It has also been shown to mediate

the intracellular trafficking of phosphatidylcholine to mitochondria (Horibata and Sugimoto).

StARD10

StARD10 was identified as a protein over-expressed in breast cancer. It is known to bind PC and phosphatidylethanolamine (PE) with a preference for lipids containing palmitoyl and stearoyl chains in the SN-1 position and fatty acyl chains in the SN-2 position (Olayioye, Vehring et al. 2005). StARD10 mRNA is found in many tissues like the testis, kidneys and intestine (Soccio and Breslow 2003). There is still much to be learned about the role of StARD10 in lipid metabolism.

StARD11 (GPBP, CERT)

There are two StARD11 transcripts; the long form Goodpasture antigen-binding protein (GPBP) and the short form ceramide transfer protein (CERT) (Hanada, Kumagai et al. 2003). Both forms are expressed highly in striated muscle and brain, but poorly in placenta, lung and liver.

GPBP has a N-terminal pleckstrin homology, two serine rich domains and a C-terminal START domain (Soccio and Breslow 2003). It binds and phosphorylates Goodpasture antigen, the target of autoantibodies in goodpasture syndrome (Raya, Revert-Ros et al. 2000). Although lacking a conventional serine/threonine domain, it is inactive if missing the C-terminus. The presence of a kinase site is unknown and it is speculated

that the START domain is regulatory and not catalytic (Soccio and Breslow 2003).

Both isoforms can bind and transport ceramide, in a stochiometric 1:1 fashion, leading to the hypothesis that the proteins are responsible for delivery of ceramide from the ER, the site of synthesis, to the Golgi where it is converted to sphingomyelin (Hanada, Kumagai et al. 2003). Knockout of the StARD11 homologue in Drosophila Melongaster results in premature death, reduced ATP, reduced thermal tolerance, increased glucose levels and a reduction in sphingomyelin that leads to increased membrane fluidity (Rao, Yuan et al. 2007). Finally, it seems StARD11 might interact with other sterol transporters, as RNAi knockdown of OSBP decreases StARD11 activity and sphingomyelin synthesis (Perry and Ridgway 2005).

Acyl-CoA Thioesterase Subfamily: StARD14 & StARD15

StARD14 (BFIT, ACOT & THEA)

StARD14, also known as brown fat-inducible thioesterase (BFIT), acyl-CoA thioester hydrolase 11 (ACOT11) or thioesterase adipose associated (THEA), appears in obesity models due to its role in energy metabolism (Adams, Chui et al. 2001). It has 60% homology to StARD15 (or better known as cytosolic acetyl-CoA hydrolase – CACH), but lacks the acetyl-CoA hydrolase activity (Suematsu, Okamoto et al. 2001). Instead, it seems to hydrolyze medium and long chain acyl-CoA's (Adams, Chui et al. 2001). Humans produce two splice variants that encode different c-

terminal regions and whose expression pattern varies by tissue (Adams, Chui et al. 2001). The change in C-terminus leads to different α-helix lids and therefore might lead to different lipid binding profiles (Soccio and Breslow 2003). In correspondence with its nomenclature, StARD14 mRNA in mouse brown adipose tissue is induced by cold exposure and decreases by 2.5 fold in obese (ob/ob) mice compared to lean wild-type littermates (Adams, Chui et al. 2001). Finally, StARD14 maps to mouse chromosome 4 in the dietary obese locus, suggesting a role for StARD14 in energy metabolism.

StARD15 (CACH, ACOT12)

StARD15, also known as cytosolic acetyl-CoA hydrolase (CACH) or acyl-CoA thioesterase (ACOT12), has hydrolase activity for acetyl-CoA (C_2) and low activity for short chain acyl-CoAs (C_4 - C_6), but lacks activity for medium (C_{12}) and long chain acyl-CoA (C_{14}) (Suematsu, Okamoto et al. 2001). It therefore might act to maintain an equilibrium between acetyl-CoA and its coenzyme A-SH. Interestingly, starvation and a fat free diet have both been shown to increase activity, suggesting that StARD15 also plays a role in regulation of fatty acid oxidation and synthesis (Matsunaga, Isohashi et al. 1985). Additionally, activity is increased by cholesterol feeding and by inhibitors of cholesterol activity, both of which normally decrease the level of acetyl-CoA intracellularly (Ebisuno, Isohashi et al.

1988). Finally, both sterotozotocin induced diabetes and clofibrates elevate StARD15 activity.

StARD15 is active enzymatically when it homodimerizes or tetramerizes and binds ATP (Isohashi, Nakanishi et al. 1983; Isohashi, Nakanishi et al. 1983). Expression of StARD15 has been localized to the liver, muscle, spleen and testes, but its enzymatic activity has only been demonstrated in the liver and kidneys. Overall, little is known about the StARD15 protein and continuing molecular and functional studies are necessary to hash out the details of StARD15's characteristics.

RHOGAP Subfamily: StARD8, StARD12 & StARD13

The human genome normally encodes over 50 RhoGAPs, of which three have START domains (Soccio and Breslow 2003). Rho family of small GTPases signal in a variety of cell process like cell growth, morphogenesis, cell motility, cytokinesis, trafficking and cytoskeletal organization, as well as some more detrimental processes like tumor transformation and metastasis (Moon and Zheng 2003).

StARD8 (DLC-3)

StARD8, otherwise known as deleted in liver cancer 3 (DLC-3) is a tumor suppressor gene (Durkin, Ullmannova et al. 2007). It is widely expressed, a characteristic that is reduced or lost in various cancers like lung, ovarian, kidney, prostate and breast. There are two structures for StARD8, α, which is similar to its two other family members and β, which

lacks the N-terminal SAM domain. Similar to other family members, StARD8 activates phospholipase C-δ-1 (PLCδ1) and has RhoGAP activity (Durkin, Ullmannova et al. 2007)

StARD12 (DLC-1)

Also known as deleted in liver cancer 1 (DLC-1), StARD12 is a widely expressed tumor suppressor gene that is frequently homozygously deleted in primary hepatocellular carcinoma and breast tumors (Yuan, Zhou et al. 2003). Many cancer cell lines, ranging from liver and breast to colon and prostate, have StARD12 expression deleted or lost, possibly due to promoter hypermethylation (Yuan, Zhou et al. 2003).

StARD12 appears to have dual functions. First, it appears to interact with PLCδ1, activating phosphatidylinositol 4,5-bisphosphate (PIP2) hydrolyzing activity, raising intracellular Ca^{2+} levels rapidly (Homma and Emori 1995). Second, its RhoGAP activity, specific for RhoA, enhances the conversion of RhoA from its active, GTP bound state to its inactive GDP bound state (Homma and Emori 1995). GFP tagged localization studies have found StARD12 in the punctate structures of the PM and particularly in caveolae, which makes sense based on previous findings reporting interaction of StARD12 with caveolin-1 (Yamaga, Kawai et al. 2008). Homozygous knockout of StARD12 in mice leads to embryonic lethality at day 10.5 and heterozygotes are phenotypically normal (Durkin, Avner et al. 2005).

STARD13 (DLC-2)

Like the other family members, StARD13 is also known as deleted in liver cancer 2 (DLC-2). It too was found as a gene whose expression was decreased or absent in hepatocellular carcinomas. Similarly, it encodes a RhoGAP specific for RhoA and Cdc42 (Nagaraja and Kandpal 2004). Localization studies have found it in the cytoplasm, mitochondria and lipid droplets (Ching, Wong et al. 2003). Additionally, it has four isoforms (Ching, Wong et al. 2003). Cellular over-expression increases cell proliferation, motility, transformation and RhoA activity and inhibits Ras signaling and Ras induced cellular transformation (Leung, Ching et al. 2005).

More work is needed to be done for all three members of the RHOGAP subfamily of StAR proteins to further elucidate functionality and importance of each of the proteins.

StARD9

StARD9 is one of the least studied StAR proteins. It is found in sequence databases as a partial 1820 amino acid human coding sequence with a C-terminal StART domain and an undefined N-terminal (Soccio and Breslow 2003). EST evidence hints that it is highly expressed in nervous tissue. StARD9 exists in full length and exon 8 deleted forms (Halama, Grauling-Halama et al. 2006). Much more work is needed to be done to further characterize StARD9.

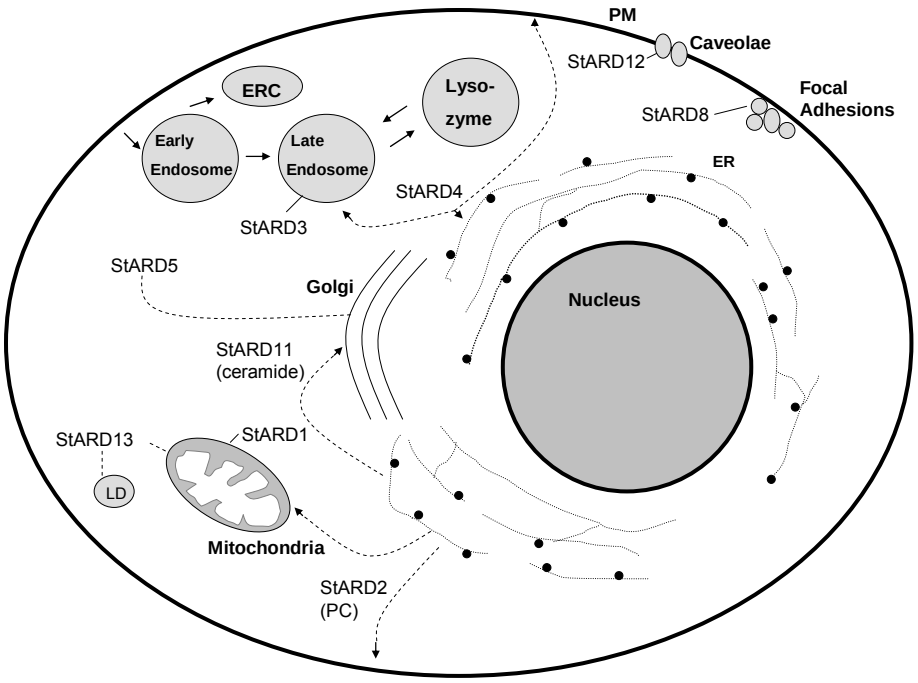

Figure 1.10 - Proposed Intracellular Localization of Various StAR Proteins:

Depicted above is the proposed localization of many of the described StAR proteins known to date.

StARD1- Has been shown to localize to the outer membrane of the mitochondria where it plays a role in steroidogenesis.

StARD2 (PCTP) – Has been proposed to transport phosphotidylcholine from the ER to both the PM and the mitochondria.

StARD3 (MLN64) - Has been localized to Late Endosomes where it plays a role in cholesterol sorting.

StARD4 – Lacks a localization sequence and thus is thought to be cytoplasmic, helping to shuttle cholesterol from the PM and Endosomes to the ER.

StARD5 – Also contains no localization sequence, but has been immunohistochemically stained and found to localize perinucularly near the Golgi Apparatus.

StARD6 – Is known to be expressed in testis and the CNS. Little is known about its intracellular localization (not shown).

StARD7 – Very little is known about StARD7 (not shown).

StARD8 (DLC-3) – StARD8 has been shown to immunohistochemically localize to Focal Adhesions.

StARD9 – Very little is known about StARD9 (not shown).

StARD10 (PCTP-like) – Implied in phospholipid delivery to canilicular membranes, but never been shown (not shown).

StARD11 (Cert) – GFP tagging studies show StARD11 in the cytoplasm and the Golgi.

StARD12 (DLC-1) – GFP tagging experiments find StARD12 at the plasma membrane, specifically interacting with Caveolae.

StARD13 (DLC-2) –StARD13 is thought to localize to lipid droplets and the mitochondria (not shown).

StARD14 (BFIT) – little is known about the localization of StARD14 (not shown).

StARD15 (CACH) - little is known about the localization of StARD15 (not shown).

Abbreviations: ERC – Endoplasmic Recycling Compartment; ER – Endoplasmic Reticulum; LD – Lipid Droplet: PM – Plasma Membrane

Dash lined = proposed routes or anchorings; Solid lines = known routes or anchorings.

Conclusion

By binding lipid ligands, StART domains likely serve as transporters, shuttling lipids from subcellular compartments, or as lipid dependent regulators of cell signaling events. This means that StAR proteins likely play roles in lipid metabolism, atherosclerosis, fertility, autoimmune disease and cancer, making them possible targets for drug therapy. Although still in its nascent form, research into the StAR proteins proves to be promising for our understanding of these complicated processes. To this end, this thesis focuses on work done to characterize the role of StARD4 *in-vivo*.

Chapter 2: Generation and Characterization of the StARD4 K.O.

Targeted Knockout of the StARD4 gene

We knocked out the StARD4 gene in a manner that allows for complete knockout, tissue specific knockout and time dependent knockout using the strategy developed by Copeland and available from the NCI-Fredrick website, http://recombineering.ncifcrf.gov/ (Liu, Jenkins et al. 2003). Through multiple steps of cloning and subsequent homologous recombination, loxP sites were introduced into the introns flanking exon 3 of the StARD4 gene. In the presence of cre-recombinase, this initiates excision of the exon 3, resulting in out of frame splicing of exon 2 to exon 4, causing premature termination of transcription and ultimately a non-functional StARD4 protein (Matthaei 2007). Cre-recombinases expression can be driven by a variety of different promoters (i.e. CMV-cre – full knockout, Alb-cre – liver specific, Lys-cre – macrophage specific) allowing for generalized or tissue specific knockout of the StARD4 gene. It is also possible to use an inducible promoter for the cre-recombinase or a viral delivery protocol to allow for StARD4 gene inactivation in a time dependent manner.

StARD4 is a 6 exon gene located on mouse chromosome 18 (Figure 2.1) (Soccio, Adams et al. 2002). The process of generating the StARD4 knockout mouse was a complicated multi-step process. To begin, a C57BL/6 background BAC clone (BacPac Resources, clone # RP23-

46E14) was ordered that contained amongst many other genes, the StARD4 genomic DNA. Next, a targeting construct was created by excising the StARD4 genomic DNA from the BAC and inserting it into the MC1-TK plasmid that contains two LoxP sites. As a positive selection marker, the downstream loxP sites on the plasmid also contained a Frt-PgK-Neo-Frt cassette. Specifically, the upstream loxP site was placed 573 bp before exon 3 and the downstream Frt-PgK-Neo-Frt-loxP was placed 942 bp after exon 3.

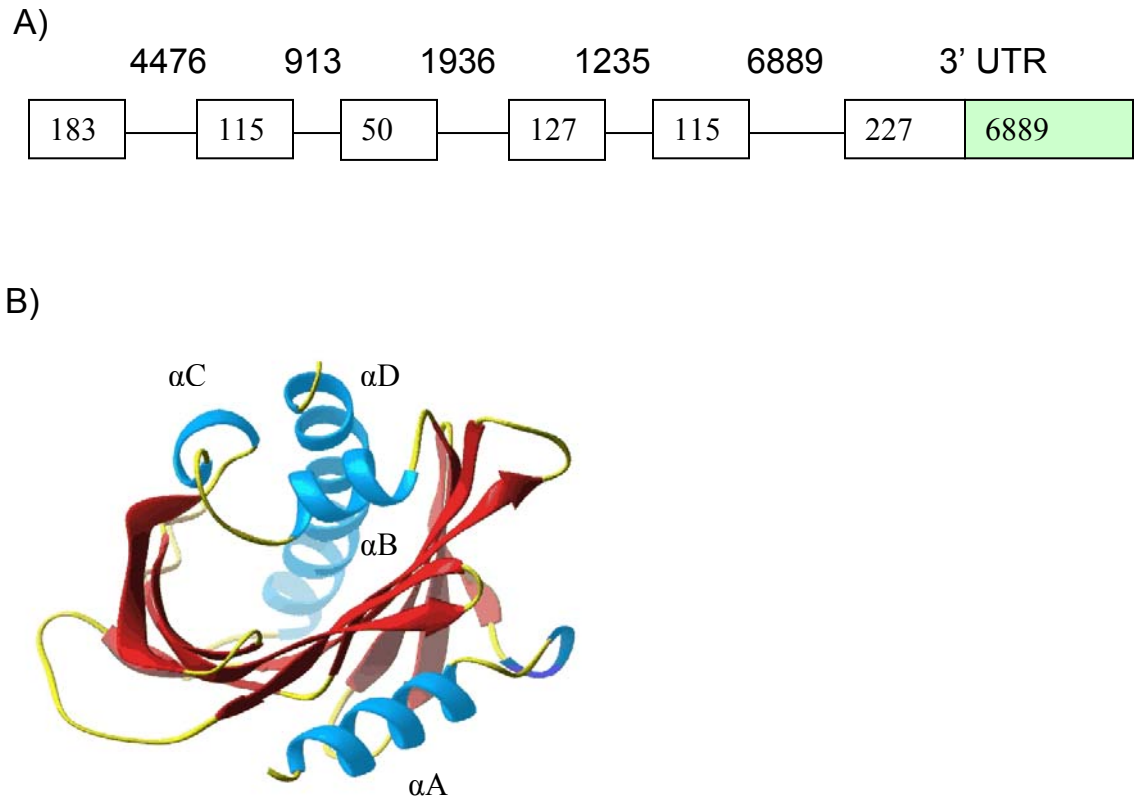

Figure 2.1 - Exonic Structure and Secondary and Tertiary Structure of mStARD4
A) StARD4 is a 272 amino acid protein encoded by 6 exons. Exons are represented as boxes with base pair lengths written inside. Exonic sequences are white and the 5' UTR is green. Introns are represented by lines connecting the boxes, with base pair lengths indicated above.
B) **Start Domain x-ray crystal structure.** StARD4 has four α-helices (blue) and nine β-strands (red) that form a u shaped capsule. The C-terminal α-helix sticking upwards (αD), may open or unfold to allow lipid binding in the hydrophobic pocket locating internally. The crested lipid binding pocket is the area affected by deletion of exon 3 and was the basis of its choice as a candidate exon to eliminate. (Romanowski, Soccio et al. 2002).

Upon successful creation of the targeting construct, the next step was to recombine the targeted construct into mouse embryonic stem (ES) cells. Correctly targeted ES cells were identified by Southern Blotting, using EcoRI and EcoRV to digest the genomic DNA, with subsequent probing by 5' and 3' probes designed by using the StARD4 sequence found on http://www.ensembl.org/index.html. Only one correctly targeted mouse ES clone was found and this was used to inject mouse blastocysts to produce chimera mice that were bred to determine germ-line transmission.

Figure 2.2 - Gene Targeting and Generation of a Conditional Knockout (Floxed) Allele of the StARD4 Gene.
A) The targeting strategy employed to insert loxP sites on either side of exon 3 of StARD4. First, a targeting vector was constructed by placing a Neo selectable marker flanked by Frt sites with a loxP site in intron 3. Next, a second loxP site was introduced in intron 2. B) PCR analysis to determine the presence of the floxed allele only found in heterozygotes and knockout mice (primer set AH. A is a 5' primer located in exon 2 and H is a 3' primer located ~ 975bp downstream of exon 3). The Wt allele for AH is over 2000 bp and not normally seen in a conventional PCR. C) PCR analysis to determine the presence of the wild-type allele only found in heterozygotes and wild-type mice (primer set CH. Primer C is located in exon 3. Primer H is the same as above). D) Western Blot analysis was performed on livers of 12 week old StARD4 mice. All samples were run in duplicate. StARD4 is represented by a 23.5 KDa band. E) β-Actin loading control for Western blot. Expected size = 45 KDa.

Figure 2.2

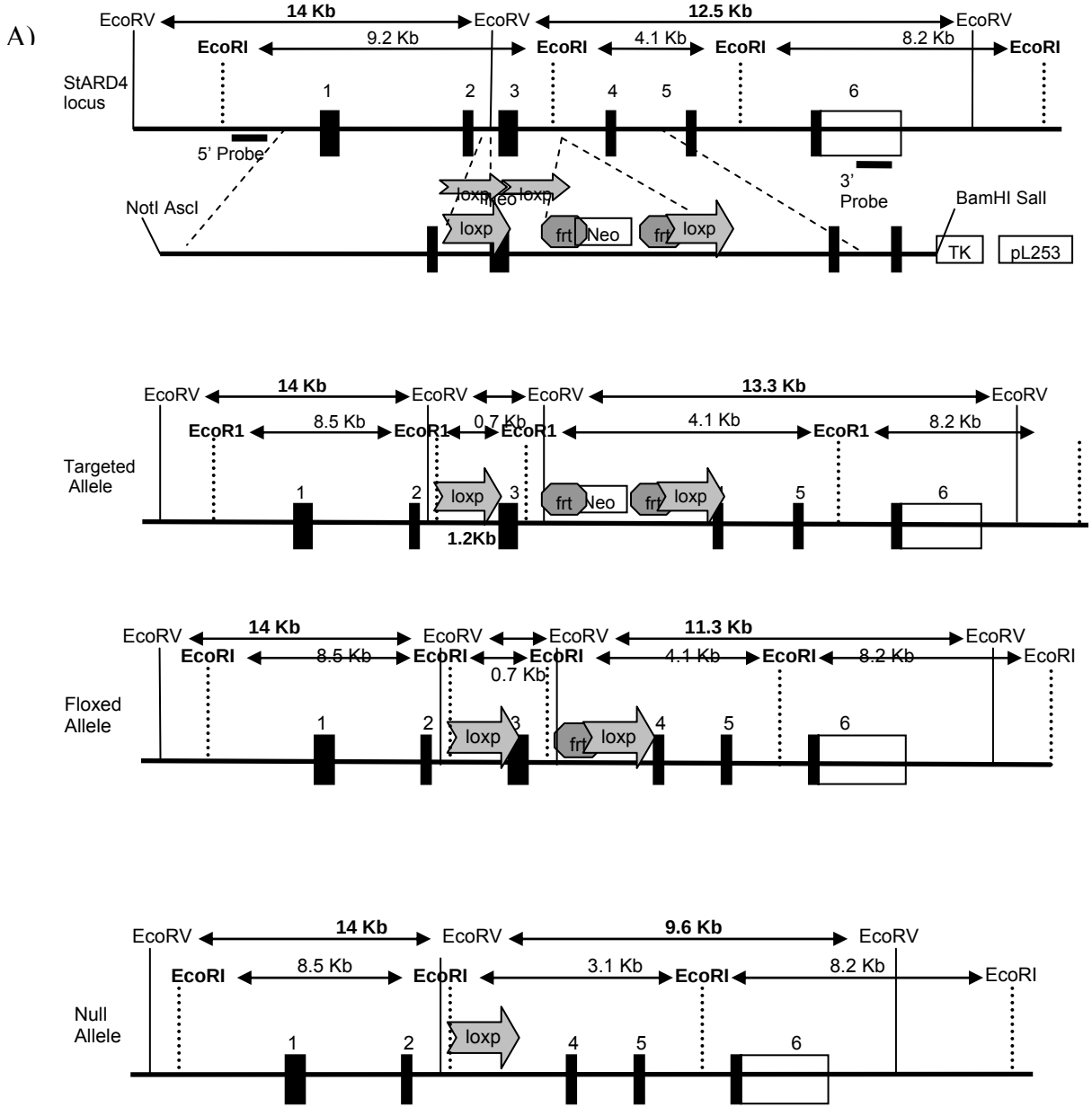
A)
EcoRV
14 Kb
EcoRV
12.5 Kb
EcoRV
EcoRI
9.2 Kb
EcoRI
4.1 Kb
EcoRI
8.2 Kb
EcoRI
StARD4
locus
1
2
3
4
5
6
5' Probe
3'
Probe
NotI AscI
loxp
Neo
loxp
loxp
frt
Neo
frt
loxp
BamHI SalI
TK
pL253
EcoRV
14 Kb
EcoRV
EcoRV
13.3 Kb
EcoRV
EcoR1
8.5 Kb
EcoR1
0.7 Kb
EcoR1
4.1 Kb
EcoR1
8.2 Kb
Targeted
Allele
1
2
loxp
3
frt
Neo
frt
loxp
5
6
1.2Kb
EcoRV
14 Kb
EcoRV
EcoRV
11.3 Kb
EcoRV
EcoRI
8.5 Kb
EcoRI
EcoRI
4.1 Kb
EcoRI
8.2 Kb
EcoRI
0.7 Kb
Floxed
Allele
1
2
loxp
3
frt
loxp
4
5
6
EcoRV
14 Kb
EcoRV
9.6 Kb
EcoRV
EcoRI
8.5 Kb
EcoRI
3.1 Kb
EcoRI
8.2 Kb
EcoRI
Null
Allele
1
2
loxp
4
5
6

Figure 2.2 continued

PCR

B) **Wt Het K.O.**

600 bp

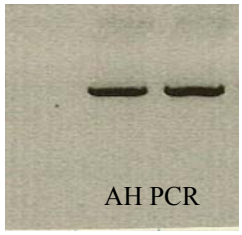

C) **Wt Het K.O.**

1000 bp

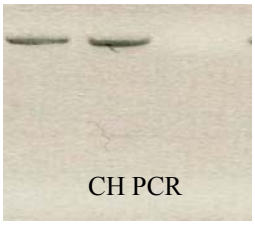

Western

D) **Wt Het K.O.**

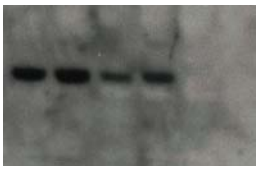

StARD4

E) **Wt Het K.O.**

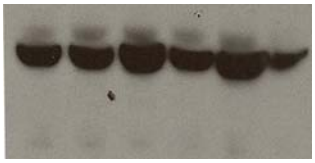

β-actin

Viability and Fertility of the StARD4 KO Mouse Line

Upon successful incorporation of the targeted construct into the mouse blastocysts and confirmation of germ-line transmission, mating between the chimera mouse containing the targeting construct and C57Bl6 wild-type mice was undertaken. The resulting heterozygous mice were bred to homozygosity and named Neo-floxed. The Neo-floxed mice were then mated to the C57BL/6-ACT-FLPe homozygous mouse to excise the Frt-PgK-Neo-Frt cassette. The progeny of this cross, named "Floxed", were then bred to homozygosity. The Floxed mice serve as the starting point for creation of the full knockout, tissue specific and time dependent knockout mice (Figure 2.3).

Next, to create a full knockout of the StARD4 gene, a Floxed homozygous mouse was mated to a C57BL/6 CMV-Cre homozygous mouse. The Cre-recombinase, driven by the powerful CMV promoter, interacts with and removes all of the nucleotides between the two LoxP sites, creating a non-functional StARD4 gene and protein. Brother-sister mating of the progeny yields deleted/null homozygous mice, which have been used throughout this thesis to evaluate the effects of the complete StARD4 knockout. The absence or presence of StARD4 was verified at the mRNA level by PCR and the protein level by Western blotting (Figure 2.1). The genotype and gender of the offspring were also determined to

see if the KO affected the ratio of KO:Wt:Het and males: females. The offspring fit an expected or normal Mendelian ratio (Table 2.1).

A)

	Female	Male
Wt	14	14
Het	25	20
KO	16	13

B)

	No. of breedings	No. of pregnancies	Litter Size (mean +/- S.D.)
Male +/- x female +/+	16	16	6.56 +/- 1.93
Male +/+ x female +/-	11	11	6.36 +/- 3.17
Male -/- x female -/-	5	5	7.02 +/- 1.35

Table 2.1 - Mendelian Ratio of Mating to Homozygosity of the Neo Floxed StARD4 Gene.
A) The ratio of WT/Het/KO of 102 mice born from the mating of two StARD4 mice heterozygous for the Floxed allele recombined by the cre-recombinase. The progeny fit a normal Mendelian distribution for mice born under the expected 1:2:1 ratio of Wt:Het:KO (observed ratio = 28:45:29) . When scrutinized with a chi square test, χ^2 = 1.922 with 2 degrees of freedom. The two tailed *p-value* for this was 0.3826 meaning that by conventional criteria, this difference is considered to be not statistically significant. B) Both female and male heterozygous mutant mice were fertile and had similar litter sizes.

A liver specific knockout was also created by mating the Floxed mouse with a C57BL/6 Alb-Cre mouse. Although not studied in this thesis, this mouse was made because it will allow others to study the role of liver StARD4 expression in lipid metabolism.

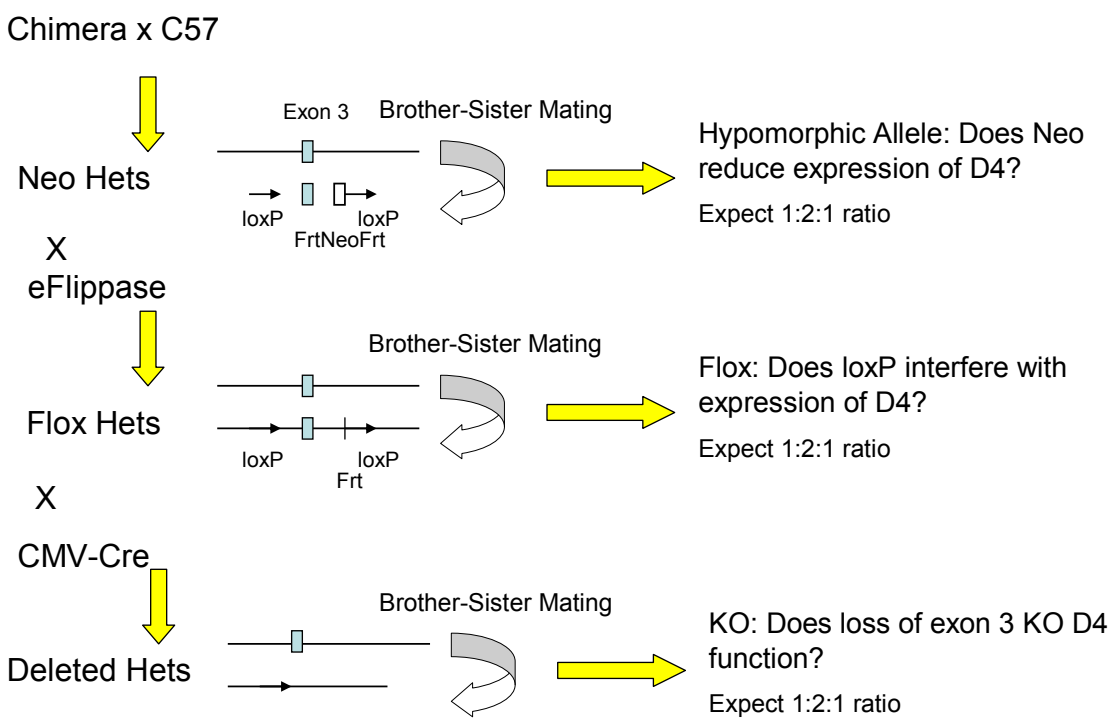

Figure 2.3 - Mating Strategy in Generation of the StARD4 Knockout.
Chimera mice were mated to C57Bl6 to generate Neo heterozygotes which were then brother-sister mated in attempt to generate Neo homozygotes. The Neo heterozygotes were also mated to the ACT-FLPe transgenic mice to remove the FrtNeoFrt cassette. These Floxed heterozygotes were brother-sister mated in an attempt to generate Floxed homozgotes. The Floxed homozygotes were mated to CMV-Cre transgenic mice to remove exon 3 and to generate Null/Deleted heterozygotes. These Null heterozygotes were brother-sister mated in an attempt to generate Null homozygotes. Brother-sister matings resulted in the normal Mendelian ratio for breeding of mouse lines with average liter size between 6-7 pups. Teal squares represent exons, triangles represent loxP sites, a white square represents the FrtNeoFrt cassette and thick arrows represent matings.

Expression of StARD4 in Various Tissues

To determine sites of StARD4 expression, I analyzed StARD4 mRNA and protein levels in various tissues. Three individual mice were sacrificed, various organs collected, RNA isolated and qPCR run for StARD4 expression. StARD4 is most highly expressed in the liver and macrophages, followed by the kidney and lung. Expression of StARD4 is not found in muscle or adipose tissue (Figure 2.4).

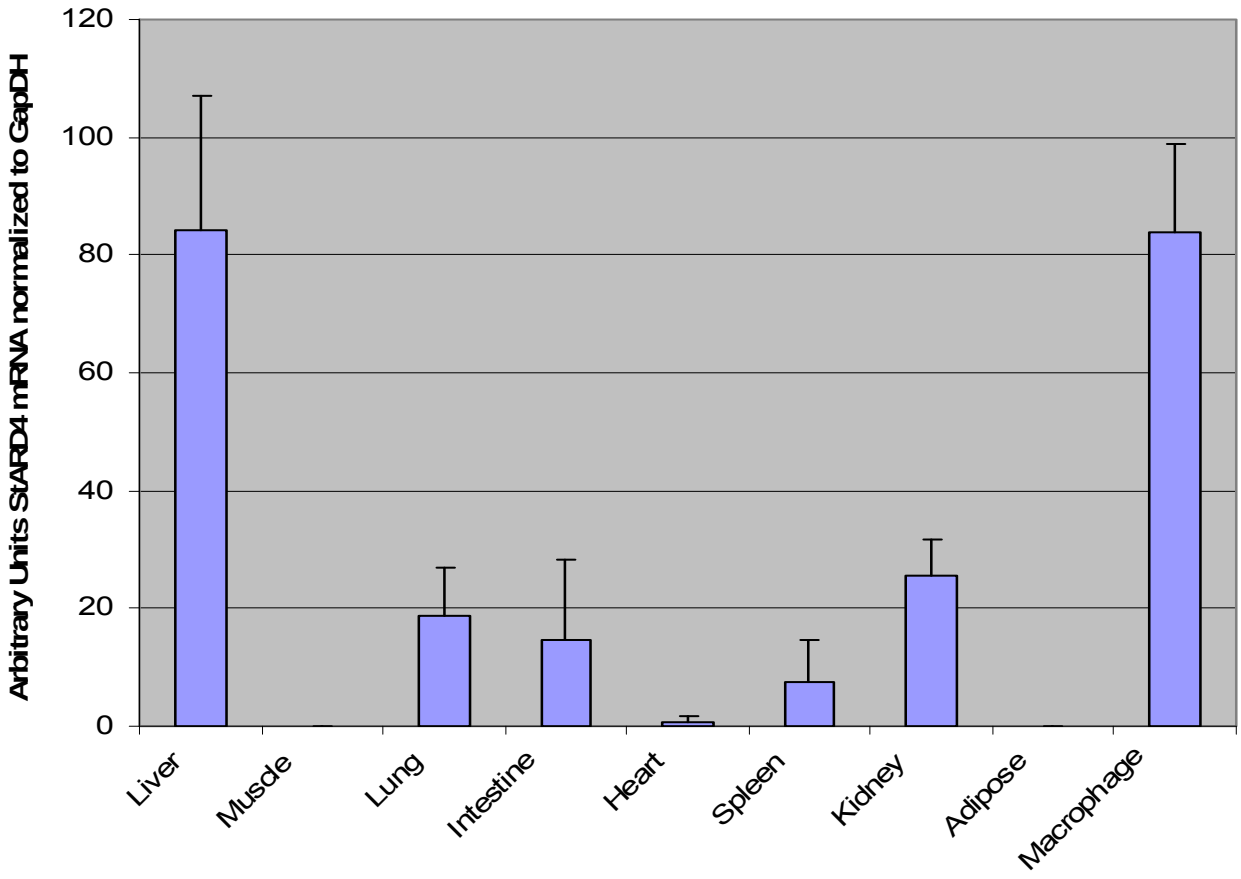

Figure 2.4 Expression Level of StARD4 in Various Tissues as Confirmed by qPCR. Tissues from 3 male WT mice were collected, RNA isolated and tested for expression of StARD4 RNA expression by qPCR. All samples are normalized to GapDH and shown as relative ratios. Std is represented by lines above the bar graphs.

Initial Screening of the StARD4 Knockouts

I initially determined a growth curve for the StARD4 knockout mice from 4 to 12 weeks of age. At 12 weeks, mice were sacrificed to determine levels of total cholesterol, cholesterol ester, free cholesterol, triglyceride and glucose as well as plasma lipoprotein levels. In addition, at autopsy, organs were evaluated for pathology at both the gross and microscopic levels.

At 12 weeks, both male and female knockout mice, fed a standard chow diet, showed a decrease in body weight compared to wild-type littermates (Figure 2.4). The change was more evident in male mice in which the weight difference was significant, starting at 5 weeks of age, whereas in female mice, a significant difference was only seen at 12 weeks of age (Table 2.2).

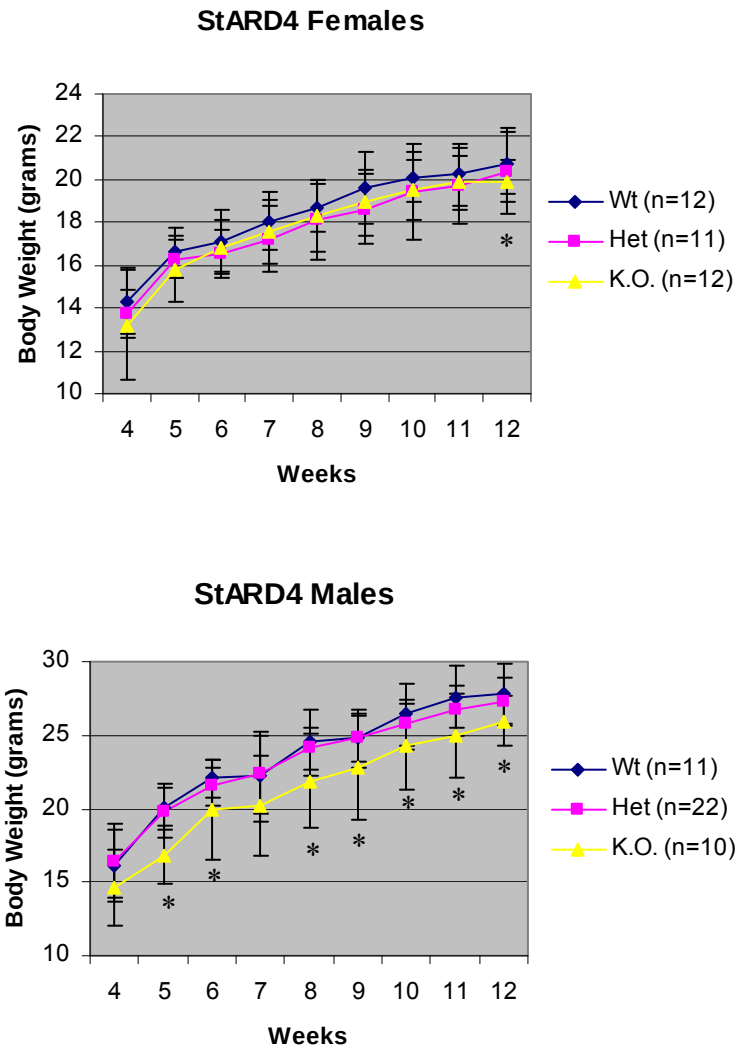

Figure 2.5 - Growth Curve of StARD4 Knockout Mice
StARD4 mice (Wt/Het/KO) from 4 weeks of age after weaning, until 12 weeks of age, fed a chow diet. Weights of mice were recorded weekly. Weights are represented as means with the Std indicated by the vertical lines.
* indicates a *p-value* < 0.05

Table 2.2 - Weights of StARD4 Knockout Mouse & Wild-type Littermate, Week 4-12

Week	4	5	6	7	8	9	10	11	12
Female									
Wt	14.3	16.6	17.1	18.1	18.7	19.6	20.1	20.3	20.9
	+/-	+/-	+/-	+/-	+/-	+/-	+/-	+/-	+/-
***n*=12**	1.6	1.2	1.5	1.3	1.1	1.7	1.2	1.5	1.5
K.O.	12.8	14.8	15.5	17.4	17.8	18.4	19.1	19.5	19.8
	+/-	+/-	+/-	+/-	+/-	+/-	+/-	+/-	+/-
***n*=12**	2.6	1.6	1.3	1.5	1.7	1.5	1.4	1.2	0.1
***p*-value**	**0.21**	**0.18**	**0.45**	**0.35**	**0.52**	**0.30**	**0.24**	**0.53**	**0.02**
Male									
Wt	16.1	20.1	22.0	22.1	24.5	24.8	26.4	27.6	28.0
	+/-	+/-	+/-	+/-	+/-	+/-	+/-	+/-	+/-
***n*=11**	2.4	1.6	1.3	3.0	2.3	2.0	2.1	2.1	2.0
K.O.	14.7	16.9	20.0	20.2	22.0	22.8	24.3	25.0	26.0
	+/-	+/-	+/-	+/-	+/-	+/-	+/-	+/-	+/-
***n*=10**	2.6	2.0	3.4	3.4	3.2	3.6	2.9	2.8	1.7
***p*-value**	**0.22**	**0.01**	**0.01**	**0.07**	**0.003**	**0.05**	**0.04**	**0.02**	**0.03**

All values are means +/- Std.
n = number of mice.

To evaluate the physiological significance of the weight difference, at 12 weeks of age, measurements were also made of length (rump to head) and the size of the feet and hands. Both male and female knockout mice were shorter and had smaller feet and hands. This suggests that the knockout mice were not failing to just gain weight, but rather have a generalized growth abnormality. Using weight and length measurements, BMI was calculated and there was no difference between StARD4 knockout and wild type mice (Figure 2.6)

		Weight (g)	**Height**	**BMI (g/mm^2)**
Male	**Wt** ***n* = 14**	28.0 +/- 2.0	9.3 +/- 0.2	(3.1 +/- 0.1) x 10-3
	K.O. ***n* = 9**	26.0 +/- 1.7	8.9 +/- 0.3	(3.3 +/- 0.1) x 10-3
	***p*-value**	0.034	0.001	0.101

Figure 2.6 - Length Measurements of StARD4 Knockout Mice
StARD4 mice (Wt/KO) at 12 weeks of age, fed a chow diet. Heights of mice were recorded with mice euthanized and laid flat on their backs. Lengths are indicated in cm. *n*=number of mice.

The weights of various organs were also analyzed including liver, kidney, heart, spleen, lung and epididymal fat pads. In knockout mice, male liver, kidney and hearts and female hearts were significantly lighter than in wild type mice, but all were in proportion to the overall decrease in weight and none stood out as being especially affected (Table 2.3).

Table 2.3 - Organ Weights of StARD4 Mice at 12 Weeks of Age

	Liver (g)	Kidney (g)	Heart (g)	Spleen (g)	Lung (g)	Adipose (g)
Female						
Wt	0.83 +/- 0.09	0.14 +/-0.62	0.12+/- 0.02	0.14 +/- 0.09	0.24 +/- 0.19	0.11 +/- 0.03
***n* = 11**						
K.O.						
***n* = 10**	0.77 +/- 0.06	0.13 +/- 0.03	0.10 +/- 0.01	0.09 +/- 0.03	0.16 +/- 0.03	0.10 +/-0.06
***p*-value**	0.136	0.358	0.040	0.107	0.244	0.609
Male						
Wt	1.12 +/- 0.14	0.17 +/- 0.03	0.13 +/-0.02	0.09+/- 0.03	0.16 +/- 0.04	0.19 +/- 0.05
***n* = 16**						
K.O.						
***n* = 10**	0.98 +/- 0.31	0.15 +/- 0.05	0.11 +/- 0.03	0.08 +/- 0.04	0.15 +/- 0.04	0.16 +/- 0.05
***p*-value**	0.019	0.007	0.00004	0.656	0.094	0.237

All values are means +/- Std.
n = number of mice.
* indicates a *p*-value < 0.05.

Pathology of StARD4 Knockout Mice

A complete pathological examination was performed on StARD4 knockout mice and their wild-type littermates by the Tri-institutional Core Facility located in the Memorial Sloan Kettering Cancer Center Pathology Department. No anatomical or histological differences between StARD4 knockout and wild type mice were found in any of the organs analyzed including; brain, heart, lung, spleen, liver, gallbladder, stomach, deudenum, jejunum, ileum, colon, cecum, thymus, tongue, kidney, esophagus, pancreas, renal lymph nodes, salivary glands, brown fat, adrenal glands, sciatic nerve, spinal chord, thyroid glands. In addition, no

differences were found in blood chemistries as well as blood count including: alkaline phosphotase, alanine aminotransferase, asparagine aminotransferase, γ-Glutamyl Transpeptidase, albumin, globulin, creatinine, phosphorous, chloride, potassium, sodium, albumin to globulin ratio, BUN to creatine ratio, osmalality, anion gap, red blood cells, white blood cells, neutrophils, lymphocytes, monocytes, eosinophils and platelets.

Plasma Cholesterol, Triglycerides and Glucose Concentrations

At 12 weeks of age, plasma lipids were compared between StARD4 knockout and wild type mice and no significant differences were found in concentraions of cholesterol, HDL, triglycerides, glucose, free cholesterol and cholesterol esters (Table 2.4).

Table 2.4 - Plasma Lipid Concentrations of StARD4 Mice at 12 Weeks of Age Fed a Chow Diet

	Female		Male	
	Wt	**KO**	**Wt**	**KO**
Total Chol. (mg/dl)	62 +/- 12	63 +/- 2	64 +/- 13	68 +/- 11
***n*=**	9	9	12	9
HDL (mg/dl)	25 +/- 4	25 +/- 5	37 +/- 8	32 +/- 8
***n*=**	9	8	10	8
Non – HDL (mg/dl)	37 +/- 8	38 +/- 3	27 +/- 5	36 +/- 3
***n*=**	9	8		
(calculated)				
Free Chol. (mg/dl)	10 +/- 3	11 +/- 3	21 +/-10	17 +/- 4
***n*=**	13	11	15	9
Chol. Ester (mg/dl)	50 +/-10	53 +/- 3	46 +/- 15	56 +/- 12
***n*=**	9	9	12	9
Triglycerides (mg/dl)	21 +/- 6	27 +/- 8	30 +/- 8	35 +/- 8
***n*=**	10	12	11	14
Glucose (mg/dl)	138 +/- 24	116 +/- 20	160 +/- 36	163 +/- 28
***n*=**	11	8	11	9

All values are means +/- std.
n = number of mice per sample.
All *P*-values were not significant.

Hepatic Lipid Concentrations

Since StARD4 expression is highest in liver and in primary hepatocytes, it is logical to examine the effect of the StARD4 knockout on liver lipids (Rodriguez-Agudo, Ren et al. 2008). Furthermore, it has been

published that StARD4 over expression in primary mouse hepatocytes has led to increase cholesterol ester synthesis (Rodriguez-Agudo, Ren et al. 2008). At 12 weeks of age, hepatic lipids were extracted by the Folch method from StARD4 knockout and wild type mice and total cholesterol, free cholesterol, cholesterol ester, and triglyceride levels were determined, but no significant differences found (Table 2.5).

Table 2.5 - Hepatic Lipid Concentrations of StARD4 Mice at 12 Weeks of Age Fed a Chow Diet

	Female		Male	
	Wt	**KO**	**Wt**	**KO**
Total Chol.(mg/g)	2.8 +/- 0.5	2.4 +/- 0.4	1.6 +/- 0.3	2.1 +/- 0.7
***n*=**	8	9	10	8
Free Chol. (mg/g)	2.2 +/- 0.5	1.9 +/- 0.4	1.2 +/- 0.3	1.5 +/- 0.6
***n*=**	8	9	10	8
Chol. Ester(mg/g)	0.6 +/- 0.4	0.54 +/- 0.3	0.4 +/- 0.1	0.4 +/- 0.2
***n*=**	8	9	10	8
TG (mg/g)	14.2 +/- 4.9	12.2 +/- 4.6	7.9 +/- 3.5	7.4 +/- 2.5
***n*=**	7	8	10	8

All values are means +/- std.
n = number of mice per sample.
All *P*-values were not significant.

Gallbladder Bile Concentrations

Gallbladder bile was extracted from 12 week old StARD4 knockout and wild-type mice and concentrations of cholesterol, phospholipids and bile acids analyzed. Female knockout mice showed a significant reduction in both total cholesterol and phospholipids, whereas in males there was no

significant difference in bile concentration (Table 2.6). The results in females are compatible with the hypothesis that StARD4 plays a role in delivering cholesterol to the hepatocyte canalicular membrane for excretion into bile.

Table 2.6 - Gallbladder Bile Levels of StARD4 Mice at 12 Weeks of Age Fed a Chow Diet

	Female		Male	
	Wt	**KO**	**Wt**	**KO**
Total Chol. (mg/dl)	190 +/- 50	135 +/- 64*	186 +/- 59	161 +/- 88
***n*=**	10	10	15	11
Phospholipids (mg/dl)	2065 +/- 573	1576 +/- 591*	1446 +/- 256	1532 +/- 424
***n*=**	13	13	15	9
Bile Acids (mg/dl)	94 +/- 35	76 +/- 6	43 +/- 15	46 +/-16
***n*=**	9	11	15	10

All values are means +/- Std.
n = number of mice per sample.

Glucose Tolerance (IPGTT Test)

Aside from lipid measurements, the StARD4 mice were examined for glucose metabolism by and intraperitoneal glucose tolerance test (IPGTT) three to five days before sacrifice at 12 weeks of age. After injecting a glucose bolus of 2g/kg, plasma glucose levels were determined at 0, 15, 30, 60 and 120 minutes. This test did not reveal any difference in glucose tolerance between StARD4 knockout and wild-type littermates (Figure 2.7).

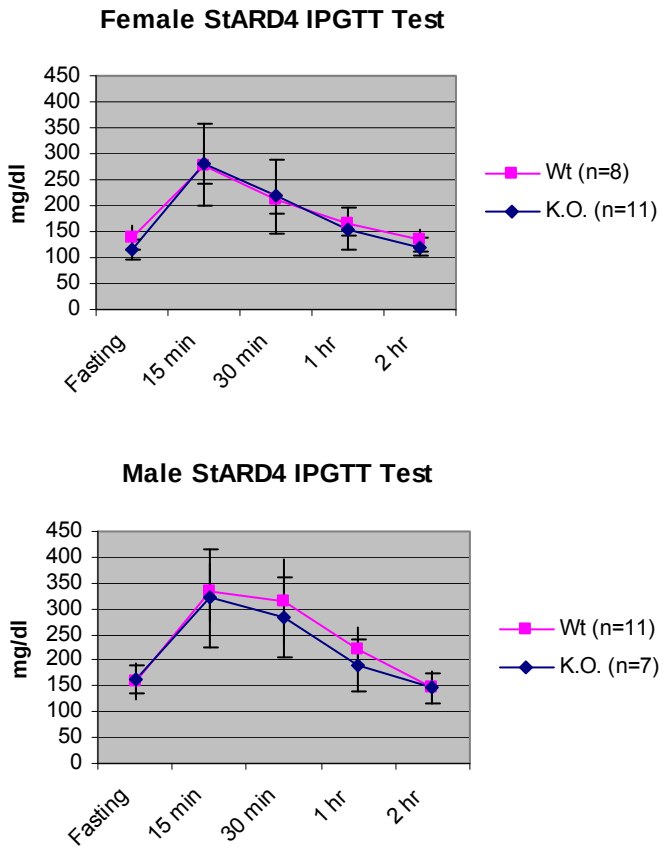

Figure 2.7 - Intraperitoneal Glucose Tolerance Test of StARD4 Mice
11.5 week old StARD4 knockout mice and their wild-type littermates were injected with a 2g/kg of body weight bolus of glucose and glucose measurements were made at the above indicated times. All values indicated averages of the indicated n. Std error bars are represented above and below the data points.

Food Intake of StARD4 Mice, Week 6-8

To better understand the weight difference between StARD4 knockout and wild-type mice, 5 male mice of each group were single caged at 6 weeks of age and food intake and body weight recorded daily for two weeks. At 8 weeks, a trend to decreased body weight was observed in the StARD4 knockouts and the weight difference between knockout and wild type mice became significant in the last 3 days of this period. However, there was no significant difference in food intake or food intake per body weight during this period (Figure 2.8). These observations suggest that the decreased body weight of StARD4 knockouts is not due to decreased appetite, but rather the result of a metabolic abnormality.

A)

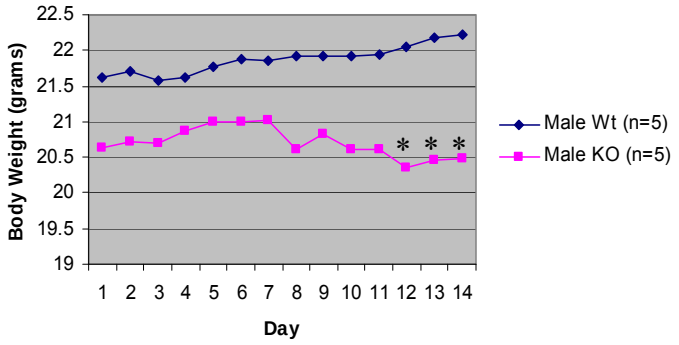

B)

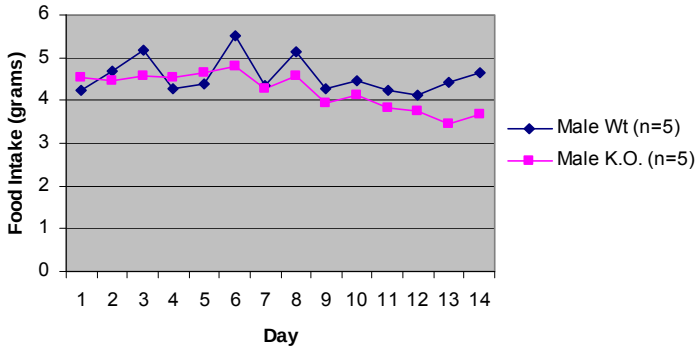

C)

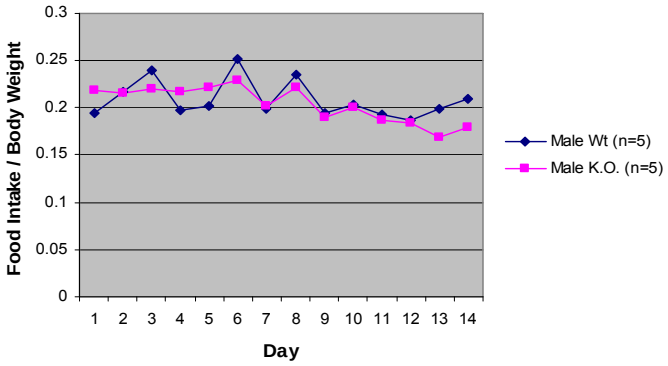

Figure 2.8 - Food Intake Experiment on StARD4 Mice, Week 6-8
Five 6 week old StARD4 mice and five 6 week old wild-type mice's food intake and body weight were recorded daily at 4pm for two weeks straight. Although weights seem to diverge as previously recorded, reaching and then maintaining significance from day 11 onwards, the corresponding food intake did not seem to be responsible for the change. A) Body Weight. B) Food Intake. C) Food Intake / Body Weight. indicates a p-value < 0.05

High Fat Diet Study and Dual Energy X-Ray Absorptiometry (DEXA) Scan

To better understand the mechanism underlying the StARD4 weight phenotype, the 10 mice used above for the food intake study, underwent DEXA scan for body composition at 8 weeks of age, were fed a high fat diet (60% of calories from fat) for 12 weeks, and rescanned at 20 weeks of age. Weights were determined weekly and on the high fat diet the StARD4 knockout mice caught up to the wild type mice and no difference in weight was observed through to week 20 (Figure 2.9). The DEXA scans at 8 and 20 weeks showed no difference between StARD4 knockout and wild type mice in lean mass, fat mass, the ratio of lean to fat mass and bone mineral density (Figure 2.10, 2.11).

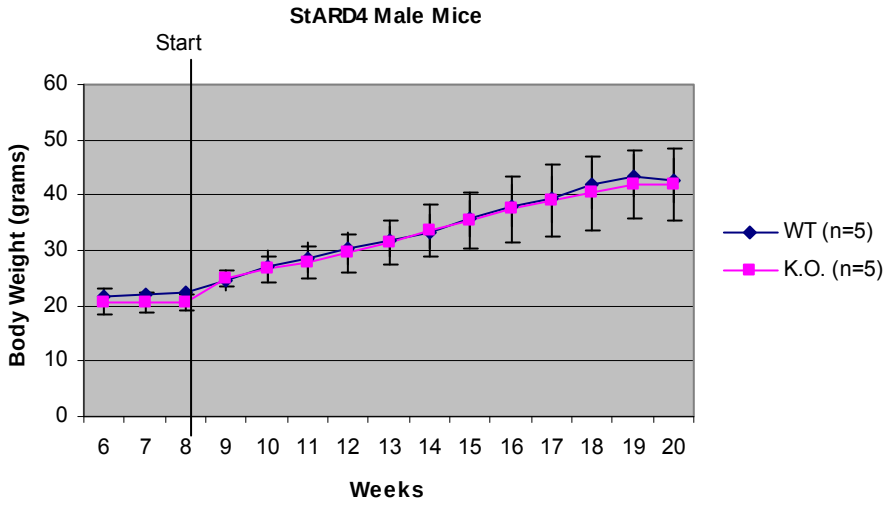

Figure 2.9 - High Fat Diet Experiment on StARD4 Mice, Week 6-8
Five 8-20 week old StARD4 mice and 5 wild-type littermates were fed a 60% high fat diet. Their weights were recorded weekly starting at week 6, 2 weeks before feeding began. There appears to be no difference in weight phenotype of the knockout mice when compared to their wild-type littermate controls.

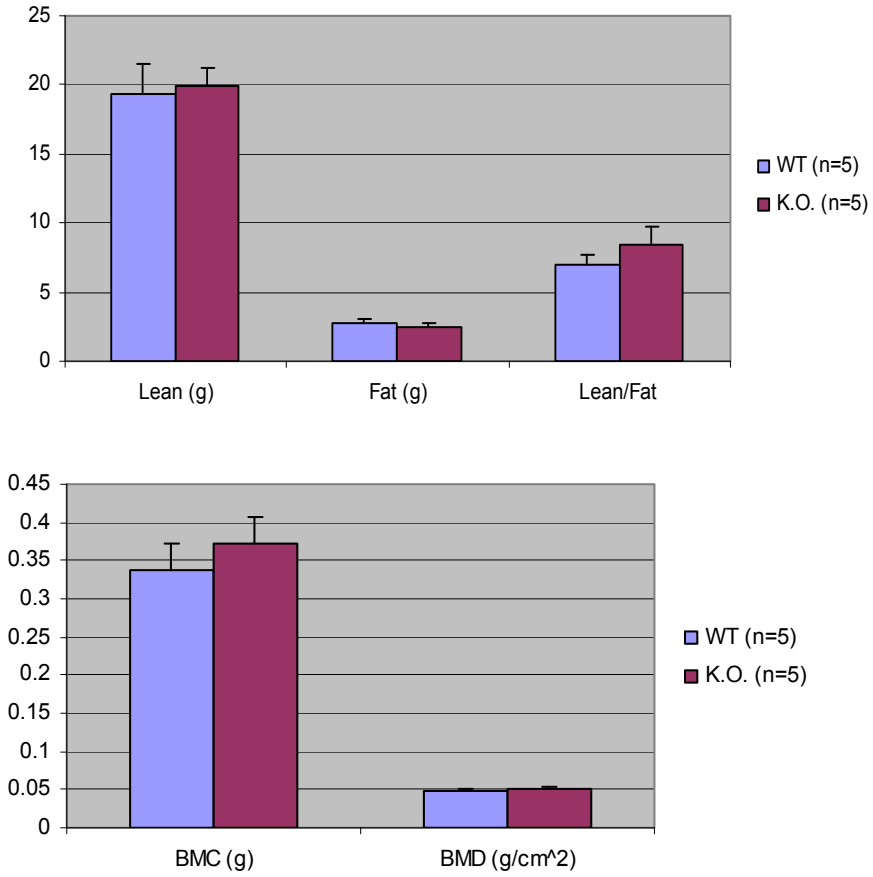

Figure 2.10 - Dexa Scan of StARD4 Mice at Week 8
Five 8 week old StARD4 mice and 5 wild-type littermates were subjected to a Dexa Scan to elucidate their body and bone composition. There appears to be no difference in lean versus normal fat or between bone mineral content and density of knockout and wild-type littermate controls.

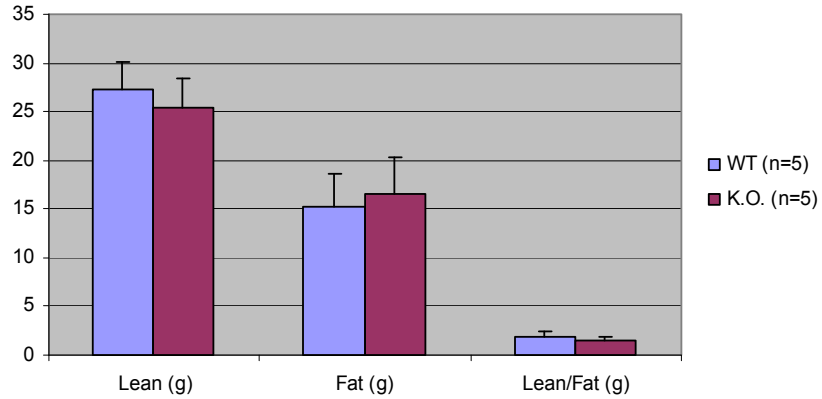

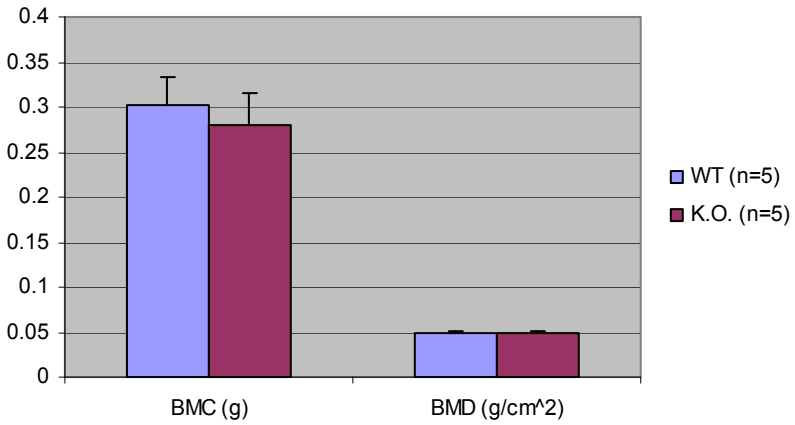

Figure 2.11 - Dexa Scan of StARD4 Mice at Week 20 After 12 Weeks of High Fat Diet Feeding

Five 8-20 week old StARD4 mice and 5 wild-type littermates were fed a 60% high fat diet. At week 20, a day before sacrifice, mice were subjected to a Dexa Scan to elucidate their body and bone composition. There appears to be no difference in lean versus normal fat or between bone mineral content and density of knockout and wild-type littermate controls.

Microarray of StARD4 Mice

The effect of StARD4 knockout on liver gene expression was next examined, by extracting RNA from the livers of 4 StARD4 knockout and 4 wild-type mice at 12 weeks of age. Each of these RNA samples were analyzed separately. The RNA was analyzed using the Illumina Mouse-Ref-8 array, which evaluates expression of over 23,000 genes.

The data was analyzed with GeneSpring GX 10 software. As a first step, I determined whether the StARD4 knockout and wild type data differed in their output readings (i.e. were there differences that can linked back to differences in plate reading, fluorescence level, etc.). If this were the case, it is necessary to normalize the 2 data sets so that they could be compared. Since this was not the case I did not apply normalization prior to comparison of each sample group expression profile (Figure 2.12).

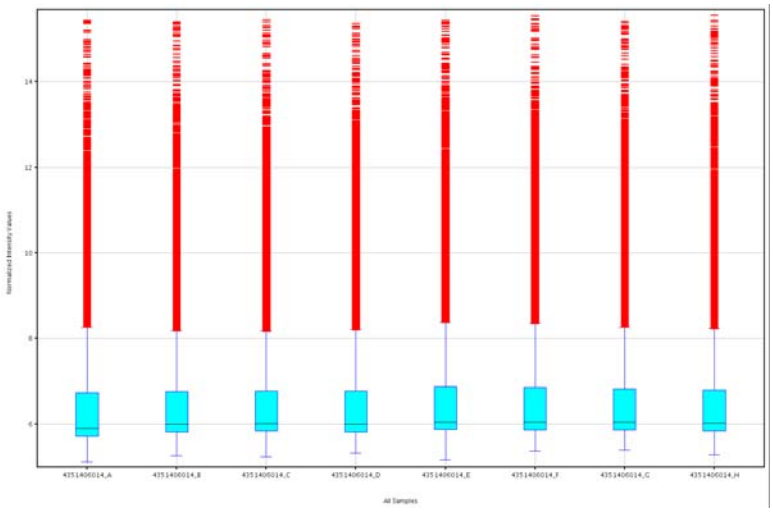

Figure 2.12 - Non-normalized Data of Microarray of StARD4 Mice
RNA from Liver of 12 week old mice analyzed with the Illumina Mouse-Ref-8 gene chip. Picture above represents all eight samples with no normalized expression patterns.

Expression profiles were then compared between StARD4 knockout and wild type mice. I found only 2 genes that showed a 2-fold difference in expression; LCN2 & HAMP. There were 10 genes with greater than a 1.5-fold difference in expression, 20 genes greater than 1.4-fold, 38 genes greater than 1.3-fold, 84 genes greater than 1.2-fold and 1,371 genes greater than 1.1-fold. Comparing expression of these genes between StARD4 knockout and wild type mice by an unpaired t-test revealed no significance difference between the genotypes at the $P<0.05$ level for any expression fold change above 1.1. When fold change was lowered to low level fold changes, such as 1.036, was a list of 288 genes extracted that had significant changes, $P<0.05$ (these genes also survived basic multiple testing corrections otherwise known as Bonferroni Hochberg false discovery rate testing). Given the putative role of StARD4 in intracellular cholesterol transport, surprisingly we did not find expression differences between the genotypes in genes known to play roles in hepatic cholesterol metabolism including: ABCG5/8, SREBP1a/1c/2, HMCGR, Cyp7α1, Cyp27α1, MDR2, NPLC1, LDLR, LXR, FXR, PPARα, BSEP, Insig1/2, ApoA1, ApoB and other StAR proteins (Figure 2.13).

[ko]	▲ [wt]	Unigene_ID	Symbol
0.7920798	-0.68130153		Lcn2
0.16498435	-0.48885572		Ppp1r3c
0.13858354	-0.4614581		Fgl1
0.50647354	-0.43298876		Saa2
0.40875852	-0.23970342		Saa1
0.4374863	-0.15226185		Gadd45g
0.68813026	-0.15157235		Hba-a1
0.64342797	0.007437587		Saa3
-1.1992146	0.066131234		Hamp
0.7050891	0.071314454		Slc4a1
-0.26139653	0.5368248		Hamp2

Figure 2.13 - List of Genes Who's Fold Change is Greater Than 1.391
Genes found to have fold change expression above 1.391. Many of the genes here are acute phase reaction proteins such as Saa1/2 and FGL1. Others like Hba-a1 is a hemoglobin peptide.

A few of the genes involved in cholesterol transport were examined for expression changes to verify the microarray data. These genes included StARD5, StARD1, MLN64, NPC1, NPC2, Cav-1, Cav-2. None of the genes varied from the results found on the gene chip (Figure 2.14).

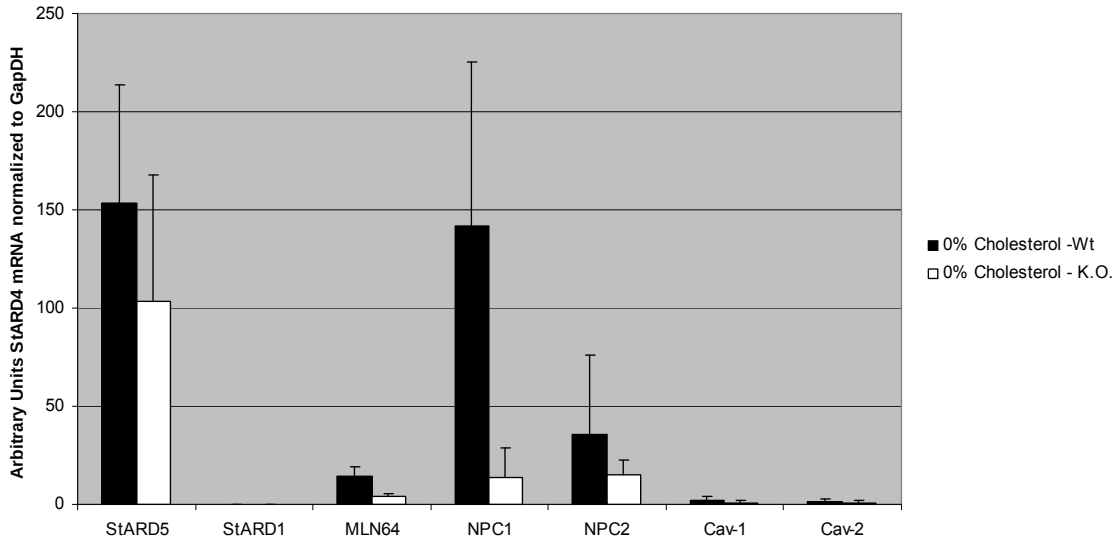

Figure 2.14 - RNA Expression Levels of Intracellular Cholesterol Transporters
Five male mice at 12 weeks of age fed a chow diet were sacrificed, their livers extracted and the RNA expression of the above genes were determined via qPCR.

The list of all genes extracted by the microarray study was then imported into Ingenuity and the Broad Institute's GSEA (gene set enrichment analysis) program to analyze for the possibility of linking genes together by network, whose otherwise small fold change might go undetected as insignificant. Ingenuity network analysis pulled out one enriched gene called HGF or hepatic growth factor. It had a 1.1 fold change above baseline and its expression is associated with a decrease in lipid droplets formation in developing mice (Tahara, Matsumoto et al. 1999). This is interesting because it has been reported that StARD4 overexpression in primary mouse hepatocytes leads to increase in lipid droplet formation (Rodriguez-Agudo, Ren et al. 2008). One would suspect decreased lipid droplet formation in a StARD4 knockout and the HGF expression increase seems to correlate with this hypothesis that StARD4 knockout would decrease lipid droplet formation.

GSEA analysis pulled out two lists of genes. One was for glutathione metabolism, while the other was for xenobiotic metabolism. The lists of these genes are reported in Table 2.7.

Table 2.7 - List of Genes Enriched by GSEA Analysis

Glutathione Metabolism	Xenobiotic Metabolism
GSTT1	ADHFE1
GPX3	GSTM2
GSTP1	GSTT2
GSTO2	CYP1B1
GSTA4	ADH4
GCLM	ADH7
GSTA3	CYP1A2
IDH2	GSTT1
MGST3	ADH5
GSTA2	GSTP1
GSTA1	GSTO2
	GSTA4
	GSTA3
	MGST3
	GSTA2
	GSTA1

0.2% Lovastatin and 0.5% High Cholesterol Feeding Study

Although a phenotype of decreased bile secretion in females of the StARD4 mice was found, no overall plasma lipid phenotype, a major marker for studying the phenomenology of atherosclerosis heart disease, was found. To study this further, two diet studies were undertaken to determine differences in the lipid profile. The diets were implemented as follows. Wild-type and knockout mice, male and female, were started at week 6 on a 0% cholesterol diet and then switched at week 7 to either a 0.2% lovastatin (0% cholesterol) enriched diet or a 0.5% high cholesterol diet. At week 8, the mice were sacrificed for analysis.

The first step in analysis was to check for the effect each diet had on StARD4 mRNA expression and protein levels. RNA was extracted from 6 wild-type mice and mRNA expression of StARD4 was measured via qPCR. Significant increase in StARD4 message was found in mice fed a 0.2% lovastatin diet, while StARD4 expression levels only increased modestly in mice fed a 0.5% cholesterol diet.

Next, protein was extracted from 2 individual wild-type mice from each diet group, and protein levels were analyzed via western blotting for StARD4. Concordant with the RNA work, StARD4 protein levels of wild-type mice on the 0.2% lovastatin diet were elevated when compared to both the 0% cholesterol control and 0.5% cholesterol diets.

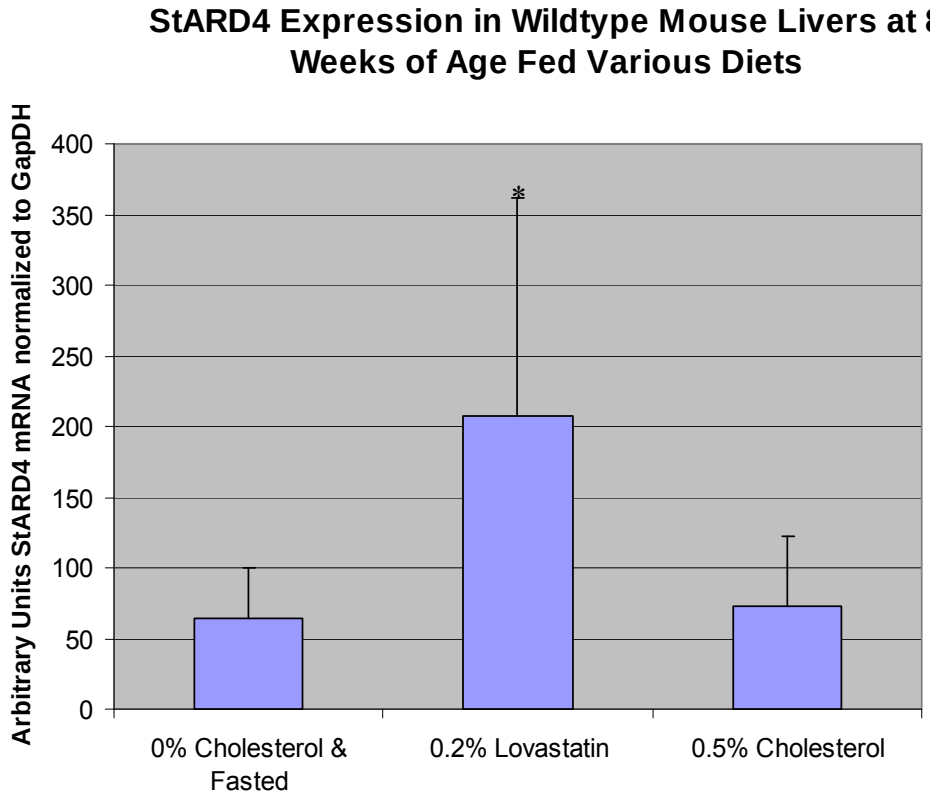

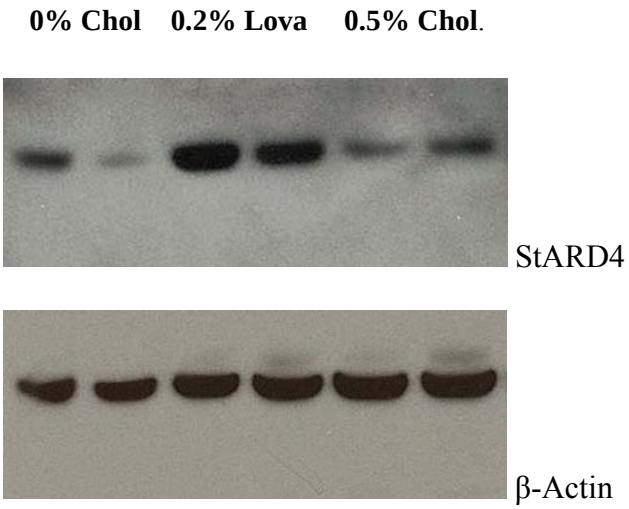

Figure 2.15 - Wild-type RNA Expression and Protein Levels of StARD4 on Three Diets

Mice at 6 weeks of age were fed 0.0% cholesterol diets for one week and then switched to either a 0.0% cholesterol diet, 0.0% cholesterol + 0.2% lovastatin diet or to a 0.5% cholesterol diet. At 8 weeks of age, mice were sacrificed. Then StARD4 expression and protein levels were delineated by qPCR or by western blotting. For RNA work *n*=6 and for protein all samples were analyzed in duplicate.

Plasma Lipid Concentrations on the 0.2% Lovastatin Diet

At 8 weeks of age, plasma lipids were compared between StARD4 knockout and wild type mice on the 0.2% lovastatin diet and no significant differences were found in levels of cholesterol, HDL, non-HDL, free cholesterol, cholesterol esters and triglycerides (Table 2.8).

Table 2.8 - Plasma Lipid Concentrations of StARD4 Mice at 8 Weeks of Age Fed a 0.2% Lovastatin Diet for One Week

	Female		Male	
	Wt	**K.O.**	**Wt**	**K.O.**
Total Cholesterol	53 +/- 12	50 +/- 16	73 +/- 12	75 +/- 20
(mg/dl) *n*=	12	12	12	9
HDL	26 +/- 8	27 +/- 7	42 +/- 15	42 +/- 10
(mg/dl) *n*=	8	7	12	9
Non - HDL	27 +/- 4	23 +/- 9	31 +/- 3	33 +/- 10
(mg/dl) *n*=	8	7	12	9
(calculated)				
Free Cholesterol	14 +/- 4	13 +/- 6	19 +/- 4	21 +/- 4
(mg/dl) *n*=	12	12	12	9
Cholesterol Ester	39 +/- 10	33 +/- 17	54 +/- 9	45 +/- 18
(mg/dl) *n*=	12	12	12	9
Triglycerides	34 +/-17	35 +/-14	39 +/- 12	35 +/- 14
(mg/dl) *n*=	12	12	12	9

All values are means All values are means +/- Std.
n = number of mice per sample.
All *p*-values were insignificant.

Hepatic Lipid Concentraions on the 0.2% Lovastatin Diet.

At 8 weeks of age, hepatic lipids were extracted by the Folch method from StARD4 knockout and wild type mice and total cholesterol, free cholesterol, cholesterol ester, and triglyceride levels were determined, but no significant differences found (Table 2.9).

Table 2.9 - Hepatic Lipid Concentrations of StARD4 Mice at 8 Weeks of Age Fed a 0.2% Lovastatin Diet for One Week.

	Female		Male	
	Wt	**K.O.**	**Wt**	**K.O.**
Total Chol.(mg/g)	2.4 +/- 0.5	2.9 +/- 0.9	2.8 +/- 0.6	2.4 +/- 0.7
***n*=**	11	11	12	7
Free Chol. (mg/g)	2.0 +/- 0.8	2.6 +/- 0.7	2.3 +/- 0.8	1.6 +/- 0.5
***n*=**	10	10	10	7
Chol. Ester(mg/g)	0.4 +/- 0.4	0.4 +/- 0.3	0.48 +/- 0.4	0.76 +/- 0.5
***n*=**	10	10	10	7
TG (mg/g)	13 +/- 5.2	11 +/- 5.2	9.3 +/- 3.7	7.7 +/- 3.4
***n*=**	11	11	12	7

All values are means +/- Std.
n = number of mice per sample.
All *p*-values were insignificant.

Plasma Levels on the 0.5% Cholesterol Diet

At 8 weeks of age, plasma lipids were compared between StARD4 knockout and wild type mice on a 0.5% cholesterol diet and no significant differences were found in levels of HDL, triglycerides, free cholesterol and triglycerides. However, there was a significant decrease in total cholesterol, LDL and cholesterol ester in female mice at week 8 (Table 2.10).

Table 2.10 - Plasma Lipid Concentrations of StARD4 Mice at 8 Weeks of Age Fed a 0.5% Cholesterol Diet for One Week

		Female		Male	
		Wt	**K.O.**	**Wt**	**K.O.**
Total Chol.	**(mg/dl)**	101 +/- 17	83 +/- 19 *	88 +/- 15	90 +/- 20
	***n*=**	12	12	12	9
HDL	**(mg/dl)**	28 +/- 6	23 +/- 4	35 +/- 8	34 +/- 4
	***n*=**	7	9	10	5
LDL	**(mg/dl)**	32 +/- 18	17 +/- 8 *	23 +/- 9	18 +/- 5
	***n*=**	7	9	10	5
VLDL	**(mg/dl)**	18 +/- 9	14 +/- 5	9 +/- 6	7 +/- 3
	***n*=**	7	9	10	5
Free Chol.	**(mg/dl)**	18 +/- 5	15 +/- 4	19 +/- 3	19 +/- 5
	***n*=**	12	12	12	9
Chol. Ester	**(mg/dl)**	83 +/- 14	69 +/- 17 *	69 +/- 13	72 +/- 16
	***n*=**	12	12	12	9
TG	**(mg/dl)**	24 +/- 8	24 +/- 8	26 +/- 4	27 +/- 5
	***n*=**	12	12	12	9

All values are means +/- Std.
n = number of mice per sample.
* = *p-value* < 0.05

Hepatic Lipid Levels on the 0.5% Cholesterol Diet

At 8 weeks of age, hepatic lipids were extracted by the Folch method from StARD4 knockout and wild type mice and total cholesterol, free cholesterol, cholesterol ester, and triglyceride levels were determined, but no significant differences found (Table 2.11)

Table 2.11 - Hepatic Lipid Concentrations of StARD4 Mice at 8 Weeks of Age Fed a 0.5% Cholesterol Diet for One Week

	Female		Male	
	Wt	**K.O.**	**Wt**	**K.O.**
Total Chol.(mg/g)	13 +/- 4.8	13 +/- 5.5	8.5 +/- 2.6	8.0 +/- 4.5
***n*=**	8	9	8	8
Free Chol. (mg/g)	4.9 +/- 1.2	4.2 +/- 2.1	3.1 +/- 1.1	3.0 +/- 0.8
***n*=**	8	9	8	8
Chol. Ester(mg/g)	8.0 +/- 4.6	8.6 +/- 5.2	5.4 +/- 2.2	5.0 +/- 4.6
***n*=**	8	9	8	8
TG (mg/g)	15 +/- 3.9	16 +/- 7.3	13 +/- 7	8.6 +/- 2.7
***n*=**	8	9	8	8

All values are means +/- Std.
n = number of mice per sample.
All *p*-values were insignificant.

RNA Expression of Select Genes Known to be Involved in Intracellular Cholesterol Dynamics and Metabolism.

Some of the genes that are known to play a role in intracellular cholesterol transport or metabolism, like StARD5, MLN64, NPC1, NPC2, LDLR and HMGCR, were validated for their expression levels on the 0% cholesterol, 0.2% lovastatin and 0.5% cholesterol diets. For each sample, five individual male mice were sacrificed at week 8 and RNA was extracted using standard TRIzol isolation. Interestingly, after a deeper analysis, it was found that NPC1, a gene found to be decreased 2.5 fold in the StARD4 knockout, was not one of the annotated genes present in the Illumina Mouse-Ref8 gene array. There were also significant increases in expression found for StARD5 on both the 0.2% lovastatin diet and the 0.5% cholesterol diet.

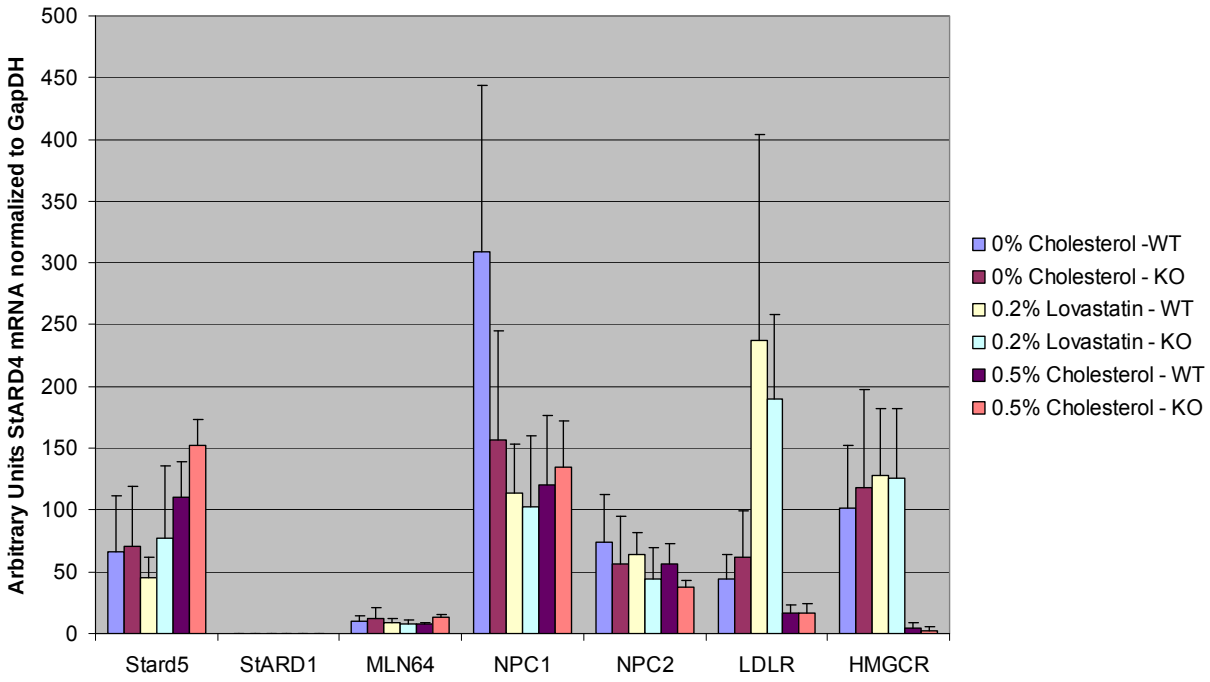

Figure 2.16 - RNA Expression Levels of Intracellular Cholesterol Transporters on Various Diets
Mice at 6 weeks of age were fed 0.0% cholesterol diets for one week and then switched to either a 0.0% cholesterol diet, 0.0% cholesterol + 0.2% lovastatin diet or to a 0.5% cholesterol diet. At 8 weeks of age, mice were sacrificed. Then RNA was extracted from livers and expression determined by qPCR.

Cholesterol Efflux from Bone Marrow Primary Macrophages

As there are two important sites implicated in the development of atherosclerosis, the liver since it is the major organ of cholesterol synthesis and the endothelial space where the actual plaque builds and ultimately ruptures, it was next prudent to check processes involved in the endothelial space of the atherosclerotic model. One of these processes and perhaps the best understood and most studied, is the process of effluxing cholesterol from macrophages to HDL particles, a part of the RCT pathway (Tall, Yvan-Charvet et al. 2008). This process is important, as it is thought

capable of removing cholesterol from the site of plaque formation, ultimately reversing the deleterious effects of high plasma cholesterol and is a major area of interest for drug development. To this end, in collaboration with one of the leading laboratories in macrophage efflux, Alan Tall's laboratory at Columbia University, efflux experiments were performed from bone marrow primary macrophages extracted from both wild-type and StARD4 knockout mice. The experiment was run under two separate conditions and with two different acceptors to test the two efflux channel proteins involved in cholesterol efflux. The conditions were with and without the LXR agonist, T0903170, which is known to stimulate cholesterol efflux (Tall, Yvan-Charvet et al. 2008). The two acceptors were HDL2 and ApoA-1. HDL2 accepts its cholesterol from the protein channel ABCG1 and ApoA-1 from ABCA1. Unfortunately, no differences were found between the StARD4 knockout and the wild-type macrophages in any of the conditions tested (Figure 2.17).

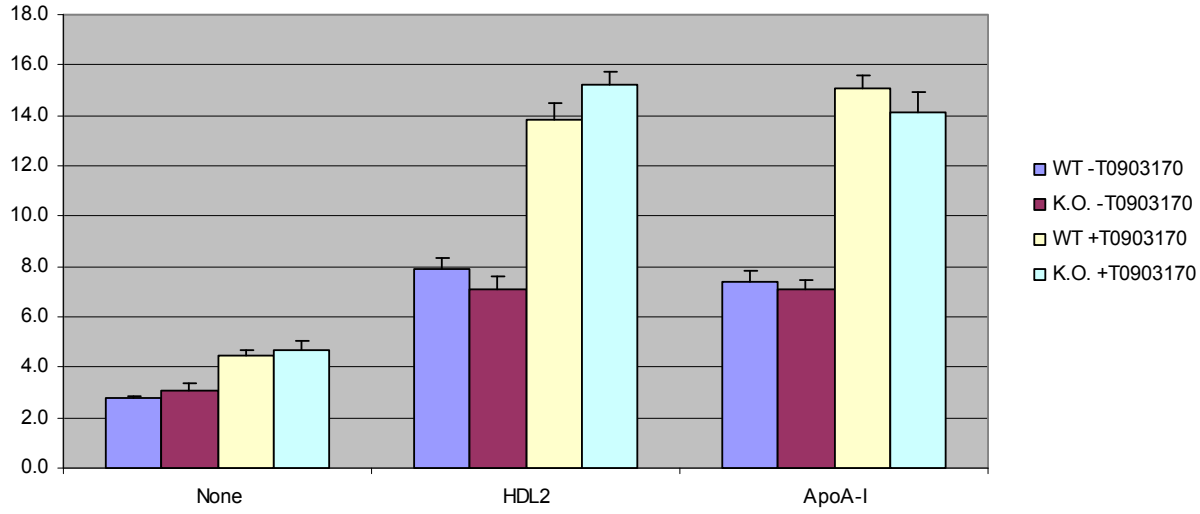

Figure 2.17 Cholesterol Efflux in Primary Bone Marrow Macrophages to HDL2 and ApoA-1 With and Without the LXR Agonist T093170
Mice at 8 weeks of age were fed a chow diet, sacrificed and their bone marrow macrophages isolated for efflux assays. Macrophages were plated 4x and either exposed to the LXR agonist T093170 or not. Then the rate of efflux of cholesterol was measured to the acceptor HDL2 or ApoA-1.

Filipin Stain

It has been shown in the Breslow lab that StARD4 knockdowns in HepG2 cells can lead to a rather profound phenotype. As the PM is the main site for storage for intracellular cholesterol (Simons and Ehehalt 2002), knockdowns appear to have a marked localization of cholesterol in the PM as shown by filipin staining. For comparison, the wild-type controls appear to have cholesterol all over the cytoplasm, indicative of its shuttling, presumably by StARD4. To verify this, primary hepatocytes of StARD4 knockouts have been isolated, cultured and then stained with filipin, in a manner similar to the cell culture work. Unfortunately, the

drastic change between PM cholesterol and intracellular cholesterol seen *in-vitro* is not as striking in the primary hepatocyte model used from StARD4 knockout mice (Figure 2.18).

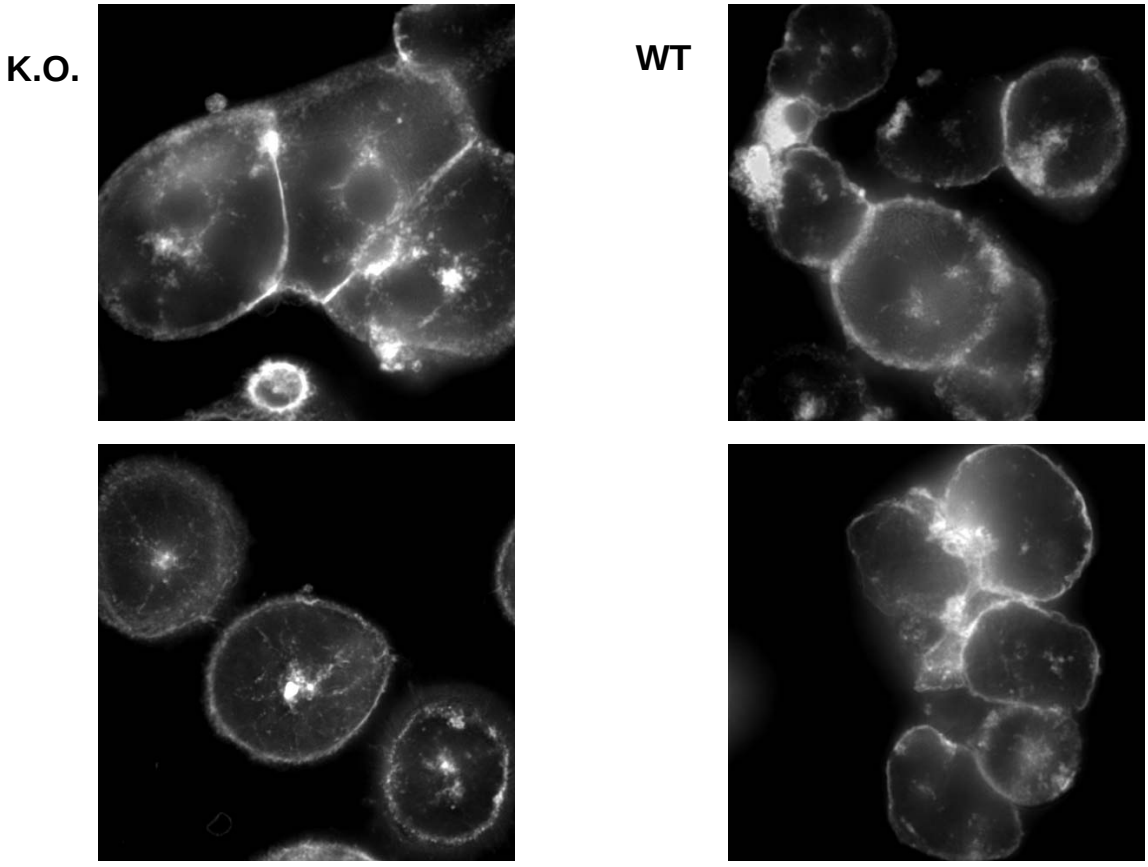

Figure 2.18 - Filipin Staining of Primary Mouse Hepatocytes
Primary hepatocytes from both StARD4 knockout and wild-type mice were isolated, seeded and ultimately stained for free cholesterol using filipin staining. Unlike the *in-vitro* model, there appeared to be no drastic change with localization of cholesterol in the plasma membrane knockout primary hepatocytes. Filipin stain is seen in white in the photo delineating the patterning of free cholesterol around the cell.

Crossing the StARD4 K.O. onto the LDLR K.O. Background

To elucidate the possible effect StARD4 has on the progression or regression of atherosclerosis, StARD4 knockout mice were crossed onto the atherosclerotic-susceptible B6.LDLR K.O. background. After weaning at 4 weeks of age, double knockout mice and their wild-type littermates were fed a low-fat, low-cholesterol, semi-synthetic diet (called the AIN76-A, Clinton Cybulsky diet) for 16 weeks (Teupser, Persky et al. 2003). The animals were sacrificed at week 20 and aortic root cross sectional lesion areas were compared between wild-type and knockout StARD4 mice. Comparisons were also made of the body weight and plasma lipids similar to what was done for the mice on a chow diet.

Plasma Lipid Concentrations on the 0.02% Cholesterol Diet

StARD4 K.O. effect on plasma lipids was next tested on the LDLR K.O. background on a 0.02% cholesterol diet. Plasma was collected at 20 weeks of age, calorimetric assays were conducted and there were no significant differences found between wild-type and knockout mice, in their overall levels of total cholesterol, HDL, LDL and VLDL. However, there was a significant decrease in triglycerides in female mice at week 20 (Table 2.12).

Table 2.12 - Plasma Lipid Concentrations of StARD4 Mice at 20 Weeks of Age Fed an AIN76a 0.02% Cholesterol Diet for 16 Weeks

		Female		Male	
		Wt	**K.O.**	**Wt**	**K.O.**
Total Chol.	**(mg/dl)**	417 +/- 179	402 +/- 193	406 +/- 163	464 +/- 145
	***n*=**	13	10	8	8
HDL	**(mg/dl)**	39 +/- 10	40 +/- 12	58 +/- 22	52 +/- 13
	***n*=**	13	10	8	8
LDL	**(mg/dl)**	127 +/- 55	150 +/- 88	200 +/- 85	263 +/- 103
	***n*=**	13	10	8	8
VLDL	**(mg/dl)**	154 +/- 91	93 +/- 46	51 +/- 31	52 +/- 40
	***n*=**	13	10	8	8
TG	**(mg/dl)**	209 +/- 91	124 +/- 57*	134 +/- 69	147 +/- 71
	***n*=**	13	10	8	8

All values are means +/- Std.
n = number of mice per sample.
* = *p*-value < 0.05

Atherosclerosis Lesions in StARD4 Mouse Aortas on the 0.02% Cholesterol Diet

Percent atherosclerotic lesion in StARD4 knockout mouse fed a 0.02% cholesterol diet was checked. To quantify cross-sectional lesion area in the aortic root, heparinized flushed hearts were embedded in OCT. Cutting was begun immediately once the valves were viewed and sections were saved on glass slides every 12μm in thickness. Sections were stained with oil red O and lesion area quantified by the level of staining of the

internal elastic lamina in every fourth section. For any mouse in which atherosclerosis was assessed, aortic root lesion area was the average of 5 of these sections. Unfortunately, no significant changes were found in the percent atherosclerotic lesions between wild-type and StARD4 knockout mice.

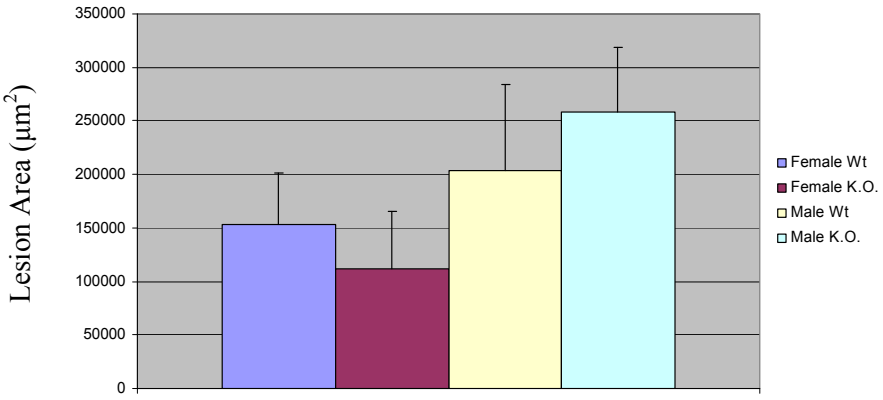

Figure 2.19 - Atherosclerotic Lesion Area in StARD4 Knockout Mice Aortas
StARD4 knockout mice and their wild-type littermates were fed a 0.02% AIN76a cholesterol diet. Atherosclerotic lesions were calculated as described above and no significant changes were found in the development of atherosclerosis in the StARD4 mouse aorta.

Summary

This chapter describes my attempts to study the physiological role of StARD4 *in-vivo* through the creation of a StARD4 knockout mouse model and the subsequent experiments completed to characterize the knockout. This work revelead some findings that can hopefully be used to build upon for future experimentation. StARD4 knockout mice do show a weight difference and although not seemingly directly linked to metabolism, there are potential other avenues discussed in later sections that can be explored to analyze StARD4's role in this context. StARD4 also showed changes in bile in female knockout mice that link its role to cholesterol excretion through the biliary system, a key component of the RCT pathway (Rodriguez-Agudo, Ren et al. 2008). Finally, StARD4 decreases another intracellular transporter, NPC1's expression. NPC1 is involved in intracellular uptake of cholesterol from endocytosed particles that enter the endosomes. Its mutation leads to a deadly disease, Niemann Pick C disease whose pathogenesis is linked to increase lipid droplet formation (Soccio and Breslow 2004). Although the connection is unclear, StARD4, likely in combination with another yet uncharacterized protein, plays a role in shuttling the cholesterol from these endosomes to their intracellular destinations.

Chapter 3: Epigenetic Regulation Of ApoA-I

To begin to analyze the transcriptional and epigenetic regulation of the ApoA-1 promoter, an *in-vitro* based experimental system was established. Previous literature has shown that ApoA-I expression is limited to the liver and intestine, with the liver being responsible for the majority of ApoA-I production (Rader 2006). Therefore, it made sense to investigate liver cells, HepG2 and HuH7, intestinal cells, Caco2 and Ls180 and a non-expressing cells like BJ and HEK-293T fibroblasts. It was hypothesized that analysis of the differences between an expressing cell line and a non-expressing cell line could help elaborate the mechanistic steps that allowed for activation of the ApoA-I promoter or conversely reveal the inhibitory mechanism that turns the ApoA-I promoter off. With this in mind, the following experiments were undertaken.

Expression of ApoA-I in Various Cell Lines

It was first necessary to experimentally verify the expression level of ApoA-1 in the various cell lines chosen, HepG2, HuH7, HEK-293T, Caco2, BJ and LS180. To do this, ApoA-I primers were designed and qPCR run on RNA collected from 3 individual cell lines of each cell type. As expected HepG2 (liver) and Caco2 (intestine) both had high levels of relative expression, while HEK-293T and BJ (fibroblast) had near baseline expression. Surprisingly, HuH7 (liver) and LS180 (intestine), cells derived from tissues thought to express ApoA-I, had near baseline expression. This

was an unexpected and potentially exciting result as it was thought that these cell lines might provide a middle ground between the expressing and non-expressing cell lines that might require fewer steps compared to non-expressing cells for activation of wild-type like level of ApoA-I expression.

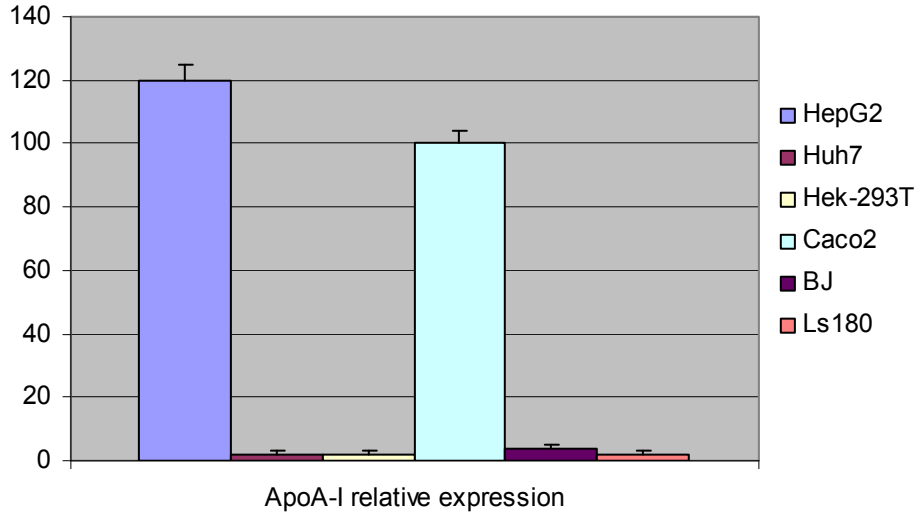

Figure 3.1 - Expression Level of ApoA-I in Various Cell Lines
qPCR was run on various cell lines, HepG2, HuH7, HEK-293T, Caco2, BJ and LS180, to check for the expression level of ApoA-I, High relative expression was found in the HepG2 and Caco2 cell line. Near baseline expression was found in the HuH7, HEK-293T, BJ and LS180 cell lines.

Perturbation of ApoA-I with 5-Aza-Deoxycytodine & Trichostatin A

To better understand the inhibitory mechanisms of ApoA-I expression, HepG2, HuH7, HEK-293T and LS180 cells were treated with two transcription "activators", 5-aza deoxycytidine, a DNA demethylating agent and trichostatin A, a HDAC inhibitor, to see if ApoA-I gene expression could be activated. This experiment was conducted with special interest in the HuH7 and Ls180 cell lines, as they are both originated from

ApoA-I expressing tissues sources, but initially had baseline ApoA-I expression. It was hoped that perhaps a one or two step treatment, could stimulate or even restore normal ApoA-I expression. To reduce the size of the experiment, only one true negative non-expressing cell line, HEK-293T and one true positive expressing cell line, HepG2, were included.

As expected, there was minimal change seen in the HepG2 cells when treated with 5-aza deoxycytidine (2.5μM) or Trichostatin A (5ng/ml). Likewise, 5-aza deoxycytidine or Trichostatin A had little effect in HEK-293T, which corroborated our initial hypothesis that these cells would have multiple levels of gene expression inhibition. However, interestingly, HuH7 when treated with 2.5 μM 5-aza deoxycytidine alone seemed to have an approximate 10 fold increase in expression over baseline. This implicated a role for methylation in the regulation of the ApoA-I promoter. Trichostatin A did not have a significant effect on the HuH7 cells, seemingly ruling out a role for histone acetylation in ApoA-I gene expression regulation. LS180 cell lines did not respond significantly to the treatments and their response was only moderate as compared to the HuH7 cells. LS180 cells were not used throughout the rest of the experiments. All quantities of 5-aza-deoxycytidine and trichostatin A were first determined with a dosing curve to determine optimal treatment levels.

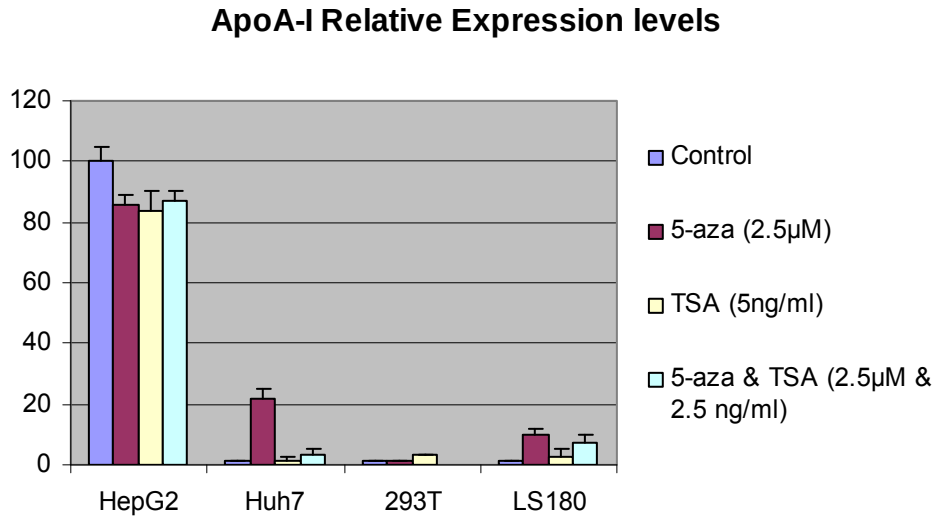

Figure 3.2 - Expression Level of ApoA-I After Treatment with 5-Aza-Deoxycytidine or Trichostatin A (TSA)
qPCR was run on various cell lines, HepG2, HuH7, HEK-293T, and LS180, to check for the expression level of ApoA-I, Cells were treated with 5-aza-deoxycytidine, trichostatin A (TSA) or both to check for perturbations in expression. High relative expression was found in the HepG2 as predicted. Near baseline expression was found in the HEK-293T and LS180 cell lines. Surprisingly, ApoA-I expression was stimulated by 5-aza-deoxycytidine treatment in HuH7 cells.

Bisulfite Sequencing of the ApoA-I Promoter

Since ApoA-I promoter methylation was previously implicated in tissue specific control of ApoA-I in embryonic cells by Razin et al., it was next examined in expressing cells, HepG2 and non expressing cells, HuH7 and HEK-293T, by bisulfite sequencing (Shemer, Kafri et al. 1991). Bisulfite sequencing acts by converting all cytosines to uracils in a stretch of DNA unless the cytosine is protected by a CpG methylation mark. Thus, when these stretches are sequenced, any cytosine that appears in the sequencing output will be from a protected methylation mark. It is in this

manner that bisulfite sequencing can determine the state of methylated in a given DNA region. A depiction of the normal ApoA-I promoter region's methylation pattern is given below (Figure 3.3).

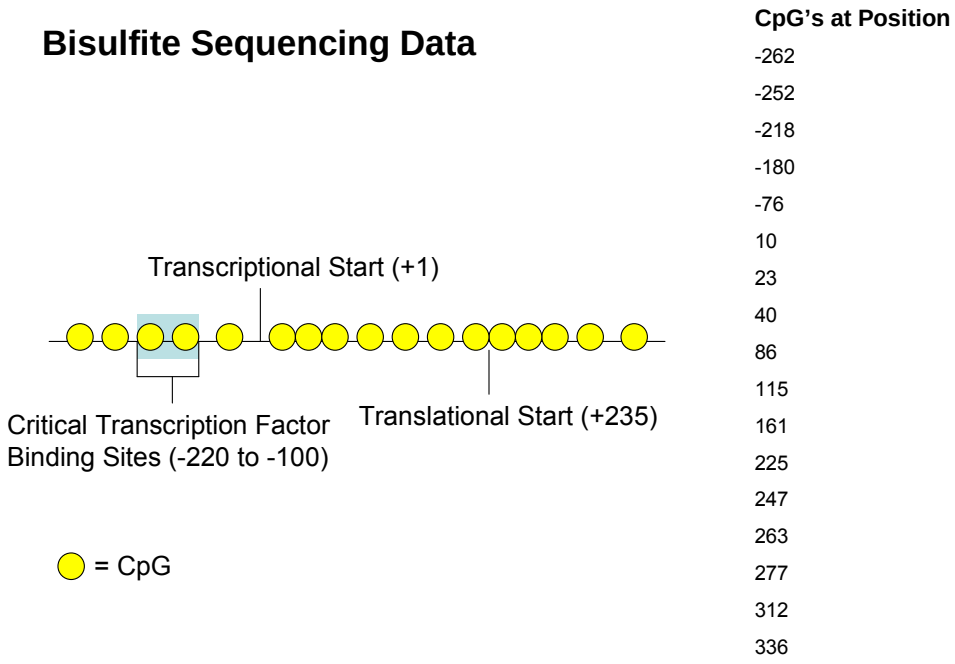

Figure 3.3 - Depiction of ApoA-I Methylation Patterning
The ApoA-I promoter between ~ -300→ 400 bp and each individual CpG island (represented by a yellow circle). The critical transcription factor binding region is represented with a blue box around it. Individual locations of CpG islands are represented to the right of the figure.

In my experimental design, particular interest was paid to the HuH7 cells, due to the increase previously found in ApoA-I expression when treated with the demethylating agent, 5-aza-deoxycytodine. The HepG2 cell line, whose ApoA-I expression is up-regulated, was used as a negative control as it was assumed it would show no signs of methylation, while the

HEK-293T were used as a positive control, since its ApoA-I expression was down-regulated and it was assumed that its ApoA-I promoter region would be highly methylated. However, it was unclear to what extent HuH7 cells lines would or would not be methylated.

As is shown in figure 3.4, HepG2 and HEK-293T cells both exhibited expected methylation patterning. HepG2, whose expression of ApoA-I is up-regulated, were unmethylated, while HEK-293T, whose expression is down-regulated, were methylated. However, HuH7 cells displayed an unexpected behavior. It appeared that all CpG islands were methylated from the critical transcription factor binding site to the CpG islands 300bp's upstream of the transcriptional start site. Conversely, the CpG islands upstream of the critical transcription factor binding site were unmethylated, in contrast to the inactivated HEK-293T cells. This was interpreted as a possible explanation for the intermediate phenotype discovered during the administration of the 5-aza-deoxycytidine. It was hypothesized that HuH7's behavior was one of a transcriptional intermediate between non-expressing and expressing cell lines and would prove a perfect candidate for further exploration of the ApoA-I promoter.

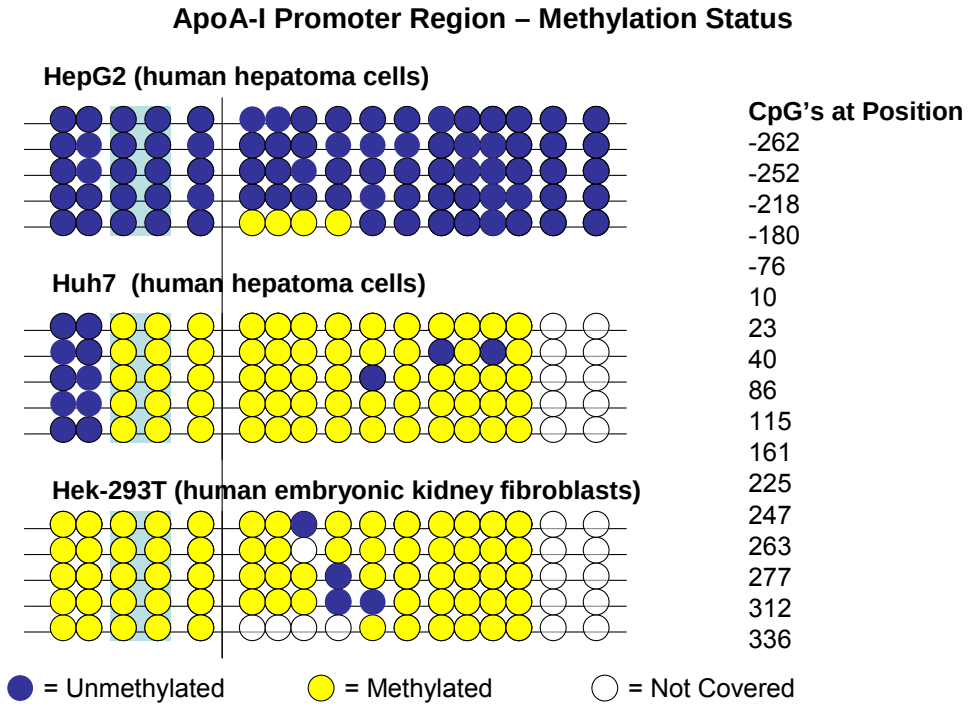

Figure 3.4 - Depiction of ApoA-I Methylation Patterning in HepG2, HuH7 and HEK-293t Cells.
The ApoA-I promoter between ~ -300→ 400 bp and each individual CpG island (represented by a yellow circle). The critical transcription factor binding region is represented with a light blue box around it. Individual locations of CpG islands are represented to the right of the figure. Blue circles represent unmethylated CpG's, yellow circles represent, methylated CpG's and clear circles represent CpG's not covered by the bisulfite sequencing. Each line represents an individual cell line's DNA, thus each experiment was done in 5 separate cell isolates.

Chromatin Immuno-Precipitation Analysis of the ApoA-I Promoter

As both a complementary and alternative approach to analyzing the ApoA-I promoter, chromatin immuno-precipitation (ChIP) was undertaken to try to localize epigenetic marks that might influence the ApoA-I promoter transcription. ChIP is similar to many traditional types of IP, but varies in that one can probe for marks that are transiently bound to DNA. This is done by crosslinking the proteins to the DNA with

formaldehyde, fragmenting the DNA into 200-800bp fragments via sonication, probing the DNA with the antibody(Ab) of choice, immunoprecipitating DNA and utilizing PCR to demonstrate the amount of protein associated with your DNA region of interest, in our case, ApoA-I. Epigenetic marks tested included, H3K27 tri-methyl, a commonly associated inhibitory mark, H3K9 di-methyl, a common inhibitory mark associated with DNA methylation inhibition, H3 acetyl and H3K9 acetyl, two common activation marks, not including the most common H3K4 tri-methyl activation mark and MBD2, the most common member of a protein family that directly binds methylation marks associated with DNA CpG islands (Jenuwein and Allis 2001). These marks were hypothesized to offer additional insights to the previously discovered methylation patterning described by bisulfite sequencing.

Initial discoveries with ChIP were inconclusive. However, it did seem to verify that inhibitory markers such as H3K9 di-methyl and H3K27 tri-methyl were present in HEK-293T cells and in HuH7 cells and not present in the HepG2 cells. Unfortunately, activation marks were not subsequently found in the HepG2 cells.

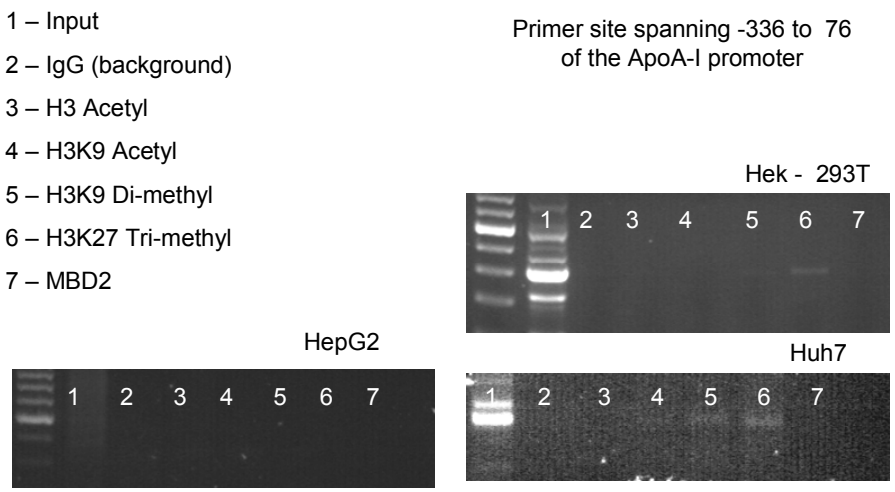

Figure 3.5 - ChiP Analysis of the ApoA-1 Region
The ApoA-I promoter was probed with the antibodies listed above. The Input is the total DNA isolated before it is exposed to any AB (positive control) and the IgG is an AB that should not immunoprecipitate anything (negative control). HepG2 cells unfortunately show now activation marks to coincide with the previous methylation pattern. HuH7 and HEK-293T both have inhibitory marks that indicate a mechanism for their phenotype. Interestingly and coinciding with the methylation work, HuH7 cells have a mark for H3K9 di-methyl, a marker for methylation inhibition.

qPCR of Various Liver Proteins and Methyl Binding Factors

Next, relative expression levels of two other common liver enriched proteins, ApoE and Albumin were measured in all three cell lines. This was done to check that the expression patterning found, specifically in HuH7, was due to actual changes in ApoA-I regulation and not an idiosyncrasy of HuH7 cells themselves, in comparison to HepG2 expression profiles. Additionally, I checked the expression of genes in the methyl binding family, MBD1, MBD2, MeCP2-1 and Kaiso to see if one in particular had an elevated expression pattern.

Both Albumin and ApoE had similar expression between HepG2 and HuH7 liver cells, with no expression in the HEK-293T cells. None of the methyl binding patterns, based on mRNA expression, showed striking differences between the cell lines.

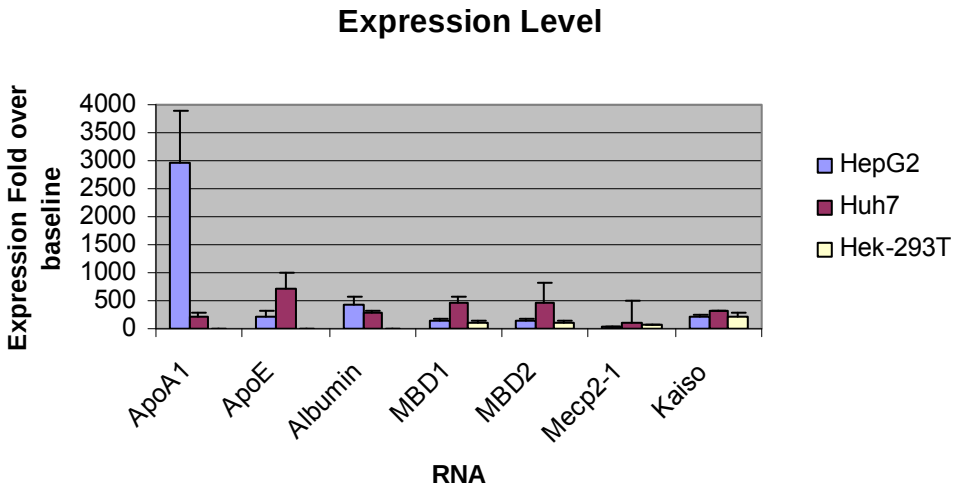

Figure 3.6 - qPCR of HepG2, HuH7 and HEK-293T Cell Lines With Common Liver and Methyl Binding Protein Primers
qPCR was run on three individual samples from HepG2, HuH7 and HEK-293T cells to check for expression patterning of the above listed genes.

Expression of ApoA-I in a New Set of HuH7 Cell Lines

To more precisely quantify ApoA-I expression absolute expression levels were determined in each cell line. At this time, it was necessary to thaw a new vial of cells, as the cells used for the last experiments were utilized and no cells remained cultivated in cell culture. Much to our surprise, the new vials of cells had a different patterning of ApoA-I expression as compared to our original results. Specifically, the new thawed HuH7 cells had higher levels of ApoA-I expression than initially

reported. This raised concerns and required the repetition of initial experiments.

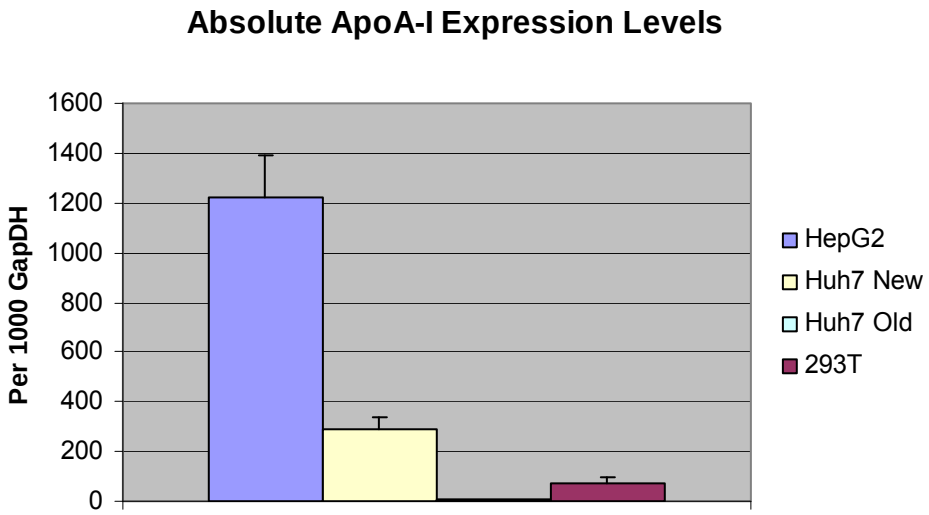

Figure 3.7 - Absolute qPCR of HepG2, HuH7 and HEK-293T Cell Lines With the ApoA-I Primers
qPCR was performed on three individual samples from all cell lines. Absolute levels of ApoA-I was highest in the HepG2 cells, with a little bit lower levels in the HuH7-new cells and baseline levels in the HuH7-old cells and HEK-293T cells.

5-Aza-Deoxycytidine Treatment of the New Set of HuH7 Cells

With the expression pattern of ApoA-I in HuH7 cells called into question, it was important to test the effect of 5-aza-deoxycytidine on the new HuH7 cells. This experiment was also repeated in HepG2 and HEK-293T cells as positive and negative controls, respectively. The cells were exposed to the two most common amounts of 5-aza-deoxycytidine, 2mM and 5mM. All numbers reflected in this experiment are absolute expression levels. Unfortunately, once the experiment was completed, it was revealed that the 5-aza-deoxycytidine treatment had no effect on the freshly thawed vial of HuH7 cells (Figure 3.8).

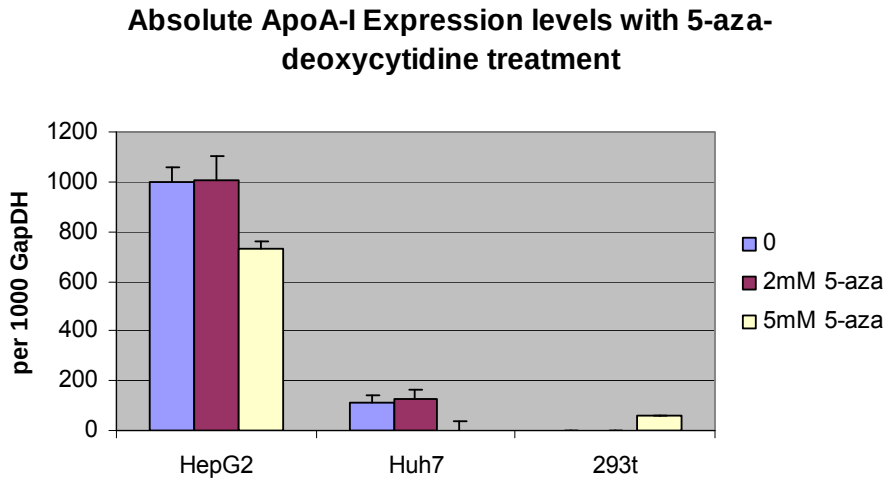

Figure 3.8 - Absolute qPCR of HepG2, New HuH7 and HEK-293T Cell Lines treated with 5-AZA-Deoxycytdine and probed with ApoA-I Primers
qPCR was run on three individual samples from all cell lines. Absolute levels of ApoA-I was highest in HepG2 and did not seem to vary in any of the lanes treated with 5-aza-deoxycytidine. This is contradictory to what we saw earlier with the old HuH7 cells.

Re-Sequencing of the Original Set of HuH7 Cells

Based on the previous two experiments, I decided to sequence the promoter regions of the cell lines and extend the bisulfite sequence to regions farther upstream of the promoter. The sequencing results revealed that the original HuH7 cell line, but not the freshly thawed vial, had a DNA deletion in the -500 to -550 region upstream of the ApoA-1. This area might be essential for binding of various elements of the transcriptional machinery and might explain the increased expression initially reported in HuH7 cells. It might also explain why that region, which was reanalyzed for CpG islands, remained unmethylated.

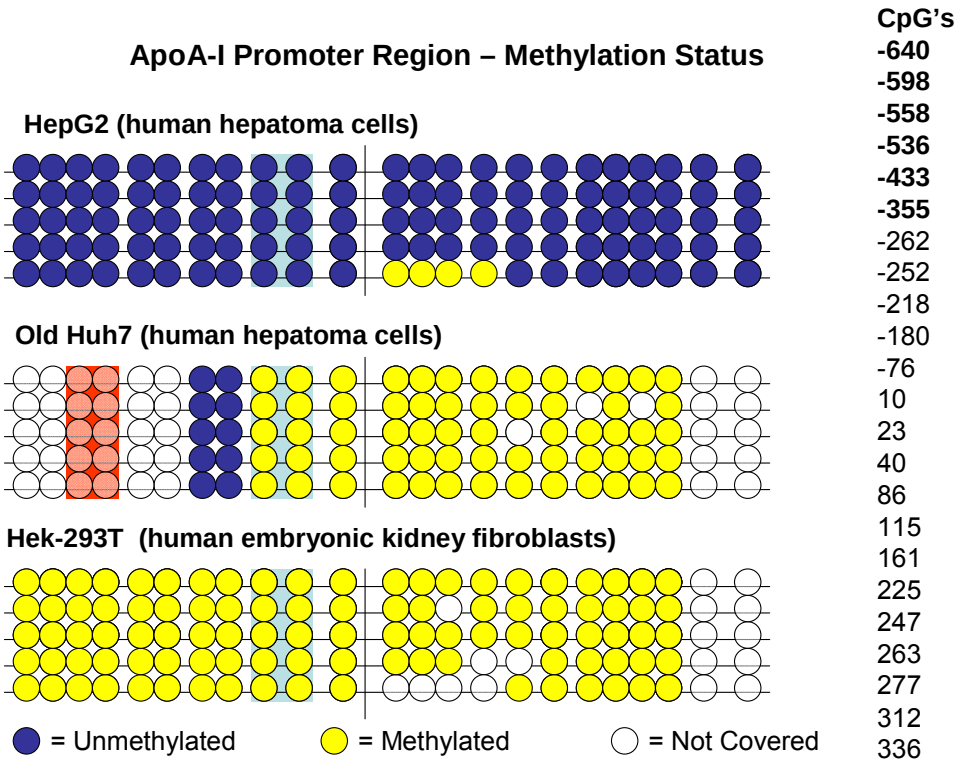

Figure 3.9 - Sequencing and Extended Bisulfite Coverage of the ApoA-I promoter Analysis of the HepG2, old HuH7 and HEK-293T cells was furthered by sequencing the promoter and extending the bisulfite analysis upstream of what was previously done. Sequencing revealed a deletion (represented in red) in the ApoA-I promoter of original HuH7 cells that could explains its increased expression patterning as compared to the same cell line thawed from a different vial.

The promoter deletion discovered in the original HuH7 cells invalidated much of my initial efforts to try and describe an intermediary step between the HepG2 activated state and the HEK-293T inhibitory state. It is possible that the discrepancy found between the two cells lines was due to a mutation that occurred due to the passaging of the original cells too many times. However, this problem still remains unsolved. Although, it would still be interesting to analyze the machinery controlling ApoA-I expression, by ChIP and other techniques, much of the work done initially

for this thesis was no longer insightful. At this point, further progress on the StARD4 project was being made and it was collectively decided to proceed in that direction.

Summary

Due to the difficulties encountered while analyzing the ApoA-I promoter and the timing of the project with the StARD4 mouse, much of the work on the ApoA-I promoter and its transcriptional machinery was abandoned. However, this remains a viable and open area of research. There remains critical issues to uncover about the mechanisms controlling the ApoA-I transcriptional machinery. The bisulfite sequencing experiment showed here the extent of the unmethylation of an activated ApoA-I gene. ChIP experiments gave hints to the role of H3K27 and H3K9 in inhibition of the ApoA-I gene. Further studies, described in greater detail in the final chapter of this thesis, will elucidate mechanism that will provide crucial insight into the machinery that controls ApoA-I and hopefully lead to a therapeutic remedy to help patients continue to manage their cholesterol in the hopes of preventing future cardiovascular events.

Chapter 4: Materials and Methods

Animals and Diets:

All animal protocols were approved by The Rockefeller University Animal Care and Use Committee. All mice were bred and housed at the Rockefeller University Laboratory Animal Research Center in a single humidity and temperature controlled room with a 12h dark-light cycle.

Fertility and Number Offspring Born/Pregnancy: To assess fertility and number offspring born/pregnancy, littermate knockout males (> 6 weeks old) were placed in cages with mature wild-type females for 1 month or longer. The same was done for female knockouts. All offspring was subsequently recorded.

Mice: Wild-type C57BL/6 male mice were obtained from the Jackson Laboratory (stock no. 00664). ACTFLPe transgenic mice on the C57BL/6 background were obtained from the Jackson Laboratory (B6.Cg-Tg (ACTFLPe) 9205Dym/J, stock no. 005703, henceforth called Flp). These mice express flippase in all mouse tissues. CMV-Cre transgenic on the C57BL/6 background were obtained from the European Mutant Mouse Archive (EMMA) (B6.129P2-Tg(CMV-cre)1Cgn/CgnIbcm, stock no. 01149, henceforth called CMVCre). These mice express Cre-recombinase in all mouse tissues. Alb-Cre transgenic mice on the C57BL/6 background were obtained from the Jackson Laboratory (B6.Cg-Tg(Alb-cre)21Mgn/J, stock no. 003574, henceforth called Alb-Cre). These mice express Cre-

recombinase in hepatocytes. LysM-Cre transgenic mice on the C57BL/6 background were obtained from Ira Tabas. These mice express Cre-recombinase mainly in the reticuloendothelial system, particularly macrophages. LDLR–/– mice on the C57BL/6 background were obtained from the Jackson Laboratory (B6.129S7-Ldlrtm1Her/J, stock no. 02207, henceforth called LDLR–/–). Albino mice on the C57BL/6 background were obtained from the Jackson Laboratory (B6(Cg)-Tyrc-2J/J, stock no. 000058, henceforth called albino).

To assess fertility, one littermate female or male (>6 weeks old) was placed in a cage with a littermate of the opposite sex for 1 month or more. The number of female mice achieving pregnancy and the number of offspring from each pregnancy was recorded.

Dietary Studies: Characterization of StARD4 knockout mice was done on animals fed a chow diet ad libitum (PicoLab Rodent Diet 20). Unless otherwise indicated, mice were weaned at 4 weeks of age, fed the chow diet for 8 weeks, and then experimented on and sacrificed at 12 weeks of age

A comparison of the effects of different diets on StARD4 knockout mice was done by placing 6 week old mice on a modified AIN76a semi-synthetic diet (12% kcal fat and 0.00% cholesterol) (Research Diets D10001) for 1 week, whereupon the mice were split into 3 groups: a control group continued the AIN76a diet, a lovastatin group fed the AIN76a diet

plus 0.2% lovastatin (Research Diets D09020602), and a cholesterol fed group fed the AIN76a diet plus 0.5% cholesterol (Research Diets D09020601). These diets were fed for 1 week and the mice were studied and sacrificed at 8 weeks of age.

Another diet study was done by switching 8 week old chow fed StARD4 knockout mice to a high fat diet (60% kcal fat) (Research Diets D09020601-02) for 12 weeks and sacrificing them at 20 weeks of age.

Atherosclerosis studies were done on StARD4 knockout mice bred on to the LDLR-/- background. These mice were fed the modified AIN76a diet containing 0.02% cholesterol (Research Diets D00110804) from weaning at 4 weeks to sacrifice at 20 weeks of age.

Sacrifice of Animals

The general mouse sacrifice protocol was as follows. On the morning of sacrifice, food was removed from the cage early in the light cycle (~9am) and mice were fasted with free access to water for the next 6 hours (~3pm). Blood glucose levels were measured from tail blood using a glucometer (Bayer). The mice were then sedated with ketamine/xylazine, weighed, blood was removed by puncturing the right and then left heart ventricles with an EDTA coated needle, the gallbladder bile was aspirated into individual tubes and finally the mice were perfused with heparinized PBS by sticking a needle into the left ventricle and allowing the PBS to flow via the circulation. Tissues were then harvested, weighed and frozen

in liquid nitrogen and stored at -80C. For atherosclerotic studies, mice were perfused with heparinized PBS and the heart was removed by cutting halfway between the aortic root and the brachiocephalic artery. The tissue was frozen in Tissue-Tek OCT compound. The brachiocephalic artery was cut at the point where it branches from the aorta and 1mm distal to its bifurcation into the subclavian and carotid arteries.

Creation of Knockout Mice

Conditional StARD4 knockout mice were made using the recombineering method originated by Copeland (http://recombineering.ncifcrf.gov/default.asp). Freshly prepared BAC DNA (BacPac Resources http://bacpac.chori.org, clone # RP23-46E14) was used. All primer sequences used for constructing the StARD4 conditional knockout vectors are listed in Table 5.1. ROCHE Expand High-Fidelity Taq kit was used for PCR amplification using the manufacturer's instructions. PCR product purification was done with QIAGEN spin columns, followed by digestion with the appropriate restriction enzyme (NEB), and purification with QIAGEN spin columns.

The retrieval vector was generated by mixing 3 μL of PCR product 1 (A-B, NotI/HindIII), 3 μL of PCR product 2 (Y-Z, HindIII, BamHI), 2 μL of MC1TK (PL253, NotI/BamHI), 1 μL of 10x ligation buffer, and 1 μL of T4 DNA ligase. The loxP-Neo-loxP targeting vector was generated by mixing 3 μL of PCR product 1 (C-D, NotI/EcoRI), 3 μL of PCR product 2

(E-F, BamHI/SalI), 2 μL of floxed Neo cassette (PL452, EcoRI/BamHI), 1 μL of pSK+ (NotI/SalI), 1.2 μL of 10x ligation buffer, and 1 μL of T4 DNA ligase. The frt-Neo-frt-loxP targeting vector was generated by mixing 3 μL of PCR product 1 (G-H, NotI/EcoRI), 3 μL of PCR product 2 (I-J, BamHI/SalI), 2 μL of floxed Neo cassette (PL451, EcoRI/BamHI), 1 μL of pSK+ (NotI/SalI), 1.2 μL of 10x ligation buffer, and 1 μL of T4 DNA ligase. The ligation mixtures were incubated at 16°C for 2 h, and 0.5 μL was transformed by electroporation into electro-competent DH10B cells (Invitrogen).

Briefly, the recombineering steps taken were as follows. 1 μL of fresh BAC DNA (100 ng) was electroporated into EL350 cells. Concomitantly, the EL350 cells were incubated with the modified retrieval vector PL253 described above. What is unique to the recombineering protocol, is that PL253 after digestion and linearization with HindIII has two ends homologous (PCR product AB and YZ) to the StARD4 genomic region of interest. Therefore, subsequent electroporation and selection with ampicillin retrieves EL350 cells containing plasmid DNA with the StARD4 genomic DNA. Second, the plasmid DNA is extracted and recombined with the modified minitargeting vector (PL452), which adds the LoxP cassette. This plasmid is then electroporation again into El350 cells and selected by ampicillin and kanamycin. Third, Cre expression, inducible in El350 cells when put into media containing arabinose, was activated and the cassette

from PL452 was removed leaving behind a singular LoxP site. Fourth, plasmid DNA was again extracted from the EL350 cells and another two FRT sites and one Loxp site were added from the modified minitargeting vector (PL451), in the same manner described above. The plasmid DNA was once again recombined in EL350 cells, selected by ampicillin and kanamycin and correctly recombined plasmid DNA recovered. This construct would ultimately be recombined in a flippase mouse to create a StARD4 gene with two LoxP sites flanking exon 3 of StARD4.

All cloning junctions and loxP and Frt site orientations were sequence verified, using forward and reverse sequencing primers. For gene targeting, 20 μg of NotI-linearized cko-targeting vector DNA was electroporated into ES cells by The Rockefeller University Gene Targeting Facility. To screen for ES clones with homologous recombination, southern blotting with probes upstream and downstream of the targeting construct were designed. For StARD4, one positive ES clone was obtained, injected into blastocysts and implanted into carrier mouse wombs, which resulted in positive chimeras.

Table 4.1 - Primers for Recombineering

Primers for Creating StARD4cKO

Primer ID	Primer Description	Sequence
A	NotI-StARD4 promoter for	ATAATGCGGCCGCTTGATCTGTACCCGAGAGGT
B	HindIII-StARD4 promoter rev	GCAGAAGCTTTGTAGTCAGGAAAGGCCAGT
C	NotI-StARD4 intron2-3 for	ATAAGCGGCCGCGTGTGGAATGGATGTACAAT
D	EcoRI-StARD4 intron2-3 rev	GCGGGAATTCCGTGTCTGATATCAGTGCAA
E	BamHI-StARD4 intron 2-3 for	ATAAGGATCCAGAGCGTGTGAGTGGACAGT
F	SalI-StARD4 intron 2-3 rev	GTCAGTCGACTTTCAGTAGCTCAGAGATCC
G	NotI-StARD4 intron3-4 for	TTATGCGGCCGCCAGAGATGAATACTCAGCAT
H	EcoRV-StARD4 intron3-4 rev	CCACGATATCCAATCTTCCTGTCCAGGTCA
I	BamHI-StARD4 intron 3-4 for	TTACGGATCCGTCAGCAGTCTAGGAATGAG
J	SalI-StARD4 intron 3-4 rev	ATCTGTCGACAACTAGGCCAGAGGGCAAAT
Y	HindIII-StARD4 intron 4-5 for	GCCTAAGCTTCACACCCACACATGAGTGAA
Z	BamHI StARD4 intron 4-5 rev	ACATGGATCCCTCAACATTCAGAAGGAGGG

To introduce ~8.5kb BAC into PL253/Retrieval Vector
AB ~280bp
YZ ~320bp
To introduce loxPNeoLoxP (PL452) into StARD5
CD ~180bp
EF ~360bp
To introduce FrtNeoFrtLoxP (PL451) into StARD5
GH ~380bp
IJ ~300bp

Genotyping Mice

Animal tail tips were digested overnight with proteinase K and then ethanol precipitated for DNA isolation. Primers and sequences are listed in Table 5.2.

Conditions for genotyping Flp: 5 min 94^0C; 35 cycles of 30 sec 94^0C, 1 min 58^0C, 1 min 72^0C; 5 min 72^0C.

Conditions for genotyping CMV-Cre: 3 min 94^0C; 12 cycles of 20 sec 94^0C, 30 sec 64^0C, 35 sec 72^0C; 25 cycles of 20 sec 94^0C, 30 sec 58^0C, 35 sec 72^0C; 5 min 72^0C.

Conditions for genotyping Alb-Cre: 5min 94^0C; 35 cycles of 30 sec 94^0C, 1 min 51^0C, 1 min 72^0C; 5 min 72^0C.

Conditions for genotyping LDLR-/-: 5 min 94^0C; 10 cycles of 20 sec 95^0C, 30 sec 64^0C, 1 min 72^0C; 30 cycles of 20 sec 95^0C, 30 sec 58^0C, 1 min 72^0C; 5 min 72^0C.

Conditions for genotyping StARD4cko AH: 5min 94^0C; 35 cycles of 30 sec 94^0C, 45 sec 54^0C, 1:00 min 72^0C; 5 min 72^0C.

Conditions for genotyping StARD4cko CH: 5min 94^0C; 35 cycles of 30 sec 94^0C, 30 sec 62^0C, 45 sec min 72^0C; 5 min 72^0C

For StARD4cko southern blotting, genomic DNA was digested with either EcoRV (5' probe) or EcoR1 (3' probe) and probed with genomic DNA upstream or downstream of the targeted genomic sequence. All probes were labeled using the Decaprime II Kit (Ambion) and 32PdATP (GE Healthcare).

Table 4.2 - Sequences of Primers Used for Genotyping

Primers Used for PCR Genotyping

Genotype	Name of Primer	Sequence
ACTFLPe	oIMR0042	CTAGGCCACAGAATTGAAAGATCT
	oIMR0043	GTAGGTGGAAATTCTAGCATCATCC
	oIMR1348	CACTGATATTGTAAGTAGTTT
	oIMR1349	CTAGTGCGAAGTAGTGATCAG
LysM-Cre	Cre8	CCCAGAAATGCCAGATTACG
	Mlys1	CTTGGGCTGCCAGAATTTCTC
	Mlys2	TTACAGTCGGCCAGGCTGAC
CMV-Cre	oIMR0042	CTAGGCCACAGAATTGAAAGATCT
	oIMR0043	GTAGGTGGAAATTCTAGCATCATCC
	oIMR0567	ACCAGCCAGCTATCAACTCG
	oIMR0568	TTACATTGGTCCAGCCACC
Alb-Cre	oIMR0042	CTAGGCCACAGAATTGAAAGATCT
	oIMR0043	GTAGGTGGAAATTCTAGCATCATCC
	oIMR1084	GCGGTCTGGCAGTAAAAACTATC
	oIMR1085	GTGAAACAGCATTGCTGTCACTT
LDLR	IMR59	CGCAGTGCTCCTCATCTGACTTGT
	IMR46	ACCCCAAGACGTGCTCCCAGGATGA
	IMR14	AGGTGAGATGACAGGAGATC
StARD4cko deletion	StARD4 A (ex2for)	CTGGAAGGACTGTCTGATGT
	StARD4 C (ex3for)	CTGCTGACCCACTTTGTAT
	StARD4 H (int3-4rev)	CTATTCTTCTCTGAGTCCCT
floxed	StARD4 C (ex3for)	CTGCTGACCCACTTTGTAT
	StARD4H (int3-4rev)	CTATTCTTCTCTGAGTCCCT
Neo	StARD4 C (ex3for)	CTGCTGACCCACTTTGTAT
	StARD4neorev	GTAGAATTTCGACGACCTGC

Primers used For Southern Blotting

Genotype	Name of Primer	Sequence
StARD4cko Upstream	5' Upstream Forward	TCATCGATTGGGTCTGAGCA
	5' Upstream Reverse	CCAGCATGTCAAGATATACCC
Downstream	5' Upstream Forward	CTGAGAGTAGAGTGGTGTGT
	5' Upstream Reverse	ATAAGCACTGTGCACATGCC

Mouse Plasma, Liver, and Gallbladder Analysis

At sacrifice, blood was immediately centrifuged and plasma separated and kept at 4°C. Lipoproteins were isolated by sequential ultracentrifugation from 60 μl of plasma at d <1.006 g/ml [very low-density lipoprotein (VLDL)], 1.006 ≤d ≥1.063 g/ml (intermediate-density lipoprotein and LDL), and d >1.063 g/ml (high-density lipoprotein). Total

plasma and lipoprotein cholesterol were measured enzymatically (Roche/Hitachi). In each fraction you measure total cholesterol, with the cholesterol esterase present and free cholesterol, without the cholesterol esterase present and the difference is cholesterol ester. Total plasma triglycerides were measured enzymatically (Roche).

Gallbladder bile was isolated and analyzed for cholesterol, phospholipids, and bile acids enzymatically (Roche, Wako).

Total liver lipids were extracted from liver by the Folch method. Briefly, snap-frozen liver tissues (~100 mg) were homogenized with a dounce homogenizer and extracted twice with chloroform/methanol (v/v = 2:1) solution. The organic layer was dried under nitrogen gas and resolubilized in chloroform containing 2% Triton X-100. This extract was dried again and resuspended in water and then assayed for total cholesterol and triglycerides enzymatically with commercial kits as described above.

Quantification of Atherosclerosis

To quantify cross-sectional lesion area in the aortic root, heparinized flushed hearts were embedded in OCT. In cutting the aortic root, orientation is important and the heart was placed in such a way that sections were cut with the 3 aortic valves in the same plane. Cutting was begun immediately once the valves are viewed and sections were saved on glass slides every 12μm in thickness. Sections were stained with oil red O and lesion area quantified by the level of staining of the internal elastic lamina

in every fourth section. For any mouse in which atherosclerosis was assessed, aortic root lesion area was the average of 5 of these sections. To quantify cross-sectional lesion area in the brachiocephalic artery, the Y-shaped piece of brachiocephalic artery was sectioned distally to proximally at 10μm thickness, beginning from the branch point for the subclavian and carotid arteries. Atherosclerotic lesions luminal to the internal elastic lamina were quantified by oil red O-stained sections at 200, 400, and 600 mm from the branching point of the brachiocephalic into the carotid and subclavian arteries.

Intraperitoneal Glucose Tolerance Test

Intraperitoneal Glucose Tolerance Tests (IPGTT) were performed on mice 3-4 days prior to sacrifice. On the morning of the test, food was removed from the cage early in the light cycle (~9am), and mice were fasted with free access to water for the next 6 hours (~3pm). Glucose was then injected intraperitoneally in physiologic saline (2g/kg of body weight) and blood drawn from the tail vein at 0, 15, 30, 60 and 120min. Glucose levels were measured in these whole blood samples with a handheld blood glucometer (Bayer).

Body Composition Analysis

Body composition and bone mineral content and density of StARD4 knockout mice were assessed by dual energy X-ray absorptiometry (Dexa) scanning. Mice were anesthetized with isofluorane and put on the scanning

plate of the Piximus 2 (Lunar) Dexa scan. Data was collected, and following the procedure the mice were allowed to recover unaided.

Sample Preparation for Gene Expression Analysis

Total RNA was isolated from cultured cells or tissues using TRIzol reagent (Invitrogen) and then subjected to RNeasy Cleanup (Qiagen) prior to analysis of gene expression by microarray and RT-PCR. In both cases the manufacturer's instructions were followed.

Quantitative RT-PCR

For RT-PCR analysis, total RNA was treated with Dnase I (Ambion), and 1-5μg was reverse transcribed using Superscript III (Invitrogen) with random hexamer primers. A 7900HT Sequence Detection System (Applied Biosystems) was used with the thermal cycling profile, 95^0C for 10 min; 40 cycles of 95^0C 30 sec, 55^0C 30 sec, 72^0C 1 min; 95^0C 15 sec, 60^0C 20 sec, 95^0C 15 sec (dissociation curve for SYBR Green reactions) unless otherwise specified. The threshold was set in the linear range of normalized fluorescence, and a threshold cycle (Ct) was measured in each well. Each sample was amplified in duplicate for the genes of interest and the housekeeping gene, GAPDH. cDNA values for genes of interest were then normalized to the corresponding value for the housekeeping gene GAPDH and expressed as a ratio, allowing for variability in the initial quantities of mRNA used in the amplification reactions. All primers are listed in Table 5.3.

Table 4.3 - Sequences of Primers Used for qPCR

Primers Used for qPCR

Gene Name (anneal)	Name of Primer	Sequence
NPC1	NPC1-For	CTTAGTGCAGGAACTCTGTCCAGG
	NPC1-Rev	TCCACATCACGGCAGGCATTGTAC
NPC2	NPC2-For	CACTCAGTCCCAGAACAGCA
	NPC2-Rev	AGTTTCCATTCCACCACCAG
MLN64	MLN64-For	CACCTCTGGAGAAGCGTAGG
	MLN64-Rev	AGAACGAGCTCTGGAAGCTG
Caveolin 1 (56°C)	Cav1-For	GCGGTTGTACCGTGCATCAAGAG
	Cav1-Rev	CGGATGTTGCTGAATATCTTGCC
Caveolin 2 (60°C)	Cav2-For	CCTCACCAGCTCAACTCTCATCTC
	Cav2-Rev	CAGATGTGCAGACAGCTGAGG
Caveolin 3 (60°C)	Cav3-For	GGAGATAGACTTGGTGAACAGAGA
	Cav3-Rev	CAGGGCCAGTGGAACACC
StAR (48°C)	StAR-For	GCAGCAGGCAACCTGGTG
	StAR-Rev	TGATTGTCTTCGGCAGCC
StARD4	StARD4-For	GTGATGCGTTACACCACTGC
	StARD4-Rev	CCACGGACAAACTCTGGTCT
StARD5	StARD5-For	GGAAGGCAATGGAGTTTCAA
	StARD5-Rev	ATCCCACACCTCTTCTGGTG
GAPDH	GAPDH-For	AACTTTGGCATTGTGGAAGG
	GAPDH-Rev	GGATGCAGGGATGATGTTCT
LDLR (60°C)	LDLR-For	TGACTCAGACGAACAAGGCTG
	LDLR-Rev	ATCTAGGCAATCTCGGTCTCC
HMGCR (60°C)	HMGCR-For	AGCTTGCCCGAATTGTATGTG
	HMGCR-Rev	TCTGTTGTGAACCATGTGACTTC
ApoA-I	ApoA-I For	GCCTTGGGAAAACAGCTAAACC
	ApoA-I Rev	AGTTTGCTGAAGGTGGAGGTC

Illumina Microarrays

All protocols were conducted as described in the Illumina GeneChip Expression Analysis technical manual with the help of Wenxiang Zhang and Connie Zhao at the Rockefeller Genomics Facility. The quality of total RNA prepared from 10 to 20mg of wet tissue was assessed using the Agilent 2100 Bioanalyzer, RNA 6000 Nano kit (Agilent Technologies Inc., Palo Alto, CA) and manually by gel electrophoresis. Quality RNA was determined by the density of the 18s and 28S fractions and by lack of DNA contamination. ~500 ng of high quality total RNA was then biotinylated

using the Ambion Illumina TotalPrep RNA Amplification Kit (Cat# AMIL1791, Applied Biosystems, Foster City, CA).

Briefly, 500 ng of high quality total RNA was used as the template for first strand cDNA synthesis by ArrayScript reverse transcriptase with an oligo primer bearing a T7 promoter (Garofalo, Orena et al.). The single-stranded cDNA was then converted into a double-stranded DNA (dsDNA) by DNA polymerase I in the presence of /E. coli/ RNase H and DNA ligase. After column purification, the dsDNA served as a template for in vitro transcription in a reaction containing biotin-labeled UTP, unlabeled NTPs and T7 RNA Polymerase. The amplified, biotin-labeled antisense RNA (Yancey, de la Llera-Moya et al.) was column purified and checked for quality with the Agilent 2100 Bioanalyzer and the RNA 6000 Nano kit. 750 ng of RNA in 5 µl of Tris-EDTA was mixed with 10 ml of hybridization reagents and heated at 65°C for 10 minutes. After cooling to room temperature, the RNA in hybridization solution was applied to Illumina MouseRef-8 v1.1 chip. The chip was incubated for 18 hours at 58°C. After washing and staining with streptavidin-Cy3, the chip was scanned using Illumina BeadArray Reader. The standard DirectHyb Gene Expression protocol was used with the following settings: Factor=1, PMT=587, Filter=100%. The raw data was extracted using Illumina BeadStudio software without normalization.

Initial Data Analysis — Genespring GX10 software was used to quantify expression levels of all genes; default values provided by Illumina were applied to all analysis parameters. Border pixels were removed, and the average intensity of pixels within the 75th percentile of expression was computed for each probe. The average of the lowest 2% of probe intensities occurring in each of 16 microarray sectors was set as background and subtracted from all features in that sector. Probe pairs were scored as positive or negative for detection of the targeted sequence by comparing signals from the perfect match and mismatch probe features. The number of probe pairs meeting the default discrimination threshold (0.015) was used to assign a call of absent, present, or marginal for each assayed gene, and a p value was calculated to reflect confidence in the detection call. A weighted mean of probe fluorescence (corrected for nonspecific signal by subtracting the mismatch probe value) was calculated using the one-step Tukey's bi-weight estimate. This signal value, a relative measure of the expression level, was computed for each assayed gene. Global scaling was applied to allow comparison of gene signals across multiple microarrays; after exclusion of the highest and lowest 2%, the average total chip signal was calculated and used to determine what scaling factor was required to adjust the chip average to an arbitrary target of 150. All signal values from one microarray were then multiplied by the appropriate scaling factor.

Western Blotting

Proteins were isolated from cells or mouse tissues by homogenization in RIPA buffer (50 mM Tris, pH 7.4/150 mM NaCl/1 mM EDTA/0.1% SDS/1% Triton X-100/1% deoxycholate) containing complete mini protease inhibitor cocktail (Roche). Crude extracts were homogenized and then centrifuged at 16,000 x g for 10 minutes at 4^{o}C to pellet cellular debris and nuclei. Total protein concentration was measured by the BCA assay (Pierce), and 10–50 μg of protein was electrophoresed on a 4-12% Bis Tris gel and then blotted via western onto a nitrocellulose membrane. Protein detection with the following antibody dilutions were carried out: anti-StARD4, 1:200 (Santa Cruz: sc-66663) and anti-beta actin (Cell Signaling), 1:10,000. To detect the antibody-protein complexes, the SuperSignal West Pico or Femto Kits (Pierce) were used according to the manufacturer's instructions. Band intensities were measured with IMAGE Pro Plus.

Data and Statistical Analysis

All data are expressed as mean ± std. Statistical analysis was performed using the student t-test. Because normality could not be assessed for our some of the small sample sizes and non-normal distributions have been reported in previous larger atherosclerosis studies in mice, the non-parametric Mann-Whitney test was used to test significance. Significance is indicated by an asterisk in the figures/tables.

Isolation of Primary Hepatocytes

Primary hepatocytes were isolated as follows: A Rainen Instrument rabbit peristaltic pump was primed by running approximately 100ml of 70% ethanol through the tubing as a disinfectant prior to the procedure. After disinfection, the pump was rinsed with 50ml of Hanks' Balanced Salt Solution (HBSS) without Ca^{2+}. Next, all of the solutions were warmed in a 40^{o}C water bath and the pump's flow rate was adjusted to 5ml/min. While this is taking place, the collagenase solution is prepared (75mg of collegenase (Worthington – collagenase type 1) in 100ml of HBSS with Ca^{2+} for each mouse. Finally, a petri dish ready to receive each liver containing 10ml of Dulbecco's Modified Eagle Medium is placed on ice.

Once the preparation is completed, the mouse is anesthetized, exsanguinated, and perfused with heparinized saline, the abdomen is opened surgically and a catheter inserted into the inferior vena cava (IVC). In the EVC, the catheter is advanced until it reaches the liver and blood flows out easily. The catheter is then connected to the pump primed with HBSS without Ca2+, which is turned on and run for 5 minutes. To reduce leakage, the chest cavity is opened and the suprahepatic inferior vena cava is clamped. Then to allow proper perfusion the portal vein is cut. After five minutes have passed, solutions in the pump are changed and the liver is then perfused with the collagenase solution for 15 minutes. At this point

the liver, spongy and soft, is removed and placed into the Petri dish that had been set on ice. This process is then repeated for the rest of the mice

After all the mouse livers have been processed, transfer them in their petri dishes to the cell culture hood. In culture, the livers were minced with a razor blade or scalpel until they are sufficiently broken apart for cells to be isolated. Next, the livers are filtered through a cell strainer (40μm nylon mesh) into a 50ml Falcon tube. Upon completion, add DMEM to the filtrate to increase the total volume to 50 ml and then pellet the cells by centrifuging for 5 minutes at 4^{o}C (20rcf, 0 brake, 0 acceleration). To rinse the cells, aspirate off the DMEM media, add 30ml fresh DMEM, gently resuspend the cells, and the repellate them by centrifugation. Repeat this washing procedure 2 more times, but use a higher spin velocity (50-100 rcf depending on machine) to repellet the cells. Finally, once the cells are sufficiently clean, suspend the cells in DMEM and count the density with a hemicytometer. Finally, seed between 500,000 – 2,000,000 cells per well of a 6 well culture dish and culture at 37°C in 95%air/5%CO_2. The next morning cells were checked to see how well they stuck to the culture dish and experimentation was started 24-48 hours after cells settled.

Filipin Staining

It is possible to stain for the localization of free cholesterol, both in the plasma membrane and intracellular compartments, within a cultured cell *in-vitro* with a filipin stain. Initially, cells are grown by seeding 1 x 10^6

cells on a cover slip resting inside a well of a 6 well plate. Once the cells reach 80% confluence they are removed from cell culture, the media removed and filipin staining was begun; all following steps are done at room temperature. For each step, use enough media to cover the cover slip adequately as to keep the cells hydrated. First, the cells were washed three times in Medium 1 (150mM Nacl, 5mM KCL, 1mM CaCL2, 20mM Hepes pH 7.4, 2g/l glucose, H_20). Immediately after the washings, fix the cells for 20 minutes in 4% paraformaldehyde. Next, wash the cells two times in PBS, aspirate off the excess solution and incubate for 2 hours with filipin stain, 1µl per 1ml Medium 1 (Stock Solution- 50mg/ml in DMSO, Sigma – F9765; Working Solution - 50µ/ml filipin in Medium 1). A Sytox Green counterstain, 2µl per ml Medium 1, is applied to visualize the nuclei for the last 15 minutes of the 2 hour incubation (Stock Solution- 5mM , Invitrogen – S7020; Working Solution – 5µM in Medium 1). At the two hour mark, wash the cells an additional three times with Medium 1, mount the cover slips onto slides with VectaShield Mounting Solution (Vector Labs – H1000) and visualize filipin by fluorescence microscopy with excitation between 335-385 nm and emission around 420nm. Sytox green is visualized at 504/523 nm excitation/emission wavelengths. Slides can be kept in the fridge for many months without degradation of signal.

Generation of Bone Marrow Macrophages (to differentiate them into SRA Expressing Macrophages)

Bone Marrow Macrophages were generated as follows. To start, sacrifice a mouse, open up its leg cavity, clear the muscle from femur and tibia and cut of small portions from each side of the femur or tibia until the marrow, which should be red on the inside of the bone, is visible. Next, harvest the femur/tibia by flushing the opening of the bone, which should be cut enough that it allows the passage of liquid, with L-cell or Bone Marrow-derived Macrophage growth media (courtesy Tall lab – Columbia University) into a falcon tube (approximately 2ml of liquid that should be cloudy with cells). One leg (femur and tibia combined) should provide enough cells to seed 3 p100's or 60 wells of a 12 well. Cells should be plated in the special medias listed above as it encourages the cells to differentiate.

The following three days (day 2-4) should be sent watching and waiting, allowing the cells to settle. On day five, change the media and within a couple days macrophages should completely differentiate.

Cholesterol Efflux from Bone Marrow Macrophages

Cholesterol efflux from bone marrow derived macrophages was determined as follows. Bone marrow macrophages, cultured as above, are incubated for 24hrs with 1-2 μCi/ml 3H cholesterol in minimal essential media (MEM) containing 10% fetal bovine serum in 12-well plates at 37°C

and 5% CO_2. After the incubation is complete, wash the cells 3 times in PBS and enrich the cells with cholesterol by incubation for 5 hours with acetylated LDL(BTI), 50 μg protein/ml, along with 1- 2 μCi/ml 3H cholesterol (GE) in minimal essential medium (MEM) containing 10% fetal bovine serum. After the incubation, the medium is removed, the cells washed with phosphate-buffered saline (PBS) and then the cells are incubated with serum free MEM with either no acceptor, lipid free ApoA-I (10ug/ml) (BTI), or HDL (50ug/ml) (BTI). Incubation with these different acceptors was done for various lengths of time (4, 8, 24hours). Finally, the media is removed, centrifuged, and 100ul aliquots were counted in a scintillation counter. Additionally, the cells themselves were dissolved in 0.1M NaOH for several hours and 100ul aliquots were counted. The percent efflux of lipid was calculated as cpm in medium divided by the sum of the cpm in the media and in the cells. Cholesterol efflux experiments were performed in triplicate, and the data (% efflux) are expressed as mean ± std for 3-4 animals per genotype.

Bisulfite Sequencing

Bisulfite sequencing was carried out using the Qiagen Epitect Bisulfite Kit (Product # - 59104) by following the manufacturer's instructions. Briefly, prepare bisulfite mix as indicated. Mix, 1 μg of DNA with 85μl of bisulfite mix, 35 μl DNA protect buffer and use RNase-free water to bring to 140 μl final volume. Then put the reaction in a PCR

machine and run the following reaction. Denaturation for 5 minutes at 99°C, incubation for 25 minutes at 60°C, denaturation again for 5 minutes at 99°C, incubation again for 85 minutes at 60°C, denaturation a final time for 5 minutes at 99°C, incubation for 175 minutes at 60°C and finally hold for until ready at 20°C. Afterwards, centrifuge the tubes, transfer the reaction to a new 1.5µl tube and add 560µl buffer BL. Add the reaction to an epitect column and briefly spin so it sticks to the column. Wash the column with 500 µl buffer BW. Desulfonate the reaction with buffer BD (500µl), wash again with 500 µl buffer BW and then elute with 20 µl buffer EB.

Chromatin Immunoprecipitation (ChIP)

All ChIP procedures were done following the protocol provided with the Upstate Chip Kit (Catalog # 17-295). Briefly, cells were grown to 1 x 10^6 cells in a 10 cm dish. Next, crosslink the cells by adding formaldehyde directly to the culture medium to a final concentration of 1% and incubate for 10 minutes at 37°C. Aspirate off the medium and wash the cells twice with ice cold PBS containing protease inhibitors. Scrape the cells into a conical tube. Pellet the cells by spinning for 4 minutes at 200 RPM at 4°C. Resuspend the cells in 200 µl of warm SDS Lysis Buffer plus protease inhibitors and incubate on ice for 10 minutes. Sonicate the lysate to shear DNA to length of 200-1000 bp's. Keep on ice during the sonication. Add 8µl 5M NACL and reverse crosslink at 65°C for 4hrs→o/n. Centrifuge the

samples for 10 minutes at 13,000 RPM at 4°C and transfer supernatant to a new tube. Discard the pellet. Dilute the supernatant 10x in ChIP Dilution Buffer plus protease inhibitors. To reduce background, pre-clear the 2ml diluted supernatant with 75µl of Protein Agarose/Salmon Sperm DNA (50% slurry) for 30 minutes at 4°C with agitation. Pellet agarose by brief centrifugation and collect supernatant. Add AB of choice to the 2ml fraction and incubate overnight at 4°C with rotation. The next day, add 60µl of Protein A Agarose/Salmon Sperm DNA (50% slurry) for one hour at 4°C with rotation. Pellet agarose again with gentle centrifugation (700-1000 RPM, 4°C, ~ 1 minute). Wash the complex for 3-5 minutes on a rotating platform with 1ml of each of the following buffers on order, Low Salt Immune Complex Wash Buffer, High Salt Immune Complex Wash Buffer, LiCL Salt Immune Complex Wash Buffer, and 2X TE Buffer Salt Immune Complex Wash Buffer. Elute cells in 250µl of fresh elution buffer (1% SDS, 0.1M $NaHCO_3$), vortex gently and incubate at room temp for 15 minutes with rotation. Spin down agarose and carefully transfer the supernatant fraction to another tube and repeat elution. Combine eluates (500µl). Add 20µl 5M NaCL to the eluate and reverse histone crosslink for 4hrs at 65°C. Add 10µl of 0.5 M EDTA, 20µl of 1M Tris-HCL, pH 6.5 and 2µl of 10 mg/ml Proteinase K to the eluate and incubate for one hour at 45°C. Recover DNA with a phenol/chloroform extraction. Use in PCR reaction.

AB's Used - H3K9 dimethyl – Abcam catalog # ab1220, H3K27 trimethyl – Upstate catalog # 07-449, MBD2 – Upstate catalog # 07-198, H3K9 Anti Acetyl – Upstate catalog # 07-352, H3 Anti Acetyl -Upstate Catalog # 06-599.

Chapter 5: Discussion and Future Direction

Discussion of StARD4

The START domain-containing family of proteins have been shown to be involved in many pathways of intracellular lipid trafficking (Ponting and Aravind 1999; Strauss, Kishida et al. 2003; Prinz 2007). It has been proposed that all proteins with a START domain, contain a similar binding pocket, that binds varying ligands or cholesterol derivatives based on modification of that binding domain (Iyer, Koonin et al. 2001). StARD4 belongs to the StARD4 subfamily, a START domain subfamily containing StARD4, StARD5 and StARD6. StARD5 has previously been shown to bind cholesterol and 25-hydroxycholesterol while StARD4, StARD1 and MLN64 have been shown to only bind cholesterol (Rodriguez-Agudo, Ren et al. 2006; Rodriguez-Agudo, Ren et al. 2008). Unlike StARD1 and MLN64, StARD4 and StARD5 do not have N-terminal localization sequences and are therefore predicted to be cytoplasmic proteins. START domain cytoplasmic localization is not uncommon, exemplified by PCTP/StARD2, a protein that plays a crucial role in phosphatidyl choline intracellular transport (Feng, Chan et al. 2000; Kanno, Wu et al. 2007). Additionally, StARD4 and StARD5 share over 30% homology. This thesis describes the first studies completed to directly examine the role of StARD4 *in*-vivo. To this end, I created a StARD4 mouse knockout model to probe the physiological role of StARD4 in lipid metabolism.

Much to our surprise, mice homozygous for a mutation disrupting StARD4's Start domain were healthy and displayed next to no abnormalities in plasma lipid dynamics, or in liver cholesterol metabolism. Dietary manipulations, as performed in this study, had no effect on overall lipid metabolism. However, it can not be ruled out that a different dietary manipulation might be able to exacerbate the phenotype of the StARD4 knockout. Additionally, the time of exposure to a particular diet may also be of importance. Finally, although candidate experimentation was done in areas related to lipid metabolism and atherosclerosis, other organ systems such as testis or adrenal glands, related to hormone production, might also serve as areas of investigation to uncover novel effects of StARD4.

In total, six START family members have been knocked out in mice; StARD1, StARD2 (PCTP), StARD3 (MLN64), StARD11 (CERT) and StARD12 (DLC1 – deleted in liver cancer 1) and now StARD4. StARD1 knockout has provided a striking and clinically relevant phenotype as the knockout is the model used to study the human disease, congenital lipoid adrenal hyperplasia (Caron, Soo et al. 1998). Both male and female StARD1 homozygous knockout mice have female external genitalia due to a generalized defect in steroid hormone biosynthesis. Additionally, knockout mice die shortly after birth due to a generalized defect in steroid hormone production. However, it has proven difficult to uncover and characterize lipid phenotypes in the other StAR protein mouse knockout

models. Initial studies of PCTP disruption showed no difference in phospholipid metabolism, but did show increases in core body temperature and enlarged mitochondria in brown adipose tissue (van Helvoort, de Brouwer et al. 1999; Kang, Ribich et al. 2009). However, when pushed with a lithogenic diet (15% fat, 1.225% cholesterol and 0.5% sodium cholate) known to form cholesterol gallstones, PCTP knockouts showed an impaired excretion of lipid into bile and an improper balance in the bile of cholesterol to phospholipids (Kanno, Wu et al. 2007; Scapa, Pocai et al. 2008). Mice with MLN64 mutations also have no apparent abnormalities in lipid metabolism or storage when pushed with a chow, high cholesterol or high fat diet (Kishida, Kostetskii et al. 2004). StARD11 and StaRD12 are both embryonic lethal. StARD11 knockouts are embryonic lethal at day E11.5, caused by degeneration of the mitochondria (Wang, Rao et al. 2009). StARD12 knockouts are embryonic lethal at day E10.5 with defects in neural tube, brain, heart, placenta, actin filaments and focal adhesions (Durkin, Yuan et al. 2007). StARD12 heterozygous mice are phenotypically normal. This hints towards the level of complexity found between various START domain proteins that make a single mouse knockout model difficult to use for investigation of the START domain related proteins.

In support of this idea, a family of proteins related to the StAR proteins, because their ligands are cholesterol dervitives or oxysterols is the

Oxysterol Binding Proteins (OSBP). OSBPs are part of a large family of lipid binding proteins of which there are at least 12 members that play numerous roles in lipid distribution and metabolism (Prinz 2007). A large amount of the work on ORPs (oxysterol related proteins) has been done in yeast *S. cerevisiae*, which has seven OSH (OSBP homolog) proteins all with a putative sterol binding pocket(Prinz 2007). Yeast mutants for any one of the seven OSH genes have little to no defect in PM to ER sterol transfer suggesting a level of redundancy (Raychaudhuri, Im et al. 2006). However, conditional deletion of all seven genes slows exogenous sterol transport, causes vacuolar fragmentation and accumulation of lipid droplets ultimately ending in cell death (Beh, Cool et al. 2001; Beh and Rine 2004).

Overall, there are many families of intracellular transporters, including, Niemann Pick C (NPC) proteins, the caveolins, OSBP and sterol carrier protein 2 (SCP-2) that all might play some role in compensating for the missing StARD4 protein. A logical place to start would be to look at StARD5, a gene that as previously stated has 30% homology to the StARD4 protein. StARD5 mouse knockouts were created in this laboratory by a previous graduate student Marc Waase, although the data remains unpublished. Homozygous knockouts are embryonic lethal, much like StARD11 and StARD12. The lethality happens before E3.5, indicative of an issue with fertilization, cleavage and compaction, making the embryos difficult to study. Initial studies by Soccio et al. showed that StARD4 and

StARD5 are both capable of increasing cholesterol transport *in*-vitro, indicating a role for a compensatory mechanism between the two (Soccio and Breslow 2003). It might therefore be interesting to cross the StARD4 knockout with the StARD5 heterozygote. However, it should also be noted that at least in liver, StARD5 appears to be expressed in Kuppfer cells, while StARD4 is expressed in parenchymal cells.

Furthermore, it has even been suggested, that only a limited number of the genes involved in lipid transport and associated membrane trafficking have to date been identified (Chang, Chang et al. 2006). Just recently, TMEM97 has been identified by an RNAi screen as a novel transporter binding to the NPC1 protein in the regulation of endosomal uptake of cholesterol from LDL particles (Bartz, Kern et al. 2009).

It is important to emphasize that part of the construction of the knockout left room for the creation of tissue specific knockouts. Although this thesis used a CMV-cre promoter to create a ubiquitous knockout, it is possible that tissue specific knockouts, perhaps a LysM-cre promoter for macrophage specific knockout, could be used to test for the role of StARD4 as it relates to atherosclerosis. The Tabas lab has shown successful use of gene specific knockouts to show increased apoptosis in mice with macrophage specific deletion of bcl2 (Thorp, Li et al. 2009). Although in *in-vitro* bone marrow macrophage efflux assays, no significant differences were found in the rate of efflux of cholesterol to ApoA-I or HDL, it is

possible that StARD4, perhaps in combination with another protein, plays a role in the development of atherosclerosis by influencing macrophage cholesterol efflux.

Interestingly, StARD4 mice seemed to have a weight related phenotype weighing about 2 grams less than wild-type littermate controls. It seemed that this was not due to issues involving food intake and the weight difference was not affected by a high fat diet. This was suprising, but it is possible that some other metabolic change, perhaps alterations in resting thermodynamic state (a change in body heat), or in the rate of excersize of the animals can account for the weight changes. Additionally, the lengths of the animals were smaller, indicating that the size observation might be due to a more complicated metabolic defect of the StARD4 mice. It has been shown that non-steroidogenic COS-1 cells co-transfected with P450scc, 3β-hydroxysteroid reductase, necessary proteins for progesterone production, and StARD4 have mildly increased steroidogenesis (Soccio, Adams et al. 2005). So, one could speculate that the absence of StARD4 may impair steroid hormone production and compromise energy metabolics and growth (West and York 1998). However, the decreased weight and length are in proportion with the mice overall being smaller, a phenotype that is very complex and could be related to any number of factors not discussed.

Another possible clue relating to the metabolic defect affecting StARD4 relates to the AKT signaling pathway. Peripherally, the connection to Akt appears to be loose at best, although there is literature connecting Akt sequestration and signaling to lipid rafts; cholesterol rich scaffolding domains in the plasma membrane (Calay, Vind-Kezunovic et al.). However, work done by one of the post docs in the laboratory, Jeanne Garbarino, has shown that a 60% ShRNA knockdown of StARD4 in HepG2 cells cultured in lipid deficient serum (LPDS) is capable of affecting Akt phosphorylation. Specifically, of the two phosphorylation sites on Akt, serine 473 and threonine 308, StARD4 knockdown appears to decrease serine 473 activity. Serine 473 phosphorylation is required for FoxO1 phosphorylation at threonine 24, which contributes to FoxO1 inhibition via sequestration from the nucleus and increased lipogenesis. As FoxO1 is a key regulator in modulating many energy metabolic functions, such as controlling insulin and gluconeogenic genes, it is possible to see a role for StARD4's effects on Akt (Gross, Wan et al. 2009). It would therefore make sense that downstream signaling targets of StARD4 could lead to abnormal development of the StARD4 mutant mouse. Additionally, StARD4 knockdowns appear to have decreased endoplasmic reticulum cholesterol levels as found via subcellular fractionation as well as decreased cellular cholesterol ester and increased cellular triglycerides.

As support to this argument, Akt knockout mice, Akt1, Akt2 and Akt3 are all developmentally abnormal, albeit in different ways (Yang, Tschopp et al. 2004). Akt1 mutant mice are small and have increased apoptosis in their thymus (Yang, Tschopp et al. 2003). It was discovered, that Akt1 mutant mice had smaller placenta then their wild-type littermates, which deprived their embryos of normal nutrition during development and thus restricted animal growth. Akt2 plays a different role, in that it helps regulate glucose metabolism, adipogenesis and maintenance, β-cell function and animal growth (Garofalo, Orena et al. 2003). These mice also have severe diabetes and due to many complications suffer from age related loss of adipose tissue (lipoatrophy) and an overall decrease in size. Interesting to note, is that the Akt1/2 double knockout mice have severe growth retardation dying shortly after birth (Peng, Schwarz et al. 1997). It was shown that this affect was probably due to skeletal muscle atrophy and abnormal bone development. In contrast to Akt2 deficient mice, Akt3 mutant mice do not exhibit increased perinatal mortalilty. Rather, brain size and weight was reduced by 25%, attributed to a significant reduction in cell size and cell number (Yang, Tschopp et al. 2004).

Peripherally, the connection to Akt appears to be loose at best, although there is literature connecting Akt sequestration and signaling to lipid rafts; cholesterol rich scaffolding domains in the plasma membrane (Calay, Vind-Kezunovic et al.). However, work done by one of the post

doctoral fellowss in the laboratory, Jeanne Garbarino, has shown that a 60% ShRNA knockdown of StARD4 in HepG2 cells cultured in lipid deficient serum (LPDS) is capable of effecting Akt phosphorylation. Specifically, of the two phosphorylation sites on Akt, serine 473 and threonine 308, StARD4 knockdown appears to decrease serine 473 activity. Serine 473 phosphorylation is required for FoxO1 phosphorylation at threonine 24, which contributes to FoxO1 inhibition via sequestration from the nucleus and increased lipogenesis. As FoxO1 is a key regulator in modulating many energy metabolic functions, such as controlling insulin and gluconeogenic genes, it is possible to see a role for StARD4's effects on Akt (Gross, Wan et al. 2009). It would therefore make sense that downstream signaling targets of StARD4 could lead to abnormal development of the StARD4 mutant mouse. Additionally, StARD4 knockdowns appear to have decreased endoplasmic reticulum cholesterol levels as found via subcellular fractionation as well as decreased cellular cholesterol ester and increased cellular triglycerides.

Female knockout mice showed a significant impairment of cholesterol and phospholipid excretion into gallbladder bile. This is in agreement with previously published data that showed that over expression of StARD4 increased bile synthesis (Rodriguez-Agudo, Ren et al. 2008). As mentioned before, PCTP knockout mice also show an imbalance in cholesterol and phospholipids in the bile, indicating a complex mechanism

governing intracellular sterol dynamics. This same study showed that StARD4 enhanced cholesterol ester synthesis in hepatocytes from exogenous cholesterol sources. It is then tempting to postulate that the decrease in total cholesterol, LDL-C and cholesterol ester seen in females on the high cholesterol diet could somehow be mechanistically related to this earlier finding. Perhaps StARD4 plays some role in shuttling between the ER and lipid droplets.

Related to the bile phenotype found in female mice, it is known amongst physicians that females are more susceptible to gallstones, obstructive plaques in the gallbladder formed by the concentration of bile components (Kandutsch and Shown 1981). The StARD4 knockout mice that exhibited changes in bile secretion were female and thus it is interesting to hypothesize whether this sex specific phenotype holds true between mice to humans. It is known, that the primary pathophysiological defect in cholesterol gallstone disease (85% of cholelithiasis) is hypersecretion of hepatic cholesterol into bile with less frequent secretion of the two other components of bile, phospholipids and bile acids (Wang, Cohen et al. 2009). There are other known secondary gallbladder dysfunctions that contribute to gallstones including hypomotility, immune mediated inflammation, accelerated phase transitions and hypersecretion of gelling mucins (Wang, Cohen et al. 2009). StARD4 might thus be an attractive target for correcting the hypersecretion of hepatic cholesterol into

the bile. It would certainly be of interest to the pharmaceutical industry as it is estimated that 20 million Americans are affected and that this number is only rising due to the spread of the obesity epidemic (NIDDK). Considering its role in cholesterol transport, it is possible that StARD4 transports cholesterol to the ABCG5/8 transporters known to increase cholesterol gallbladder concentrations. There are other alternative pathways for cholesterol to gain entry into gallbladder bile that would also need to be investigated. Regardless, StARD4's role in delivery of cholesterol to bile would underscore its importance in the reverse cholesterol transport pathway and might highlight its significance as a possible line of treatment against gallstone disease.

It is possible that the major role of StARD4 is to transport newly synthesized cholesterol from the endoplasmic reticulum to its ultimate destination. In previous experiments, I found that wild-type and StARD4 knockout mouse macrophages pre-labeled with 3H-cholesterol did not differ in efflux of radiolabeled cholesterol to either ApoA-I or HDL. To study whether or not StARD4 transports newly synthesized cholesterol from the endoplasmic reticulum, a similar experiment could be done except macrophages would be preincubated with labeled cholesterol precursors, ^{14}C-acetate or ^{14}C-mevalonate. In addition to efflux of newly synthesized radiolabeled cholesterol, the movement of labeled cholesterol from the endoplasmic reticulum to the plasma membrane and the esterification of

labeled cholesterol in the endoplasmic reticulum by the ACAT reaction could be quantified over time.

Finally, it would be a good idea to start identifying binding partners of StARD4 *in-vitro*. A mass spectrometry experiment could identify proteins purified and pulled down along with StARD4. Does StARD4 interact with NPC1 and move around endosomes? Does it bind AKT and interact with lipid rafts in the plasma membrane? It is important to realize that these experiments might prove challenging, as StARD4 is a cytosolic protein who interactions would likely be fleeting. However, the information provided would give valuable clues about StARD4's functional role. The identity of its binding partners would help deduct where cholesterol actually docked, based on the localization of its binding partners; unless and this seems highly unlikely, it only bound other cytosolic proteins. It would be possible to take this work one step further and conduct a fluorescence resonance energy transfer (FRET) experiment between StARD4 and some of its binding partners. This would help to visualize the localization of the protein interactions in the cell. As StARD4's crystal structure has been solved, it might be possible once a binding partner is known, to reconstruct biochemically the transfer of cholesterol from a StARD4 molecule to its partner, which would be a significant breakthrough in the study of cholesterol protein transporters.

In conclusion, mutation of the START domain of StARD4, a protein thought to play a vital role in intracellular cholesterol dynamics and transport does not appear to impair cholesterol homeostasis intracellularly. These findings suggest that proteins with redundant functions exist that can supplement the role of StARD4 *in-vivo* and that the whole intracellular cholesterol milieu remains a complicated and under-developed research topic for the study of cholesterol regulation and the development of atherosclerosis.

Discussion of ApoA-I

The importance of ApoA-I as a target for increasing HDL and reverse cholesterol transport and as a candidate for development of a novel therapeutic to help regulate a patient's cholesterol levels was highlighted throughout the introductory section of this thesis. It therefore remains of great interest to the research community to continue making headway into deciphering the various transcriptional machinery controlling ApoA-I. The experiments done in the thesis highlighted the role methylation plays in facilitating transcription of ApoA-I and began to examine the ways histone marks effect transcription as well. In the next section, I will propose some future steps that can be taken to continue this line of inquiry that would hopefully shed some light on the machinery controlling the ApoA-I gene.

It would be logical to continue with the ChIP experiments to in order to determine the differential role either inhibitory mark (H3K27 tri-methyl or H3K9 tri-methyl) was playing in inhibiting ApoA-I. As each of the two genes control very different pathways, much can be learned from differential markings on ApoA-I during inhibition. H3K9 methylation by G9a, creates a binding platform for HP1 (α,β & γ) of which another protein DNMT1, a protein known to methylate stretches of genetic code, then binds, to control inhibition of certain genes (Smallwood, Esteve et al. 2007). It has been shown that a gene called Survivin can be inhibited by the recruitment of G9a, HP1 and DNMT1 alone, leading one to believe that

their might be a relatively simplified method for controlling gene repression (Smallwood, Esteve et al. 2007). In contrast, H3K27 marks when trimethylated, are known to recruit Polycomb group proteins (PcG). Polycomb proteins form multimeric complexes that exert their functions by modifying chromatin structure and by regulating the disposition and recognition of multiple post-translational histone modifications (Schuettengruber, Chourrout et al. 2007). It is therefore clear that distinguishing between these two types of marks, one relating to methylation, the other to histone modification, would be a major insight into the inhibitory state of ApoA-I. Additional ChIPs of any of the downstream marks of H3K9 or H3K27, like HP1 or Polycomb, or any of the additional marks not included here, would help reconstruct the binding complex surrounding the ApoA-I promoter. Once the marks associated with ApoA-I were established it would be interesting to do SiRNA knockdowns of any of these critical epigenetic and transcriptional marks and see in what set of combination or sequential order led to unlocking of the inhibitory marks and subsequent activation of the ApoA-I promoter.

Also interesting, would be studies *in-vitro* to try and reconstitute a chromatin with histones, associated critical histone binding proteins and the ApoA-I DNA region to see if we could create ApoA-I message from our engineered complex. Such studies have generated proof in the past for the necessity of certain transcription factors or chromatin remodeling events to

lead to the activation of a gene of interest. For example, activation of the murine-mammary-tumor-virus (MMTV) by the glucocorticoid receptor was shown to be associated with a structural change in the B nucleosome region of the viral long term repeat (Hager, Fletcher et al. 2000). This was proven by reconstituting nucleoprotein transition with chromatin assembled on MMTV long term repeat DNA with drosophila embryo extract, purified glucocorticoid receptor and HeLa cell nuclear extract. This work was then shown *in-vivo* by using a tandem array of MMTV-Ras reporter element in living cells and a form of glucocorticoid receptor labeled with GFP, which allows for direct targeting to be observed.

Some of these approaches would be extremely useful, in that they could be used to begin to map the kinetics of the interaction between ApoA-I's transcription/chromatin factors. Questions that could begin to be answered include: Is the binding transient or long lasting? How many factors are needed at one time to allow for transcription? Are any of the factors altered during the process such that transcription is inactivated? Are the remodeling events ATP dependent? These types of studies would be of interest to the general research community, as increasing ApoA-I could lead to greater HDL production and ultimately more reverse cholesterol transport. The hope of such experimention would be the creation of a novel therapeutic used to combat hypercholesteremia and ultimately decrease atherosclerosis and mortality in the world.

Finally, there are many small molecules that are being developed to enhance ApoA-I to treat atherosclerosis and Alzheimer's disease. An example is Resverlogix's RVX-208 that has already been administered for 28 days and 42 days in African green monkeys with ApoA-I levels increased 52% and HDL levels increased 75%, as compared to placebo. To date the compound is starting Phase II clinical trials. Given the nature of the development of small molecules, large library screens with the outcome predetermined and the mechanism of action not necessarily studied, understanding ApoA-I's transcriptional machinery might help predict/prevent any unwanted side effects that might occur during a large Phase III clinical trials. The benefit of this is clear and it underscores the importance of continuing research in the field of ApoAI transcription.

Publications

Original Research Articles

Riegelhaupt, **J.J.**, Waase, M.P. Garbarino J., Cruz D.E., Breslow J.L. (2009). Targeted disruption of StARD4 leads to modest weight reduction and minor alterations in lipid metabolism. *Journal of Lipid Research* (Epub).

References

Adams, S. H., C. Chui, et al. (2001). "BFIT, a unique acyl-CoA thioesterase induced in thermogenic brown adipose tissue: cloning, organization of the human gene and assessment of a potential link to obesity." Biochem J **360**(Pt 1): 135-42.

Akiyama, N., H. Sasaki, et al. (1997). "Isolation of a candidate gene, CAB1, for cholesterol transport to mitochondria from the c-ERBB-2 amplicon by a modified cDNA selection method." Cancer Res **57**(16): 3548-53.

Baez, J. M., S. E. Barbour, et al. (2002). "Phosphatidylcholine transfer protein promotes apolipoprotein A-I-mediated lipid efflux in Chinese hamster ovary cells." J Biol Chem **277**(8): 6198-206.

Baez, J. M., I. Tabas, et al. (2005). "Decreased lipid efflux and increased susceptibility to cholesterol-induced apoptosis in macrophages lacking phosphatidylcholine transfer protein." Biochem J **388**(Pt 1): 57-63.

Barter, P. J., S. Nicholls, et al. (2004). "Antiinflammatory properties of HDL." Circ Res **95**(8): 764-72.

Bartz, F., L. Kern, et al. (2009). "Identification of cholesterol-regulating genes by targeted RNAi screening." Cell Metab **10**(1): 63-75.

Beh, C. T., L. Cool, et al. (2001). "Overlapping functions of the yeast oxysterol-binding protein homologues." Genetics **157**(3): 1117-40.

Beh, C. T. and J. Rine (2004). "A role for yeast oxysterol-binding protein homologs in endocytosis and in the maintenance of intracellular sterol-lipid distribution." J Cell Sci **117**(Pt 14): 2983-96.

Bernstein, B. E., A. Meissner, et al. (2007). "The mammalian epigenome." Cell **128**(4): 669-81.

Bloch, K. (1975). "Some aspects of the control of lipid biosynthesis." Adv Exp Med Biol **60**: 1-12.

Bodzioch, M., E. Orso, et al. (1999). "The gene encoding ATP-binding cassette transporter 1 is mutated in Tangier disease." Nat Genet **22**(4): 347-51.

Bose, H., V. R. Lingappa, et al. (2002). "Rapid regulation of steroidogenesis by mitochondrial protein import." Nature **417**(6884): 87-91.

Bose, H. S., T. Sugawara, et al. (1996). "The pathophysiology and genetics of congenital lipoid adrenal hyperplasia. International Congenital Lipoid Adrenal Hyperplasia Consortium." N Engl J Med **335**(25): 1870-8.

Brown, M. L., A. Inazu, et al. (1989). "Molecular basis of lipid transfer protein deficiency in a family with increased high-density lipoproteins." Nature **342**(6248): 448-51.

Byskov, A. G., M. Baltsen, et al. (1998). "Meiosis-activating sterols: background, discovery, and possible use." J Mol Med **76**(12): 818-23.

Caron, K. M., S. C. Soo, et al. (1997). "Targeted disruption of the mouse gene encoding steroidogenic acute regulatory protein provides insights into congenital lipoid adrenal hyperplasia." Proc Natl Acad Sci U S A **94**(21): 11540-5.

Chang, T. Y., C. C. Chang, et al. (2006). "Cholesterol sensing, trafficking, and esterification." Annu Rev Cell Dev Biol **22**: 129-57.

Ching, Y. P., C. M. Wong, et al. (2003). "Deleted in liver cancer (DLC) 2 encodes a RhoGAP protein with growth suppressor function and is underexpressed in hepatocellular carcinoma." J Biol Chem **278**(12): 10824-30.

Choudhury, A., M. Dominguez, et al. (2002). "Rab proteins mediate Golgi transport of caveola-internalized glycosphingolipids and correct lipid trafficking in Niemann-Pick C cells." J Clin Invest **109**(12): 1541-50.

Claudel, T., M. D. Leibowitz, et al. (2001). "Reduction of atherosclerosis in apolipoprotein E knockout mice by activation of the retinoid X receptor." Proc Natl Acad Sci U S A **98**(5): 2610-5.

Cohen, A. W., R. Hnasko, et al. (2004). "Role of caveolae and caveolins in health and disease." Physiol Rev **84**(4): 1341-79.

Collins, J. L., A. M. Fivush, et al. (2002). "Identification of a nonsteroidal liver X receptor agonist through parallel array synthesis of tertiary amines." J Med Chem **45**(10): 1963-6.

Dansky, H. M., S. A. Charlton, et al. (1999). "Genetic background determines the extent of atherosclerosis in ApoE-deficient mice." Arterioscler Thromb Vasc Biol **19**(8): 1960-8.

de Brouwer, A. P., J. Westerman, et al. (2002). "Clofibrate-induced relocation of phosphatidylcholine transfer protein to mitochondria in endothelial cells." Exp Cell Res **274**(1): 100-11.

Dietschy, J. M. and S. D. Turley (2002). "Control of cholesterol turnover in the mouse." J Biol Chem **277**(6): 3801-4.

Drab, M., P. Verkade, et al. (2001). "Loss of caveolae, vascular dysfunction, and pulmonary defects in caveolin-1 gene-disrupted mice." Science **293**(5539): 2449-52.

Durand, S., S. Angeletti, et al. (2004). "GTT1/StarD7, a novel phosphatidylcholine transfer protein-like highly expressed in gestational trophoblastic tumour: cloning and characterization." Placenta **25**(1): 37-44.

Durkin, M. E., M. R. Avner, et al. (2005). "DLC-1, a Rho GTPase-activating protein with tumor suppressor function, is essential for embryonic development." FEBS Lett **579**(5): 1191-6.

Durkin, M. E., V. Ullmannova, et al. (2007). "Deleted in liver cancer 3 (DLC-3), a novel Rho GTPase-activating protein, is downregulated in cancer and inhibits tumor cell growth." Oncogene **26**(31): 4580-9.

Durkin, M. E., B. Z. Yuan, et al. (2007). "DLC-1:a Rho GTPase-activating protein and tumour suppressor." J Cell Mol Med **11**(5): 1185-207.

Eberle, D., B. Hegarty, et al. (2004). "SREBP transcription factors: master regulators of lipid homeostasis." Biochimie **86**(11): 839-48.

Ebisuno, S., F. Isohashi, et al. (1988). "Acetyl-CoA hydrolase: relation between activity and cholesterol metabolism in rat." Am J Physiol **255**(5 Pt 2): R724-30.

Egger, G., G. Liang, et al. (2004). "Epigenetics in human disease and prospects for epigenetic therapy." Nature **429**(6990): 457-63.

Espenshade, P. J. (2006). "SREBPs: sterol-regulated transcription factors." J Cell Sci **119**(Pt 6): 973-6.

Fairn, G. D. and C. R. McMaster (2008). "Emerging roles of the oxysterol-binding protein family in metabolism, transport, and signaling." Cell Mol Life Sci **65**(2): 228-36.

Fels, D. R. and C. Koumenis (2006). "The PERK/eIF2alpha/ATF4 module of the UPR in hypoxia resistance and tumor growth." Cancer Biol Ther **5**(7): 723-8.

Feng, L., W. W. Chan, et al. (2000). "High-level expression and mutagenesis of recombinant human phosphatidylcholine transfer protein using a synthetic gene: evidence for a C-terminal membrane binding domain." Biochemistry **39**(50): 15399-409.

Foufelle, F. and P. Ferre (2007). "[Unfolded protein response: its role in physiology and physiopathology]." Med Sci (Paris) **23**(3): 291-6.

Frank, P. G., H. Lee, et al. (2004). "Genetic ablation of caveolin-1 confers protection against atherosclerosis." Arterioscler Thromb Vasc Biol **24**(1): 98-105.

Fraser, J. D., D. Keller, et al. (1997). "Utilization of recombinant adenovirus and dominant negative mutants to characterize hepatocyte nuclear factor 4-regulated apolipoprotein AI and CIII expression." J Biol Chem **272**(21): 13892-8.

Friedland, N., H. L. Liou, et al. (2003). "Structure of a cholesterol-binding protein deficient in Niemann-Pick type C2 disease." Proc Natl Acad Sci U S A **100**(5): 2512-7.

Fu, X., J. G. Menke, et al. (2001). "27-hydroxycholesterol is an endogenous ligand for liver X receptor in cholesterol-loaded cells." J Biol Chem **276**(42): 38378-87.

Gallegos, A. M., B. P. Atshaves, et al. (2001). "Sterol carrier protein-2 expression alters plasma membrane lipid distribution and cholesterol dynamics." Biochemistry **40**(21): 6493-506.

Ginsburg, G. S., J. Ozer, et al. (1995). "Intestinal apolipoprotein AI gene transcription is regulated by multiple distinct DNA elements and is synergistically activated by the orphan nuclear receptor, hepatocyte nuclear factor 4." J Clin Invest **96**(1): 528-38.

Glomset, J. A. (1968). "The plasma lecithins:cholesterol acyltransferase reaction." J Lipid Res **9**(2): 155-67.

Goldstein, J. L. and M. S. Brown (2009). "The LDL receptor." Arterioscler Thromb Vasc Biol **29**(4): 431-8.

Goldstein, J. L., R. A. DeBose-Boyd, et al. (2006). "Protein sensors for membrane sterols." Cell **124**(1): 35-46.

Gondre-Lewis, M. C., R. McGlynn, et al. (2003). "Cholesterol accumulation in NPC1-deficient neurons is ganglioside dependent." Curr Biol **13**(15): 1324-9.

Gotto, A. M., Jr., H. J. Pownall, et al. (1986). "Introduction to the plasma lipoproteins." Methods Enzymol **128**: 3-41.

Hake, S. B. and C. D. Allis (2006). "Histone H3 variants and their potential role in indexing mammalian genomes: the "H3 barcode hypothesis"." Proc Natl Acad Sci U S A **103**(17): 6428-35.

Halama, N., S. A. Grauling-Halama, et al. (2006). "Identification and characterization of the human StARD9 gene in the LGMD2A-region on chromosome 15q15 by in silico methods." Int J Mol Med **18**(4): 653-6.

Hanada, K., K. Kumagai, et al. (2003). "Molecular machinery for non-vesicular trafficking of ceramide." Nature **426**(6968): 803-9.

Hansson, G. K. (2005). "Inflammation, atherosclerosis, and coronary artery disease." N Engl J Med **352**(16): 1685-95.

Haze, K., H. Yoshida, et al. (1999). "Mammalian transcription factor ATF6 is synthesized as a transmembrane protein and activated by proteolysis in response to endoplasmic reticulum stress." Mol Biol Cell **10**(11): 3787-99.

Homma, Y. and Y. Emori (1995). "A dual functional signal mediator showing RhoGAP and phospholipase C-delta stimulating activities." Embo J **14**(2): 286-91.

Hong, C., K. S. Moorefield, et al. (2007). "Epigenome scans and cancer genome sequencing converge on WNK2, a kinase-independent suppressor of cell growth." Proc Natl Acad Sci U S A **104**(26): 10974-9.

Horton, J. D., J. L. Goldstein, et al. (2002). "SREBPs: activators of the complete program of cholesterol and fatty acid synthesis in the liver." J Clin Invest **109**(9): 1125-31.

Huuskonen, J., V. M. Olkkonen, et al. (2001). "The impact of phospholipid transfer protein (PLTP) on HDL metabolism." Atherosclerosis **155**(2): 269-81.

Ikonen, E. (2006). "Mechanisms for cellular cholesterol transport: defects and human disease." Physiol Rev **86**(4): 1237-61.

Ikonen, E. (2008). "Cellular cholesterol trafficking and compartmentalization." Nat Rev Mol Cell Biol **9**(2): 125-38.

Isohashi, F., Y. Nakanishi, et al. (1983). "Effects of nucleotides on a cold labile acetyl-CoA hydrolase from the supernatant fraction of rat liver." Biochemistry **22**(3): 584-90.

Isohashi, F., Y. Nakanishi, et al. (1983). "Factors affecting the cold inactivation of an acetyl-coenzyme-A hydrolase purified from the supernatant fraction of rat liver." Eur J Biochem **134**(3): 447-52.

Iyer, L. M., E. V. Koonin, et al. (2001). "Adaptations of the helix-grip fold for ligand binding and catalysis in the START domain superfamily." Proteins **43**(2): 134-44.

Jamroz-Wisniewska, A., G. Wojcicka, et al. (2007). "Liver X receptors (LXRs). Part II: non-lipid effects, role in pathology, and therapeutic implications." Postepy Hig Med Dosw (Online) **61**: 760-85.

Jenuwein, T. and C. D. Allis (2001). "Translating the histone code." Science **293**(5532): 1074-80.

Joseph, S. B., E. McKilligin, et al. (2002). "Synthetic LXR ligand inhibits the development of atherosclerosis in mice." Proc Natl Acad Sci U S A **99**(11): 7604-9.

Kandutsch, A. A. and E. P. Shown (1981). "Assay of oxysterol-binding protein in a mouse fibroblast, cell-free system. Dissociation constant and other properties of the system." J Biol Chem **256**(24): 13068-73.

Kanno, K., M. K. Wu, et al. (2007). "Structure and function of phosphatidylcholine transfer protein (PC-TP)/StarD2." Biochim Biophys Acta **1771**(6): 654-62.

Kaufman, R. J., D. Scheuner, et al. (2002). "The unfolded protein response in nutrient sensing and differentiation." Nat Rev Mol Cell Biol **3**(6): 411-21.

Kishida, T., I. Kostetskii, et al. (2004). "Targeted mutation of the MLN64 START domain causes only modest alterations in cellular sterol metabolism." J Biol Chem **279**(18): 19276-85.

Ko, D. C., J. Binkley, et al. (2003). "The integrity of a cholesterol-binding pocket in Niemann-Pick C2 protein is necessary to control lysosome cholesterol levels." Proc Natl Acad Sci U S A **100**(5): 2518-25.

Krieger, M. (1999). "Charting the fate of the "good cholesterol": identification and characterization of the high-density lipoprotein receptor SR-BI." Annu Rev Biochem **68**: 523-58.

Kuivenhoven, J. A., H. Pritchard, et al. (1997). "The molecular pathology of lecithin:cholesterol acyltransferase (LCAT) deficiency syndromes." J Lipid Res **38**(2): 191-205.

Laitinen, S., M. Lehto, et al. (2002). "ORP2, a homolog of oxysterol binding protein, regulates cellular cholesterol metabolism." J Lipid Res **43**(2): 245-55.

Lala, D. S., P. M. Syka, et al. (1997). "Activation of the orphan nuclear receptor steroidogenic factor 1 by oxysterols." Proc Natl Acad Sci U S A **94**(10): 4895-900.

Lange, Y. (1991). "Disposition of intracellular cholesterol in human fibroblasts." J Lipid Res **32**(2): 329-39.

Leung, T. H., Y. P. Ching, et al. (2005). "Deleted in liver cancer 2 (DLC2) suppresses cell transformation by means of inhibition of RhoA activity." Proc Natl Acad Sci U S A **102**(42): 15207-12.

Lewis, G. F. and D. J. Rader (2005). "New insights into the regulation of HDL metabolism and reverse cholesterol transport." Circ Res **96**(12): 1221-32.

Li, J., G. Ning, et al. (2000). "Mammalian hepatocyte differentiation requires the transcription factor HNF-4alpha." Genes Dev **14**(4): 464-74.

Liscum, L. and N. J. Munn (1999). "Intracellular cholesterol transport." Biochim Biophys Acta **1438**(1): 19-37.

Liu, P., N. A. Jenkins, et al. (2003). "A highly efficient recombineering-based method for generating conditional knockout mutations." Genome Res **13**(3): 476-84.

Malik, S. (2003). "Transcriptional regulation of the apolipoprotein AI gene." Front Biosci **8**: d360-8.

Marciniak, S. J. and D. Ron (2006). "Endoplasmic reticulum stress signaling in disease." Physiol Rev **86**(4): 1133-49.

Matsunaga, T., F. Isohashi, et al. (1985). "Physiological changes in the activities of extramitochondrial acetyl-CoA hydrolase in the liver of rats under various metabolic conditions." Eur J Biochem **152**(2): 331-6.

Matthaei, K. I. (2007). "Genetically manipulated mice: a powerful tool with unsuspected caveats." J Physiol **582**(Pt 2): 481-8.

Maxfield, F. R. and I. Tabas (2005). "Role of cholesterol and lipid organization in disease." Nature **438**(7068): 612-21.

McNeish, J., R. J. Aiello, et al. (2000). "High density lipoprotein deficiency and foam cell accumulation in mice with targeted disruption of ATP-binding cassette transporter-1." Proc Natl Acad Sci U S A **97**(8): 4245-50.

Menge, T., H. P. Hartung, et al. (2005). "Statins--a cure-all for the brain?" Nat Rev Neurosci **6**(4): 325-31.

Mineo, C., H. Deguchi, et al. (2006). "Endothelial and antithrombotic actions of HDL." Circ Res **98**(11): 1352-64.

Mobius, W., E. van Donselaar, et al. (2003). "Recycling compartments and the internal vesicles of multivesicular bodies harbor most of the cholesterol found in the endocytic pathway." Traffic **4**(4): 222-31.

Moggs, J. G. and G. Orphanides (2001). "Estrogen receptors: orchestrators of pleiotropic cellular responses." EMBO Rep **2**(9): 775-81.

Moggs, J. G. and G. Orphanides (2004). "The role of chromatin in molecular mechanisms of toxicity." Toxicol Sci **80**(2): 218-24.

Moog-Lutz, C., C. Tomasetto, et al. (1997). "MLN64 exhibits homology with the steroidogenic acute regulatory protein (STAR) and is over-expressed in human breast carcinomas." Int J Cancer **71**(2): 183-91.

Moon, S. Y. and Y. Zheng (2003). "Rho GTPase-activating proteins in cell regulation." Trends Cell Biol **13**(1): 13-22.

Mukherjee, S., X. Zha, et al. (1998). "Cholesterol distribution in living cells: fluorescence imaging using dehydroergosterol as a fluorescent cholesterol analog." Biophys J **75**(4): 1915-25.

Nagaraja, G. M. and R. P. Kandpal (2004). "Chromosome 13q12 encoded Rho GTPase activating protein suppresses growth of breast carcinoma cells, and yeast two-hybrid screen shows its interaction with several proteins." Biochem Biophys Res Commun **313**(3): 654-65.

Naureckiene, S., D. E. Sleat, et al. (2000). "Identification of HE1 as the second gene of Niemann-Pick C disease." Science **290**(5500): 2298-301.

Olayioye, M. A., S. Vehring, et al. (2005). "StarD10, a START domain protein overexpressed in breast cancer, functions as a phospholipid transfer protein." J Biol Chem **280**(29): 27436-42.

Osgood, D., D. Corella, et al. (2003). "Genetic variation at the scavenger receptor class B type I gene locus determines plasma lipoprotein concentrations and particle size and interacts with type 2 diabetes: the framingham study." J Clin Endocrinol Metab **88**(6): 2869-79.

Pandak, W. M., S. Ren, et al. (2002). "Transport of cholesterol into mitochondria is rate-limiting for bile acid synthesis via the alternative pathway in primary rat hepatocytes." J Biol Chem **277**(50): 48158-64.

Parton, R. G. and K. Simons (2007). "The multiple faces of caveolae." Nat Rev Mol Cell Biol **8**(3): 185-94.

Payne, A. H. and D. B. Hales (2004). "Overview of steroidogenic enzymes in the pathway from cholesterol to active steroid hormones." Endocr Rev **25**(6): 947-70.

Peet, D. J., S. D. Turley, et al. (1998). "Cholesterol and bile acid metabolism are impaired in mice lacking the nuclear oxysterol receptor LXR alpha." Cell **93**(5): 693-704.

Peng, Y., E. J. Schwarz, et al. (1997). "Cloning, human chromosomal assignment, and adipose and hepatic expression of the CL-6/INSIG1 gene." Genomics **43**(3): 278-84.

Perry, R. J. and N. D. Ridgway (2005). "Molecular mechanisms and regulation of ceramide transport." Biochim Biophys Acta **1734**(3): 220-34.

Plump, A. S., N. Azrolan, et al. (1997). "ApoA-I knockout mice: characterization of HDL metabolism in homozygotes and identification of a post-RNA mechanism of apoA-I up-regulation in heterozygotes." J Lipid Res **38**(5): 1033-47.

Plump, A. S., C. J. Scott, et al. (1994). "Human apolipoprotein A-I gene expression increases high density lipoprotein and suppresses atherosclerosis in the apolipoprotein E-deficient mouse." Proc Natl Acad Sci U S A **91**(20): 9607-11.

Ponting, C. P. and L. Aravind (1999). "START: a lipid-binding domain in StAR, HD-ZIP and signalling proteins." Trends Biochem Sci **24**(4): 130-2.

Portincasa, P., A. Moschetta, et al. (2006). "Cholesterol gallstone disease." Lancet **368**(9531): 230-9.

Prinz, W. (2002). "Cholesterol trafficking in the secretory and endocytic systems." Semin Cell Dev Biol **13**(3): 197-203.

Prinz, W. A. (2007). "Non-vesicular sterol transport in cells." Prog Lipid Res **46**(6): 297-314.

Qiu, J. (2006). "Epigenetics: unfinished symphony." Nature **441**(7090): 143-5.

Rader, D. J. and A. Daugherty (2008). "Translating molecular discoveries into new therapies for atherosclerosis." Nature **451**(7181): 904-13.

Raghow, R., C. Yellaturu, et al. (2008). "SREBPs: the crossroads of physiological and pathological lipid homeostasis." Trends Endocrinol Metab **19**(2): 65-73.

Rao, R. P., C. Yuan, et al. (2007). "Ceramide transfer protein function is essential for normal oxidative stress response and lifespan." Proc Natl Acad Sci U S A **104**(27): 11364-9.

Rawson, R. B. (2003). "The SREBP pathway--insights from Insigs and insects." Nat Rev Mol Cell Biol **4**(8): 631-40.

Raya, A., F. Revert-Ros, et al. (2000). "Goodpasture antigen-binding protein, the kinase that phosphorylates the goodpasture antigen, is an alternatively spliced variant implicated in autoimmune pathogenesis." J Biol Chem **275**(51): 40392-9.

Raychaudhuri, S., Y. J. Im, et al. (2006). "Nonvesicular sterol movement from plasma membrane to ER requires oxysterol-binding protein-related proteins and phosphoinositides." J Cell Biol **173**(1): 107-19.

Redgrave, T. G. (2004). "Chylomicron metabolism." Biochem Soc Trans **32**(Pt 1): 79-82.

Reid, P. C., N. Sakashita, et al. (2004). "A novel cholesterol stain reveals early neuronal cholesterol accumulation in the Niemann-Pick type C1 mouse brain." J Lipid Res **45**(3): 582-91.

Repa, J. J. and D. J. Mangelsdorf (2002). "The liver X receptor gene team: potential new players in atherosclerosis." Nat Med **8**(11): 1243-8.

Rietra, P. J., K. W. Slaterus, et al. (1978). "Clostridial toxin in faeces of healthy infants." Lancet **2**(8084): 319.

Rodriguez-Agudo, D., S. Ren, et al. (2006). "Localization of StarD5 cholesterol binding protein." J Lipid Res **47**(6): 1168-75.

Rodriguez-Agudo, D., S. Ren, et al. (2008). "Intracellular cholesterol transporter StarD4 binds free cholesterol and increases cholesteryl ester formation." J Lipid Res **49**(7): 1409-19.

Scapa, E. F., A. Pocai, et al. (2008). "Regulation of energy substrate utilization and hepatic insulin sensitivity by phosphatidylcholine transfer protein/StarD2." Faseb J **22**(7): 2579-90.

Scheper, W. and J. J. Hoozemans (2009). "Endoplasmic reticulum protein quality control in neurodegenerative disease: the good, the bad and the therapy." Curr Med Chem **16**(5): 615-26.

Schroder, M. (2008). "Endoplasmic reticulum stress responses." Cell Mol Life Sci **65**(6): 862-94.

Schultz, J. R., H. Tu, et al. (2000). "Role of LXRs in control of lipogenesis." Genes Dev **14**(22): 2831-8.

Schwartz, C. C., J. M. VandenBroek, et al. (2004). "Lipoprotein cholesteryl ester production, transfer, and output *in-vivo* in humans." J Lipid Res **45**(9): 1594-607.

Seedorf, U., M. Raabe, et al. (1998). "Defective peroxisomal catabolism of branched fatty acyl coenzyme A in mice lacking the sterol carrier protein-2/sterol carrier protein-x gene function." Genes Dev **12**(8): 1189-201.

Shemer, R., S. Eisenberg, et al. (1991). "Methylation patterns of the human apoA-I/C-III/A-IV gene cluster in adult and embryonic tissues suggest dynamic changes in methylation during development." J Biol Chem **266**(35): 23676-81.

Shemer, R., T. Kafri, et al. (1991). "Methylation changes in the apolipoprotein AI gene during embryonic development of the mouse." Proc Natl Acad Sci U S A **88**(24): 11300-4.

Shemer, R., A. Walsh, et al. (1990). "Tissue-specific methylation patterns and expression of the human apolipoprotein AI gene." J Biol Chem **265**(2): 1010-5.

Shen, X., K. Zhang, et al. (2004). "The unfolded protein response--a stress signaling pathway of the endoplasmic reticulum." J Chem Neuroanat **28**(1-2): 79-92.

Simons, K. and R. Ehehalt (2002). "Cholesterol, lipid rafts, and disease." J Clin Invest **110**(5): 597-603.

Simons, K. and J. Gruenberg (2000). "Jamming the endosomal system: lipid rafts and lysosomal storage diseases." Trends Cell Biol **10**(11): 459-62.

Sleat, D. E., J. A. Wiseman, et al. (2004). "Genetic evidence for nonredundant functional cooperativity between NPC1 and NPC2 in lipid transport." Proc Natl Acad Sci U S A **101**(16): 5886-91.

Soccio, R. E., R. M. Adams, et al. (2005). "Differential gene regulation of StarD4 and StarD5 cholesterol transfer proteins. Activation of StarD4 by sterol regulatory element-binding protein-2 and StarD5 by endoplasmic reticulum stress." J Biol Chem **280**(19): 19410-8.

Soccio, R. E., R. M. Adams, et al. (2002). "The cholesterol-regulated StarD4 gene encodes a StAR-related lipid transfer protein with two closely related homologues, StarD5 and StarD6." Proc Natl Acad Sci U S A **99**(10): 6943-8.

Soccio, R. E. and J. L. Breslow (2003). "StAR-related lipid transfer (START) proteins: mediators of intracellular lipid metabolism." J Biol Chem **278**(25): 22183-6.

Soccio, R. E. and J. L. Breslow (2004). "Intracellular cholesterol transport." Arterioscler Thromb Vasc Biol **24**(7): 1150-60.

Sturley, S. L., M. C. Patterson, et al. (2004). "The pathophysiology and mechanisms of NP-C disease." Biochim Biophys Acta **1685**(1-3): 83-7.

Suematsu, N., K. Okamoto, et al. (2001). "Molecular cloning and functional expression of rat liver cytosolic acetyl-CoA hydrolase." Eur J Biochem **268**(9): 2700-9.

Tabas, I. (2002). "Cholesterol in health and disease." J Clin Invest **110**(5): 583-90.

Tabas, I. (2002). "Consequences of cellular cholesterol accumulation: basic concepts and physiological implications." J Clin Invest **110**(7): 905-11.

Tahara, M., K. Matsumoto, et al. (1999). "Hepatocyte growth factor leads to recovery from alcohol-induced fatty liver in rats." J Clin Invest **103**(3): 313-20.

Tall, A. R., L. Yvan-Charvet, et al. (2008). "HDL, ABC transporters, and cholesterol efflux: implications for the treatment of atherosclerosis." Cell Metab **7**(5): 365-75.

Tangirala, R. K., E. D. Bischoff, et al. (2002). "Identification of macrophage liver X receptors as inhibitors of atherosclerosis." Proc Natl Acad Sci U S A **99**(18): 11896-901.

Teupser, D., A. D. Persky, et al. (2003). "Induction of atherosclerosis by low-fat, semisynthetic diets in LDL receptor-deficient C57BL/6J and FVB/NJ mice: comparison of lesions of the aortic root, brachiocephalic artery, and whole aorta (en face measurement)." Arterioscler Thromb Vasc Biol **23**(10): 1907-13.

Teupser, D., M. Tan, et al. (2006). "Atherosclerosis quantitative trait loci are sex- and lineage-dependent in an intercross of C57BL/6 and FVB/N low-density lipoprotein receptor-/- mice." Proc Natl Acad Sci U S A **103**(1): 123-8.

Thomas, C., R. Pellicciari, et al. (2008). "Targeting bile-acid signalling for metabolic diseases." Nat Rev Drug Discov **7**(8): 678-93.

Thorp, E., Y. Li, et al. (2009). "Brief report: increased apoptosis in advanced atherosclerotic lesions of Apoe-/- mice lacking macrophage Bcl-2." Arterioscler Thromb Vasc Biol **29**(2): 169-72.

Tobert, J. A. (2003). "Lovastatin and beyond: the history of the HMG-CoA reductase inhibitors." Nat Rev Drug Discov **2**(7): 517-26.

Tomasetto, C., C. Regnier, et al. (1995). "Identification of four novel human genes amplified and overexpressed in breast carcinoma and localized to the q11-q21.3 region of chromosome 17." Genomics **28**(3): 367-76.

Tontonoz, P. and D. J. Mangelsdorf (2003). "Liver X receptor signaling pathways in cardiovascular disease." Mol Endocrinol **17**(6): 985-93.

Travis, A. J. and G. S. Kopf (2002). "The role of cholesterol efflux in regulating the fertilization potential of mammalian spermatozoa." J Clin Invest **110**(6): 731-6.

Tsujishita, Y. (2003). "Structural genomics of lipid signaling domains." Oncol Res **13**(6-10): 421-8.

Ueda, Y., E. Gong, et al. (2000). "Relationship between expression levels and atherogenesis in scavenger receptor class B, type I transgenics." J Biol Chem **275**(27): 20368-73.

van Helvoort, A., A. de Brouwer, et al. (1999). "Mice without phosphatidylcholine transfer protein have no defects in the secretion of phosphatidylcholine into bile or into lung airspaces." Proc Natl Acad Sci U S A **96**(20): 11501-6.

van Meer, G., D. R. Voelker, et al. (2008). "Membrane lipids: where they are and how they behave." Nat Rev Mol Cell Biol **9**(2): 112-24.

Veniant, M. M., S. Withycombe, et al. (2001). "Lipoprotein size and atherosclerosis susceptibility in Apoe(-/-) and Ldlr(-/-) mice." Arterioscler Thromb Vasc Biol **21**(10): 1567-70.

Warden, C. H., C. C. Hedrick, et al. (1993). "Atherosclerosis in transgenic mice overexpressing apolipoprotein A-II." Science **261**(5120): 469-72.

Watari, H., F. Arakane, et al. (1997). "MLN64 contains a domain with homology to the steroidogenic acute regulatory protein (StAR) that stimulates steroidogenesis." Proc Natl Acad Sci U S A **94**(16): 8462-7.

Welch, C. L., Y. Sun, et al. (2007). "Spontaneous atherothrombosis and medial degradation in Apoe-/-, Npc1-/- mice." Circulation **116**(21): 2444-52.

Weng, W. and J. L. Breslow (1996). "Dramatically decreased high density lipoprotein cholesterol, increased remnant clearance, and insulin hypersensitivity in apolipoprotein A-II knockout mice suggest a complex role for apolipoprotein A-II in atherosclerosis susceptibility." Proc Natl Acad Sci U S A **93**(25): 14788-94.

West, D. B. and B. York (1998). "Dietary fat, genetic predisposition, and obesity: lessons from animal models." Am J Clin Nutr **67**(3 Suppl): 505S-512S.

Wirtz, K. W. (1991). "Phospholipid transfer proteins." Annu Rev Biochem **60**: 73-99.

Wu, M. K., H. Hyogo, et al. (2005). "Impaired response of biliary lipid secretion to a lithogenic diet in phosphatidylcholine transfer protein-deficient mice." J Lipid Res **46**(3): 422-31.

Yamada, S., T. Yamaguchi, et al. (2006). "Regulation of human STARD4 gene expression under endoplasmic reticulum stress." Biochem Biophys Res Commun **343**(4): 1079-85.

Yamaga, M., K. Kawai, et al. (2008). "Recruitment and activation of phospholipase C (PLC)-delta1 in lipid rafts by muscarinic stimulation of PC12 cells: contribution of p122RhoGAP/DLC1, a tumor-suppressing PLCdelta1 binding protein." Adv Enzyme Regul **48**: 41-54.

Yan, D. and V. M. Olkkonen (2008). "Characteristics of oxysterol binding proteins." Int Rev Cytol **265**: 253-85.

Yuan, B. Z., X. Zhou, et al. (2003). "DLC-1 gene inhibits human breast cancer cell growth and *in-vivo* tumorigenicity." Oncogene **22**(3): 445-50.

Zhang, Y., J. R. Da Silva, et al. (2005). "Hepatic expression of scavenger receptor class B type I (SR-BI) is a positive regulator of macrophage reverse cholesterol transport *in-vivo*." J Clin Invest **115**(10): 2870-4.